

Chapter 7

SEISMIC DESIGN: STABILITY AND DEFORMATION ANALYSES

7.1 GENERAL

7.1.1 Design Approach

Under certain conditions, seismic loadings from an earthquake or other source can cause embankment or foundation materials to lose strength, potentially causing a structure to become unstable. Coal refuse embankments constructed using the upstream construction method may be particularly susceptible to instability from an earthquake because a portion of the dam is constructed on soft or loose saturated, hydraulically-placed material. Designers should perform an evaluation (commensurate with the hazard potential of the structure) to confirm that dam and embankment designs provide an adequate margin of safety against seismically-induced instability.

The methods of exploration, testing, and analysis presented in this chapter are based on research and practice, publications, and experience on a variety of projects. They provide a variety of options for design. These methods, ranging from basic to sophisticated, have generally been applied on coal refuse disposal sites. Commentary is provided in the text to help explain the basis for the methods and the applicability of the methods to specific situations. It is recognized that refinements in the methods, as well as new methods, may be developed in the future. Designers are encouraged to evaluate such refinements, new methods, and other approaches that are technically sound, particularly if they better address site-specific materials or conditions. Designers are also cautioned that this subject is complex and that refinements of existing methods and development of new methods can require substantial research and investigation, as well as input from geologists, seismologists, geotechnical engineers, and other professionals.

This chapter refers to dams and embankments interchangeably. Also, references to “soil” or “material” encompass soils and coal refuse materials (e.g., fine coal refuse or tailings, filter cake, combined coal refuse, mixed refuse, coarse coal refuse, and amended refuse). As there have been no reported failures of coal refuse embankments due to seismic loading within the U.S. coalfields, the various studies of strength loss due to seismic loading are predominantly from sites that contain natural soils or other mine tailings. Thus, the physical behavior of coal refuse materials must be inferred from correlations, supported by laboratory testing.

The following published papers, studies and ongoing research on coal refuse materials and seismic design of disposal sites provide an overview of information specific to slurry impoundments and potential information on testing and parameters that may be available:

- Gardner and Wu (2002) present an overview of challenges in evaluating strength loss at coal refuse disposal facilities from MSHA's perspective. They summarize the available pore-pressure-based empirical methods (field standard penetration testing and cone penetration testing) and strain-based laboratory methods (undrained steady-state shear strength approach based on triaxial compression tests) for evaluation of potential strength loss at coal refuse disposal impoundments.
- Castro (2003) presents the undrained peak strengths and undrained steady-state strengths derived from cone penetration testing, field vane-shear tests, laboratory tests on undisturbed samples and laboratory-consolidated slurry samples. These strength data show that strength loss of fine tailings is noticeable and the undrained steady-state strength values are typically between one-half and one-fourth of the peak undrained strength. The paper also provides cyclic-triaxial test data for undisturbed samples of natural clayey silt of low plasticity, similar to fine tailings, to show the degradation of peak undrained strength with strain during cyclic loading.
- Genes et al. (2000) present the undrained steady-state shear strength approach for evaluation of strength loss at five coal refuse disposal facilities in West Virginia. Isotropically-consolidated, undrained triaxial compression tests of undisturbed and remolded samples of fine coal refuse from five different disposal sites are presented to show undrained steady-state shear strength variation with void ratio and effective vertical stress.
- Ulrich et al. (1991) present a pore-pressure-based evaluation using cyclic-triaxial tests on samples of fine coal refuse from sites in Kentucky, Ohio, and Tennessee.
- Cowherd and Corda (1998) discuss pore-pressure-based empirical methods for triggering of strength loss at coal refuse dams and provide standard penetration tests data along with the measured seismic shear wave velocities for fine coal refuse, with a summary of cyclic-triaxial test results from four disposal sites.
- Hegazy et al. (2004) presents engineering properties for northern Appalachian coal refuse, including a summary of results of seismic piezocone testing and field vane-shear testing used for determining undrained shear strength.
- Kalinski and Phillips (2008) present a progress report on research being conducted at the University of Kentucky concerning development of dynamic properties of coal refuse. When completed, it will include field and laboratory testing on the dynamic behavior of coal refuse materials. Field standard penetration testing, cone-penetration testing, field vane-shear testing, seismic surface-wave testing, and downhole-seismic testing are to be performed. Complementary laboratory cyclic-triaxial testing and resonant-column testing are also proposed for determining dynamic properties of coal refuse materials.
- Zeng and Goble (2008) present the results of laboratory testing (resonant-column and cyclic-triaxial tests) for determining dynamic properties (damping ratio and shear modulus) performed on Appalachian coal refuse at Case Western Reserve University.

Seismic design of dams and embankments involves two separate requirements:

1. Prevention of seismic instability (slides)
2. Prevention of excessive deformations (translation, settlement, and cracking)

7.1.1.1 Seismic Instability

The ground motion from an earthquake can result in a reduction in the shear strength of loose, saturated materials. Seismic instability may occur when post-earthquake shear strength is less than the

pre-earthquake shear strength in one or more significant zones of an embankment or foundation. The driving force of the seismic instability is the static (gravity) weight of the embankment. Seismic instability is a particular concern for dams with substantial upstream construction because a portion of the dam is constructed on hydraulically-placed fine material. For seismic instability to occur, three conditions must develop:

1. The earthquake shaking must be strong enough to trigger undrained strength loss in one or more zones of material.
2. The strength loss must be significant enough that the post-earthquake shear strengths are less than the static driving shear stresses.
3. The location and amount of the material that experiences strength loss must be sufficient to generate instability.

Seismic stability is generally analyzed as a static (i.e., no seismic coefficient) limit-equilibrium, slope-stability problem, using post-earthquake shear strengths for the materials in the embankment and foundation. The earthquake shaking causes the material in the embankment or foundation to lose strength, but the static gravity shear stresses drive the failure. Some instability failures have been observed to occur after the earthquake shaking has stopped (Seed et al., 2003; Seed and Harder, 1990; Marcuson, Hynes and Franklin, 1992).

Experience has shown that when significant strength loss occurs in critical sections of a structure: (1) failures are often rapid, (2) they occur with little warning, and (3) the resulting deformations are often very large. Experience has also shown that the trigger events can be quite small. Hence, seismic design for significant- to high-hazard-potential dams and embankments should be carried out with caution and care.

7.1.1.2 Excessive Deformations

If seismic stability analyses indicate that an embankment is unstable, then deformations should be considered to be unacceptably large. However, if seismic stability analyses indicate that an embankment is stable, then potential seismic deformations should be assessed. Seismic deformations occur primarily during earthquake shaking. The cyclic-shear stresses induced by the earthquake contribute directly to the deformations. This contrasts with the primary mechanisms of instability. In seismic instability, the earthquake shaking causes undrained strength loss, but the static gravity stresses drive the instability failure.

The material making up the dam or embankment, the fine coal refuse or tailings retained behind and sometimes underlying the embankment, and the natural soil below the embankment must all be evaluated as part of stability and deformation analyses.

The basic elements for seismic design and analysis require evaluation of:

- Susceptibility of materials to strength loss and post-earthquake strengths
- Seismic stability using post-earthquake strengths
- Whether the design earthquake will trigger strength loss
- Deformations

7.1.2 Seismic Design Considerations and Flow Chart

The following points were considered in developing the guidance and recommendations presented in this chapter:

- The levels of analysis that should be performed vary depending on the type of facility and the consequences of failure. So, for example, no seismic analysis is required for low-hazard-potential dams (provided static stability is satisfied), while seismic stability and deformation analyses are required for high-hazard-potential dams.
- Methods for evaluating the susceptibility of a material to strength loss during an earthquake and for evaluating the degree of strength loss depend partly on whether the material is sand-like or clay-like. Fine coal refuse within a structure, and natural soil deposits in the foundation, might include zones of both sand-like and clay-like material. Therefore, methods for evaluating both sand-like and clay-like material are provided. These methods apply to both coal refuse materials and soil.
- Straightforward screening methods should be available for differentiating zones that are potentially susceptible to seismically-induced strength loss from zones that are not susceptible. Further detailed investigation and evaluation can then be focused on the potentially-susceptible zones. This chapter presents screening methods for both clay-like and sand-like material that require only the basic information provided by Standard Penetration Test (SPT) or Cone Penetration Test (CPT) data, grain-size test results, and Atterberg-limit data.
- Relatively straightforward methods of analysis should be available to designers, as well as methods that are more sophisticated. The more sophisticated methods may allow for less conservatism in the design and might be worthwhile for achieving a more economical design. However, the more sophisticated methods are optional, not required. For example, relatively straightforward field testing methods can be used to estimate post-earthquake strength, as well as more sophisticated, optional, laboratory methods. Another example is that seismic-stability analyses can be performed by simply assuming that the design earthquake triggers strength loss in materials that are potentially susceptible to strength loss, or an optional triggering analysis can be performed to evaluate whether the design earthquake is in fact strong enough to trigger strength loss. The authors of this chapter note that triggering analyses are not considered to be appropriate for sand-like materials for design earthquakes that exceed certain criteria and therefore impose significant seismic stresses on the materials. In designing new structures, it is often prudent to design based on the relatively straightforward methods rather than using more sophisticated methods to justify a design.
- The level of detail required for evaluation of the seismicity of a site should depend on the level of seismic hazard at the site. Many coal mining regions in the U.S. are in areas of low seismic hazard. Minimum parameters for the design earthquake in these areas are provided, and a site-specific evaluation is not recommended. For sites in areas of higher seismic hazard, a site-specific seismicity evaluation is recommended.
- The various credible methods employed by geotechnical engineers experienced in the seismic design of dams should be available for use. Therefore, this chapter presents three methods for analyzing the triggering of strength loss in loose, sand-like material: (1) the pore-pressure-based approach developed by Seed and updated by Youd et al. (2001), (2) the strain-based approach developed by Castro (1994), and (3) the stress-based approach developed by Olson and Stark (2003). Several field and laboratory methods and correlations for estimating post-earthquake strength of materials that are susceptible to strength loss and several methods for performing deformation analyses are also presented.
- Structures should generally have a safety factor of at least 1.2 for seismic stability based on a static stability analysis using post-earthquake material strengths. This safety factor is intended to account for uncertainties in the geometry of the structure,

in the shear strength, and in the delineation of zones that are potentially susceptible to strength loss, and it also helps achieve designs for which predicted seismic deformations are within acceptable limits.

- There may be special cases involving existing facilities for which the recommended design criteria can be relaxed. Examples of these special cases include minor modifications made as part of closure activities in which the progress toward closure will eventually improve seismic stability, and interim improvements for addressing a specific existing deficiency (e.g., adding an interim stage to provide needed free-board).

The recommended steps for a seismic evaluation or design are illustrated in the flow chart presented in [Figures 7.1a, 7.1b](#) and [7.1c](#). These steps are described in detail in [Section 7.4.4](#). A relatively straightforward path through the seismic stability portion of the flow chart (in which triggering analyses, sophisticated laboratory testing, and seismicity evaluations are avoided) is described in [Section 7.1.5](#).

The steps in the flow chart in [Figure 7.1a](#) can be summarized as follows:

1. Classify the structure and foundation based on type, size, downstream hazard potential, and anticipated performance under seismic loading, per the criteria indicated in Boxes 1, 2, and 3 of the flow chart.
2. Considering the classification in Step 1, and a conservative evaluation of post-earthquake stability (optional, Boxes 5 and 6), categorize the structure and foundation as either (1) further seismic evaluation is not needed (go to Box 4) or (2) potentially susceptible to seismic instability such that additional analysis is required (go to Box 7).
3. For those structures that are potentially susceptible to seismic instability, thoroughly characterize the soils and refuse in the structure and foundation (Box 7 of flow chart and [Section 7.3](#) of text). This step generally requires a significant effort because the spatial distribution of the refuse materials can be variable. Identify zones in the structure and foundation that may be susceptible to strength loss due to earthquake shaking ([Section 7.4.4.2](#)).
4. Analyze the stability of the embankment using post-earthquake strengths ([Section 7.4.3](#)). Post-earthquake strengths will be lower than pre-earthquake (static) strengths for zones that are susceptible to strength loss. This analysis may be relatively straightforward based on field testing data and laboratory index testing (Boxes 7, 7A, and 8). At coal refuse disposal sites where the ratio of coarse to fine refuse is large enough to allow design of massive (wide) embankments with broad crests, employing the basic and more straightforward methods are recommended because of their relative simplicity in design and regulatory review and their conservatism. Alternatively, sophisticated laboratory testing can be used to provide better estimates of post-earthquake strength, and relatively complex triggering analyses can be performed to evaluate whether the earthquake shaking is actually strong enough to trigger strength loss in the materials that are potentially susceptible to strength loss (Boxes 9 through 16 and [Sections 7.4.2](#) and [7.4.3.2](#)). A seismic hazard evaluation ([Section 7.7](#) and [Figure 7.23](#)) may be needed as part of these more sophisticated testing and analysis methods to define the magnitude and peak ground acceleration of the design earthquake and to obtain representative time histories of acceleration. These more sophisticated testing and analysis methods are often less conservative than the basic and more straightforward methods. The added costs of the more sophisticated testing and analysis may be justified by designs that are more economical or more efficient from an operational standpoint.

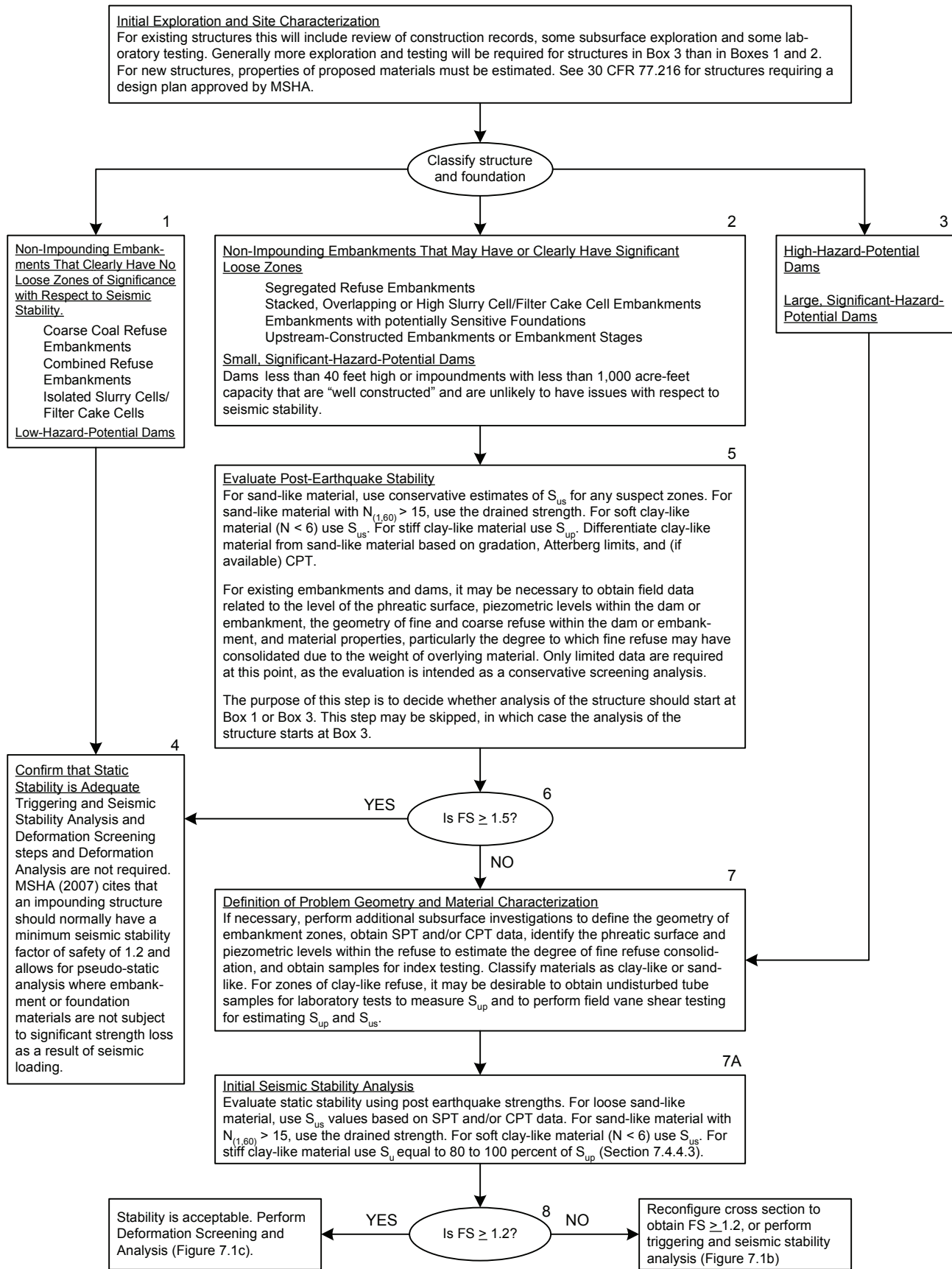


FIGURE 7.1a SEISMIC STABILITY SCREENING

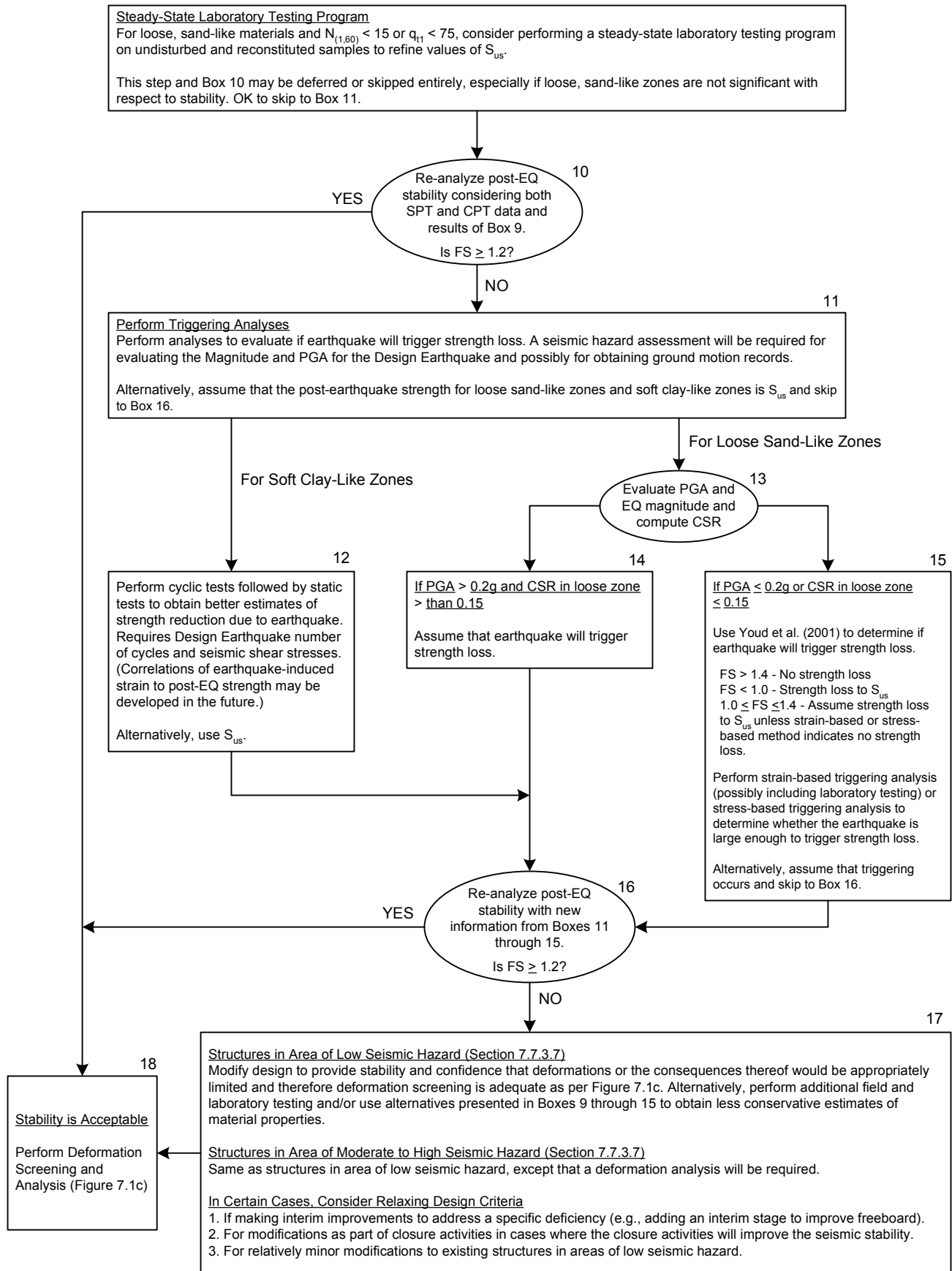


FIGURE 7.1b TRIGGERING AND SEISMIC-STABILITY ANALYSIS

DEFORMATION SCREENING

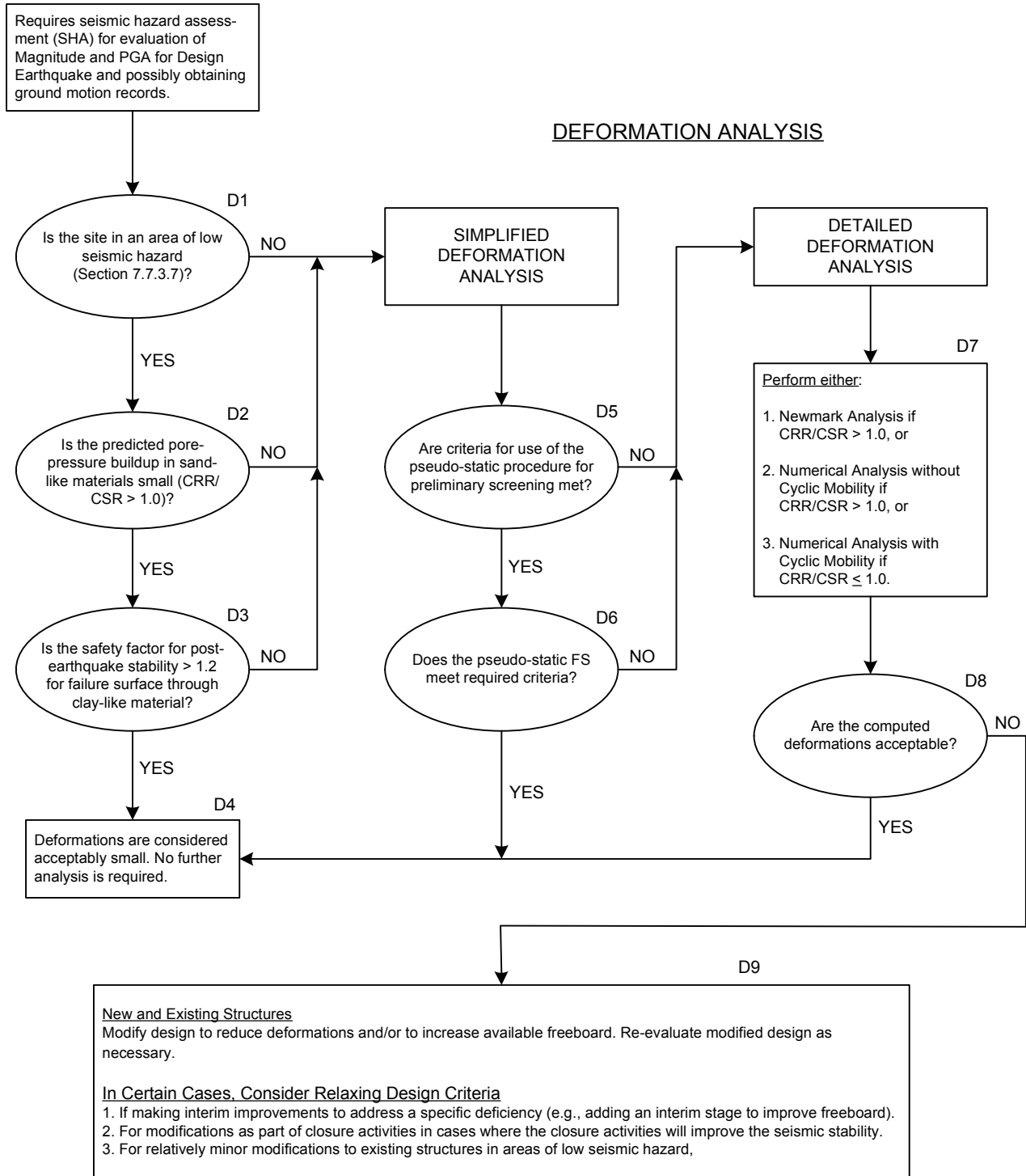


FIGURE 7.1c DEFLECTION SCREENING AND ANALYSIS

5. If stability is acceptable (safety factor of 1.2 or higher), evaluate potential deformations (Step 7).
6. If stability is not acceptable, redesign or modify the embankment until stability is acceptable (Box 17).
7. Evaluate potential deformations of the embankment caused by the earthquake shaking (Boxes D1 through D8 and [Section 7.5](#)). The deformation analysis may involve a

relatively simple screening analysis or may require sophisticated computer modeling. If not performed as part of Step 4, a seismic-hazard evaluation (Section 7.7 and Figure 7.23) will be needed as part of the deformation analysis.

8. If the estimated deformations are within an acceptable range, accept the design. Otherwise, redesign or modify the embankment (Box D9).

7.1.3 Sand-Like Versus Clay-Like Material

For many of the analyses described in this chapter, fine coal refuse and natural soils are referred to as sand-like or clay-like depending on whether they exhibit monotonic and cyclic undrained shear loading behavior that is fundamentally more similar to that of either sand or clay. The methods for evaluating susceptibility to strength loss, triggering, and post-earthquake strength are different for sand-like and clay-like materials. This differentiation is significant primarily if the material is loose enough (sands) or soft or sensitive enough (clays) that it is potentially susceptible to strength loss.

The key factors in differentiating loose sand-like material from soft or medium clay-like material, for the purposes of seismic stability and deformation analyses, are the strain at peak undrained strength and the abruptness of the drop-off in shearing resistance as strains increase beyond the strain at peak. Loose sands and highly sensitive clays can reach peak undrained strength S_{up} at small strains, and experience abrupt drop-off in resistance at higher strains. Most clays tend to reach S_{up} at higher strains, and tend to experience more gradual and limited drop-off in shearing resistance at higher strains. Fine coal refuse deposits often include materials falling within both classifications, and near the boundary of these two types of behavior.

Loose material with shear strain at peak strength of less than 2 percent in an undrained monotonic (non-cyclic) test, and a rapid drop-off in resistance after reaching peak strength, is generally considered sand-like (although highly sensitive clays may exhibit similar behavior). Loose or soft material with shear strain at peak strength of more than about 5 percent, and a gradual drop-off in resistance after reaching peak strength is considered clay-like. Figure 7.2 illustrates the associated stress-strain curves for these materials. Material with strain behavior between these descriptions is considered borderline. It should be noted that shear strain in an undrained triaxial test is 1.5 times axial strain. Peak strength refers to peak principal stress difference ($\sigma_1 - \sigma_3$).

For the analyses in this chapter, it is generally more conservative to assume that a borderline material is sand-like than to assume it is clay-like. It is very difficult to obtain or prepare samples of in-situ low plasticity material for strength testing at its in-situ void ratio. Therefore, Atterberg-limits tests, gradation tests, and, preferably, CPT data should be used first as an index of stress-strain behavior to categorize materials as sand-like or clay-like. Laboratory stress-strain testing should be used to help categorize borderline materials.

The following criteria are recommended:

- Atterberg limits and gradation – Material should be treated as sand-like if the plasticity index of the material (measured from the portion passing the No. 40 sieve) is 7 or less.

Material should be considered clay-like if all of the following criteria are met:

- The material has 35 percent or more by dry weight passing the No. 40 sieve.
- The material has 20 percent or more by dry weight passing the No. 200 sieve.
- The plasticity index of the material (as measured by the portion passing the No. 40 sieve) is 10 or higher.

Material that does not fit either set of criteria should be treated as sand-like unless optional laboratory stress-strain testing demonstrates otherwise.

Commentary: In general, it is more conservative to treat a material as sand-like rather than as clay-like. The gradation and Atterberg-limit criteria provided above were selected as reasonably conservative recommended guidance by the authors of this chapter. These Atterberg-limit and gradation criteria may include as sand-like some materials that are considered clay-like by some investigators (e.g., Boulanger and Idriss (2004) who suggested a break between sand-like and clay-like behavior at a PI of 7). Seed et al. (2003) point out that there is no general agreement on Atterberg-limit criteria, and suggest a PI of 12 as one guideline for evaluating soil behavior, but they do not specifically refer to clay-like versus sand-like behavior.

- Cone penetration test data – CPT data can be used in conjunction with Atterberg-limit and gradation data to differentiate sand-like from clay-like material. CPT Soil Behavior Type Index I_c values below 2.6 should be considered sand-like (Robertson and Wride, 1998; Youd et al., 2001). I_c values above 2.6 may be considered clay-like. Material with I_c values above 2.6, but with very low values of friction ratio, should be considered clay-like but potentially highly sensitive (Section 7.4.4.2). If CPT data conflict with Atterberg limits and gradation data, the Atterberg limits and gradation data should generally govern. CPT data may also be used as an index to compare zones where Atterberg limits and gradation were measured with zones where Atterberg limits and gradation were not measured.

Commentary: Soil Behavior Type is based on where CPT data fall on a log-log plot of normalized CPT tip resistance versus friction ratio. Olsen and Mitchell (1995), reproduced in Seed et al. (2003), suggested a similar soil characterization framework based on the same type of plot.

- Laboratory test data – As mentioned previously, borderline materials (PI between 7 and 10 or otherwise not clearly sand-like or clay-like) should be classified as sand-like unless laboratory testing demonstrates otherwise. Laboratory testing for this purpose is optional. If performed, the testing should consist of isotropically-consolidated, strain-controlled, undrained triaxial compression tests with pore-pressure measurement performed on undisturbed samples. For the purpose of this testing, undisturbed sampling as described in Section 6.4.3.5 is recommended, considering also the discussion in Section 7.3 regarding sample quality. For this testing, the material has a PI of 7 or higher and is therefore less likely to densify during sampling than a less plastic sand-like material would be. Therefore, the detailed measurements of densification discussed in Appendices 7B and 7C for sand-like materials are not necessary for this sampling and testing. A consolidation stress of two-thirds of the in-situ vertical effective stress should be used to model in-situ conditions. If the axial strain at peak strength (peak principal stress difference, $\sigma_1 - \sigma_3$) is less than or equal to 3.33 percent (5 percent shear strain), then the material should be considered sand-like. If the axial strain at peak strength is more than 3.33 percent (5 percent shear strain) then the material should be considered clay-like.
- Highly sensitive clay-like and borderline materials – In very rare occurrences, natural soils and (non-coal) mine tailings have been identified that have a Liquidity Index greater than 1 (i.e., a natural water content greater than their Liquid Limit), a very high sensitivity (i.e., significant and abrupt strength loss), and low shear strain at peak strength. If materials such as this are encountered, special evaluations outside the scope of this manual may be appropriate. As a conservative approach, these materials may be assigned a post-earthquake strength of 20 psf (Table 7.1).

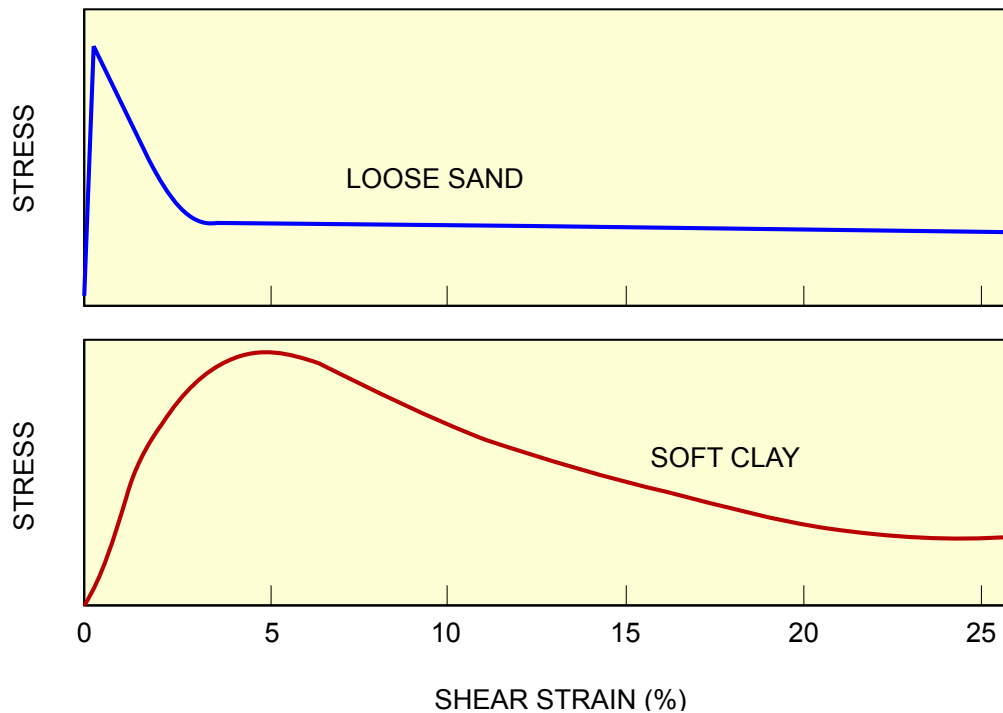


FIGURE 7.2 TYPICAL UNDRAINED STRESS-STRAIN CURVE

Loose zones of coarse refuse (e.g., zones of uncontrolled placement and compaction) should be treated as sand-like for the analyses discussed in this chapter. Combined refuse and intermixed zones of coarse and fine refuse should first be differentiated as predominantly coarse or fine refuse based on grain size and whether the coarse or fine refuse will control the response to loading. If the combined or mixed refuse is considered to be predominantly fine material, it should then be classified as sand-like or clay-like for the analyses in this chapter.

Soils, rock fill, and mixtures of soil and rock fill that are not coal refuse, whether part of a natural deposit, mine spoil, or other fill, will be referred to as natural soils. Natural soils can be described as coarse, sand-like, or clay-like, using the same general criteria as for refuse.

As discussed in Section 6.2.3.2, fine coal refuse is often classified as a slightly plastic sandy silt or clay, or a slightly plastic to non-plastic silty sand. The Plasticity Index varies from non-plastic ($PI = 0$) to $PI > 10$. In other words, fine coal refuse may be sand-like, clay-like, or borderline. Fine coal refuse (and some natural soils) may be highly stratified in very thin layers. CPT data are often useful in delineating this stratification. The designer must make a judgment as to whether clay-like or sand-like layers will control the behavior of individual zones. In general, zones consisting of stratified layers of sand-like and clay-like material should be considered sand-like, unless detailed field or laboratory data indicate otherwise.

7.1.4 Susceptibility to Strength Loss

As discussed in Section 7.4.4.2, saturated or nearly-saturated, loose, sand-like material with $N_{1,60}$ values less than 15 or q_{t1} values less than 75 tsf (as defined in Section 7.2) is considered potentially contractive (potentially susceptible to strength loss). As also discussed in Section 7.4.4.2, clay-like material with CPT values of tip resistance and side friction falling in certain ranges or with SPT N-values less than 6 (corrected for hammer efficiency per Youd et al. (2001), but not corrected for overburden pressure) is considered potentially susceptible to strength loss. These criteria are used to determine whether various zones within the embankment require further evaluation.

7.1.5 Simplified Steps for Seismic Stability

While a variety of methods for exploration, testing, and analysis are described in this chapter, simplified steps that provide a direct path for evaluating seismic stability are available. As introduced in [Section 7.1.2](#), the recommended sequence of analysis is described in the flow charts in [Figures 7.1a, 7.1b](#) and [7.1c](#), which allow the option of either skipping or incorporating sophisticated methods.

The intent of this section is to describe simplified steps for estimating soil and refuse properties for a relatively straightforward analysis without the need for extensive testing and analysis that will lead to safe designs based on supportable conservative assumptions and correlations. However, for existing structures there may be no simplified methodology for characterizing the existing conditions (i.e., finding out what types of soils are present and where). The simplified analyses and estimates of engineering soil properties are necessarily conservative, and in some cases a more detailed analysis may show them to be very conservative. Optional steps, which require additional testing and analysis to more accurately measure or predict material behavior and thereby reduce the conservatism in these simplified steps, can be considered and are discussed in other sections of this chapter.

The following basic steps describe a relatively straightforward sequence that can be followed for design or evaluation of a new or existing high-hazard-potential slurry impoundment dam (or other dam). (Box numbers refer to the flow charts in [Figures 7.1a, 7.1b](#) and [7.1c](#).) The steps described in the following text do not require sophisticated laboratory testing or relatively complex triggering analyses. A site-specific seismicity evaluation is only required for deformation analyses (not for seismic stability analyses) and may not be needed if the site is in a low-seismic-hazard area ([Section 7.7.3.7](#)).

7.1.5.1 Step 1

For a high-hazard-potential dam, proceed from Box 3 to Boxes 7 and 7A. Define the geometry of the dam and identify zones of clay-like and sand-like material (per [Section 7.1.3](#)). For an existing dam, the geometry will be based on construction records, a site survey, the results of borings and in-situ testing (preferably CPTs), and laboratory index testing (grain size and Atterberg limits). For design of a new dam, the foundation materials and properties will be based on exploration and testing programs, and embankment geometry will be based on the development plan and anticipated construction procedures and refuse properties.

7.1.5.2 Step 2

Characterize the fine refuse to address stratification, layering, distinction of sand-like and clay-like materials, and estimation of strength and associated properties. As discussed in [Section 7.3](#), Cone Penetration Testing (CPT) in combination with recovery of samples (using SPTs, for example) is recommended for addressing these issues.

7.1.5.3 Step 3

Characterize the fine refuse deposits (and other materials) as either clay-like or sand-like, per the criteria given in [Section 7.1.3](#), based on laboratory grain-size and Atterberg-limits tests.

7.1.5.4 Step 4

Screen the various zones in the dam for susceptibility to strength loss based on the SPT and (preferably) CPT data. Basically (as detailed in [Section 7.4.4.2.1](#)), sand-like material with $N_{1,60}$ values less than 15 or q_{t1} values less than 75 is considered potentially susceptible to strength loss. Clay-like material with N values less than 6 or CPT data in certain ranges is also considered potentially susceptible to strength loss. Screening to determine the susceptibility to strength loss should consider both CPT and SPT data when available. If such testing produces inconsistent results, it should be resolved in favor of the more reliable and robust data set considering the amount, consistency and quality of the

data. For design of a proposed dam, zones potentially susceptible to strength loss should be defined based on experience, available data from nearby sites, and published data for similar facilities. For slurry impoundments, consider similarities in coal seams, mining and processing methods, and fine refuse deposition.

7.1.5.5 Step 5

Perform a limit-equilibrium stability analysis using conservative post-earthquake strengths (as detailed in [Section 7.4.4.3](#)). For zones that are screened as not being potentially susceptible to strength loss, the post-earthquake strengths are the same as those used in the static stability analysis.

For sand-like material considered susceptible to strength loss, the appropriate strength is the undrained shear strength at very high strain (undrained steady-state strength S_{us}), which can be obtained from correlations with SPT and/or CPT data ([Section 7.4.3.1](#)). Even more simply, as a lower bound, S_{us} for sand-like material can be taken as $0.04 \sigma'_v$ (if the material is non-plastic or has a liquidity index of less than 1), as discussed in [Section 7.4.3.1](#) and as shown in [Table 7.1](#). For design of a new dam, S_{us} can be taken as $0.04 \sigma'_v$, or higher values may be used based on supporting data for similar materials for existing dams.

For clay-like material considered susceptible to strength loss (e.g., highly sensitive clay-like material), the appropriate post-earthquake strength is also S_{us} , which can be obtained from field vane-shear tests or from CPT data (as described in [Section 7.4.3.3](#)). A lower-bound, post-earthquake strength for clay-like material can be taken as $0.04 \sigma'_v$ (if the material has a liquidity index less than 1), as discussed in [Section 7.4.3.3](#) and as shown in [Table 7.1](#). For design of a new dam, S_{us} can be taken as $0.04 \sigma'_v$, or higher values may be used based on supporting data for similar materials at existing dams.

Commentary: The lower-bound, post-earthquake strength of $0.04 \sigma'_v$ is considered conservative for either sand-like or clay-like fine coal refuse. As more testing and analysis of fine refuse becomes available, refinements to the 0.04 relationship can be expected (initial published work is discussed in [Section 7.4.3.2.3](#)). For proposed dams, strengths estimated during design must be validated during construction by performing field investigations and obtaining samples of the actual materials.

For clay-like material that is not considered susceptible to strength loss, the appropriate post-earthquake strength is typically much higher than S_{us} . Guidance for characterizing the post-earthquake undrained shear strength of such clay-like material, based primarily on consistency and strain and/or cyclic stress level considerations, is provided in later sections.

If the safety factor for the stability analysis using post-earthquake strengths is greater than or equal to 1.2, continue by performing a deformation analysis (from Box 8 go to Box D1). If the safety factor is less than 1.2, redesign the dam (skip from Box 8 to Box 17) to reduce the influence of material zones susceptible to strength loss. Alternatively, if the safety factor is less than 1.2, consider performing more detailed evaluations of triggering and post earthquake strength, as described in [Sections 7.4.3](#) and [7.4.4](#).

7.1.5.6 Step 6

There are several methods of deformation analysis that can be used, depending on the site seismicity and the presence of material susceptible to strength loss. If the dam is in an area of low seismic hazard and is not influenced by materials that are potentially susceptible to strength loss, then a relatively simple pseudo-static procedure can be used (as described in [Section 7.5.3](#)). Otherwise, more complex analyses are required ([Section 7.5](#) and portion of flow chart in [Figure 7.1c](#)), and the computed deformations must be compared to recommended tolerable values.

TABLE 7.1 COMPARISON OF BASIC CRITERIA FOR SAND-LIKE, CLAY-LIKE AND BORDERLINE MATERIALS

	Sand-Like	Clay-Like	Borderline (Treat as Sand-Like)	Borderline (Treat as Clay-Like)
Atterberg limits	$PI \leq 7$	$PI \geq 10$	$7 < PI < 10$	$7 < PI < 10$
% passing No. 40 sieve		≥ 35		≥ 35
% passing No. 200 sieve		≥ 20		≥ 20
Triaxial tests on undisturbed samples to obtain stress-strain curve	Not Required	Not Required	Not Required	Shear strain at peak strength must exceed 5%; otherwise treat as sand-like
Lower-bound post-earthquake strength	0.04 σ'_v if non-plastic, or if LI is < 1.0	0.04 σ'_v if LI is < 1.0	0.04 σ'_v if LI is < 1.0	0.04 σ'_v if LI is < 1.0
	20 psf if $LI \geq 1.0$, but no higher than 0.04 σ'_v	20 psf if $LI \geq 1.0$, but no higher than 0.04 σ'_v	20 psf if $LI \geq 1.0$, but no higher than 0.04 σ'_v	20 psf if $LI \geq 1.0$, but no higher than 0.04 σ'_v
Other methods to obtain post-earthquake strength	1. Correlations with SPT/CPT 2. Steady-state lab testing	1. Field vane shear or CPT 2. Cyclic followed by static lab testing	Correlations with SPT/CPT	1. Field vane shear or CPT 2. Cyclic followed by static lab testing
Field vane-shear testing for peak-undrained strength and S_{us}	Not Applicable	Applicable	Potentially Applicable if it can be demonstrated that the test is undrained (Section 6.4.3.8)	Potentially Applicable if it can be demonstrated that the test is undrained (Section 6.4.3.8)
CPT to help identify layering and to differentiate sand-like from clay-like	Recommended	Recommended	Recommended	Recommended
CPT to measure peak undrained strength and S_{us}	Not Applicable	Applicable	Potentially Applicable if it can be demonstrated that the test is undrained (Section 6.4.3.7)	Potentially Applicable if it can be demonstrated that the test is undrained (Section 6.4.3.7)

Note: 1. PI is the Plasticity Index.
2. LI is the Liquidity Index.

7.2 TERMINOLOGY

The terms defined in the following list are specifically related to seismic stability and deformation analyses. These definitions should be reviewed carefully because in the literature authors may assign various meanings to the same terms. Basic terminology related to subsurface investigations, material strength, and static stability analysis is discussed in Chapter 6.

Clay-like material – This term is defined in [Section 7.1.3](#).

Contractive soil or refuse – Contractive materials compress when sheared under drained conditions. They generate positive excess pore pressures when sheared under undrained conditions. Thus the undrained strengths are lower than the drained strengths. Loose sand-like material tends to be contractive. When sheared undrained, the peak strength is typically reached at relatively low strain, and strength can decrease (i.e. strain-soften) significantly at higher strains. Soft clay-like material also tends to be contractive. However, when sheared undrained, the peak strength develops at relatively high strains and the strength decreases gradually at strains beyond the strain at peak strength.

Cyclic mobility – Cyclic mobility is the progressive softening and resulting large cyclic strains that occur in saturated soils during undrained cyclic loading in which shear stress

reversal occurs (Casagrande, 1971; Castro, 1975). In an undrained cyclic-triaxial test, stress reversal occurs during cyclic loading if the sample is loaded in extension as well as compression. In the field, stress reversal occurs when the cyclic shear stresses induced by the earthquake exceed the static shear stresses. When this occurs, the stress strain curve after some number of cycles develops an S-shape, and significant cyclic strains are generated. The condition of significant cyclic straining is defined as “cyclic mobility.” Robertson (1994) and Robertson and Wride (1998) suggested the term “cyclic liquefaction” to describe this phenomenon and suggested that the term “cyclic mobility” be used to describe the cyclic strain behavior of anisotropically consolidated soil subject to undrained cyclic loading without stress reversal. For the latter case, cyclic strains are smaller. However, the original definition of cyclic mobility will be used in this Manual.

Cyclic resistance ratio (CRR) – Used in the pore-pressure-based method of triggering analysis for sand-like material (Section 7.4.2.2). CRR is a measure of the resistance of a material to pore-pressure increase caused by earthquake shaking.

Cyclic stress ratio (CSR) – Used in the pore-pressure-based method of triggering analysis for sand-like material (Section 7.4.2.2). CSR is a measure of the shear stress generated by the earthquake shaking.

Dilative soil or refuse – Dilative materials expand at large strains when sheared under drained conditions, and they generate negative excess pore pressures when sheared under undrained conditions. Thus the undrained strengths can be higher than the drained strengths. The amount by which the undrained strength exceeds the drained strength is limited by possible cavitation of the pore water. However, it is customary to neglect strengths higher than the drained strength. Medium-dense and dense sand-like materials tend to be dilative at large strains. When sheared undrained, the strength nearly reaches its peak at moderate strain and then levels off or increases (i.e. strain-hardens) gradually at higher strains.

Commentary: During undrained monotonic (non-cyclic) loading, dilative soils normally generate small positive excess pore pressures at small strains, and then generate negative excess pore pressures at higher strains. During undrained cyclic loading, dilative soils can experience pore-pressure buildup. Depending on the cyclic strain, both positive and negative excess pore pressures can develop at different portions of the load cycle. But after each full load cycle there will normally be an increase in positive excess pore pressure. However, if loaded statically after cyclic loading, the soil tends to dilate as strains increase, the positive excess pore pressures diminish, the excess pore pressure becomes negative, and the soil strain-hardens. In other words, even though dilative material can develop positive excess pore pressures during cyclic loading, dilative material will not lose strength as a result of the cyclic loading.

Flow slide – If saturated material in an embankment or its foundation experiences strength loss, and the static (gravity) shear stresses (often referred to as the driving stresses) exceed the available shear strength, then the embankment can experience instability and failure (depending on the amount of material that experiences strength loss and the geometry of the structure). The failure is often referred to as a flow slide in cases where the material controlling the instability experiences an abrupt loss in strength such that: (1) it approaches the steady-state (residual) strength, (2) the slide mass appears to deform almost like a liquid, and (3) deformations propagate over a substantial zone, rather than along a well-defined failure surface. In such cases, the failure mass can slide a long distance before coming to rest. Although movements might commence along a well-defined failure surface, a substantial portion of the slide mass may experience strength loss as slope movements develop, and a flow slide can evolve. With sand-like materials, instability can be rapid and can occur with little warning, and deformations can be very large.

Liquefaction – The term “liquefaction” has been used in the literature to describe several related but distinctly different phenomena. These phenomena include: (1) flow slide failures of embankments and dams, (2) lateral spreading of gently sloping ground, (3) development of 100 percent excess pore pressure during undrained cyclic loading often accompanied by the appearance of sand boils at the ground surface, and (4) the development of high shear strains and/or high excess pore pressures in cyclic laboratory tests. In this Manual, the term “liquefaction” is not used. Instead, more descriptive and precise terminology is used.

Commentary: The following terms are sometimes used in the literature, but are not used in this Manual. They are presented here for completeness.

Initial liquefaction – During cyclic loading, initial liquefaction is the first occurrence of momentary zero effective stress (pore pressure = 100 percent).

Cyclic failure – Term sometimes used (Boulanger and Idriss, 2004) to describe the onset of high excess pore pressures and large shear strains during undrained cyclic loading of clay-like soils. In Boulanger and Idriss’s usage, “cyclic failure” of clay-like materials is comparable to “liquefaction” of sand-like materials.

Cyclic liquefaction – Term suggested by Robertson (Robertson, 1994; Robertson and Wride, 1998) to describe the progressive softening and resulting large cyclic strains that occur in saturated sands during undrained cyclic loading where shear stress reversal occurs. Synonymous with the definition of “cyclic mobility” used by Casagrande and others in the 1970s.

Flow liquefaction – Term sometimes used (Robertson and Wride, 1998) for “flow slide.”

Liquidity Index (LI) – The Liquidity Index is derived from the Atterberg limits. $LI = (\text{water content} - PL)/(LL - PL)$. If $LI = 1$, the natural water content equals the liquid limit.

N – The Standard Penetration Test (SPT) N-value, uncorrected.

$N_{1,60}$ – The SPT N-value, normalized to an effective overburden stress of one tsf (approximately one atmosphere) and normalized to a hammer efficiency of 60 percent (Youd et al., 2001).

Peak Ground Acceleration (PGA) – The maximum horizontal ground surface acceleration at a site caused by the design earthquake. Values of PGA obtained from seismic hazard assessments normally refer to accelerations measured at bedrock outcrops or at the ground surface of stiff soil profiles. These values of PGA are usually not directly applicable to the ground surface of sites with other types of soil profiles. Also, the PGA (maximum horizontal ground surface acceleration) at the top of an embankment will generally be different from the PGA at the ground surface at the base of the embankment. PGAs obtained from seismic hazard assessments are usually not directly applicable to the top of an embankment. A site response analysis can be used to estimate the PGA at the top of an embankment based on the PGA identified for a bedrock outcrop or stiff soil profile.

Post-earthquake shear strength – The shear strength available at the end of an earthquake, used in a static, limit-equilibrium stability analysis to evaluate post-earthquake stability. For each zone of coal refuse or natural soil, the strength used in the analysis is estimated based on the expected response of the material to earthquake shaking. The strength used could be the peak drained strength, the drained steady-state (residual) strength, the peak undrained strength, the undrained steady-state (residual) strength, or other intermediate strength.

q_c – Measured Cone Penetration Test (CPT) tip resistance.

q_t – Measured CPT tip resistance corrected for unequal end-area pore-pressure effects (Lunne et al., 1997). For CPT in clean to silty sands, q_c and q_t are essentially the same and are often used interchangeably.

q_{t1} – CPT tip resistance (q_t) normalized to an effective overburden stress of one atmosphere (typically 1 tsf), in units of stress: $q_{t1} = 1.8 q_t / (0.8 + \sigma'_v / P_a)$. (Olson and Stark, 2002)

q_{t1N} – Dimensionless CPT tip resistance, i.e., q_{t1} normalized by a reference pressure of one atmosphere and expressed in dimensionless terms. Sometimes referred to as Q or Q_t .

For clay-like material: $q_{t1N} = (q_t - \sigma_{v0}) / \sigma'_{v0}$

For sand-like material, refer to Youd et al. (2001)

$(q_{t1N})_{CS}$ – q_{t1N} corrected to an equivalent value for clean sand (Youd et al., 2001).

Sand-like material – This term is defined in [Section 7.1.3](#).

Sensitivity – Sensitivity in clays is normally defined as undisturbed strength divided by remolded strength (S_{up}/S_{us}). In this chapter, the term “highly sensitive” is used to refer to clays that have undrained stress-strain behavior similar to loose sands. Highly sensitive clays have a relatively small strain at peak undrained strength and a significant drop-off in shearing resistance (strain-softening) after the strain at peak. One example of highly sensitive clay is Norwegian quick clay. Clay-like coal refuse is generally not highly sensitive.

S_{dp} , S_{ds} , S_{up} , and S_{us} – Drained peak strength, drained steady-state (residual) strength, undrained peak strength, and undrained steady-state (residual) strength. In this Manual, these strengths are defined as being measured under monotonic loading unless noted otherwise. See also the definition of “undrained steady-state strength.”

Strength loss – The tendency for contractive soils to have lower undrained strength at high strains than at lower strains ($S_{us} < S_{up}$). The term strength loss is used to indicate a reduction in available strength from S_{up} to a lower value, not a complete loss to zero strength. If earthquake shaking causes shear strains and pore pressures to increase in a soil, the soil may experience strength loss (in the extreme, a reduction from S_{up} to S_{us}). Loose sand-like soil may experience a reduction in strength to S_{us} as the result of relatively small earthquake shaking because the strain at peak strength is relatively low. Clay-like materials (excluding highly sensitive clay soils) tend to experience less abrupt loss of strength because they reach both peak undrained strength and S_{us} at much higher strains than sand-like materials.

Commentary: In many cases the available strength before a failure has been the drained strength throughout the history of the facility, because all loads have been applied sufficiently slowly to allow drainage. During an earthquake (or other disturbance such as a relatively quick loading of additional fill or a relatively quick cut near the toe of an embankment), shear stresses are applied quickly enough that the soil behaves in an undrained manner. In contractive soils the peak undrained strength would be lower than the previously available drained strength, and thus shear deformations or failure might ensue. In these cases, strength loss has sometimes been defined as a reduction in available strength from S_{dp} to S_{up} (and then possibly to S_{us}).

For the purposes of this chapter, references to strength loss do not include reductions from S_{dp} to S_{up} . In this chapter, strength loss only refers to a decrease in available strength from S_{up} to (or toward) S_{us} . As discussed in [Section 6.6.4.2.1](#), this Manual includes analysis of the potential for strength reduction from S_{dp} to S_{up} as part of static stability analyses, with undrained peak strength (possibly reduced to account for potential progressive failure) used in zones of fine refuse.

A rise in groundwater level (or rise in the phreatic surface) can reduce stability in several ways, including the following:

- A rise in groundwater level can result in a decrease in effective stress in what was previously an unsaturated zone. This decrease in effective stress may result in a decrease

in available drained strength within that zone. This by itself is not likely to cause a failure, because the saturated drained strength is normally adequate to maintain stability.

- *In some cases of very loose materials in a previously unsaturated zone, a rise in groundwater level can trigger collapse of the material matrix. This results in a rapid rise in pore pressure and a decrease in available strength within that zone from drained to undrained. Since the material is very loose, the undrained strength can be substantially lower than the drained strength, and a failure could ensue if the zone of affected material is large enough. This is unlikely to be a concern for fine coal refuse that is deposited through water and consolidates while saturated.*
- *A rapid rise in reservoir level could cause a rapid increase in seepage forces and thus driving stresses such that the soil within the embankment behaves as undrained rather than drained. (In contractive materials, the available strength would decrease from S_{dp} to S_{up} , as discussed in the first paragraph of this commentary.)*

The term strength loss has been used to describe these phenomena related to groundwater. However, in this chapter, the term strength loss only refers to a reduction from S_{up} to (or toward) S_{us} .

Triggering – Term used to indicate that earthquake shaking is strong enough to cause, or trigger, strength loss. Some engineers propose that triggering of strength loss occurs when excess pore pressures due to cyclic loading reach 100 percent (effective stress reaches zero). Some engineers propose that triggering of strength loss occurs when a certain level of shear strain is reached, whether or not pore pressures have reached 100 percent. And some engineers propose that triggering of strength loss occurs when shear stresses exceed a certain level. The various approaches are discussed in this Manual. Triggering might also be caused by loadings other than earthquake loadings, such as rapid increases in embankment height, excavation of toe materials due to re-mining of coal refuse in an impoundment, or rapid changes in groundwater level.

Undrained residual strength – Term often used in the literature to describe the undrained soil or coal refuse shear strength at very high strains. It is synonymous with “undrained steady-state strength.” The term “residual strength” is often used in the literature to refer to drained as well as undrained strength. In this chapter, residual strength normally refers to undrained steady state (residual) strength.

Undrained steady-state strength – The undrained steady-state shear strength is the undrained shear strength of soil or coal refuse at very high strains (Poulos, 1981). This is the minimum shear strength of the material at a given void ratio. It is synonymous with terms such as “undrained residual strength,” “critical state strength,” “ultimate undrained strength,” “minimum undrained strength” and “liquefied undrained strength.” This Manual will use the term “undrained steady-state (residual) strength” or S_{us} .

7.3 CHARACTERIZATION OF SUBSURFACE CONDITIONS AND MATERIAL PROPERTIES

Previous chapters in this Manual have discussed the field exploration programs and laboratory testing needed for characterizing subsurface conditions and material properties for analysis and design. This section discusses issues related specifically to seismic analysis. These issues include:

- **Field testing and sampling quality** – Special attention to the details of field sampling and testing is required for the procedures and analyses discussed in this chapter. Drillers and other field exploration contractors should be selected and engaged based on contract terms that encourage quality over speed. Proper use of casing, drilling mud, and upward deflecting drill bits and properly maintaining a fluid head on the

borehole are important in SPT sampling, vane-shear testing, and obtaining undisturbed tube samples.

- Field vane-shear testing – Field vane-shear tests can be used to measure the undrained peak strength and undrained steady-state (residual) strength of clay-like material (Sections 6.4.3.8 and 7.4.3.3). Field vane shear tests should not be used to measure the undrained strength of sand-like material because sand-like material will drain during the course of the test, and the measured strength may be very unconservative (Table 7.1). Details of testing procedures (which differ in some important respects from the ASTM procedures) and criteria for confirming that the material remains undrained during the test are discussed in Section 6.4.3.8.
- CPT and SPT – Both cone penetration tests and standard penetration tests are recommended for characterizing fine coal refuse. CPT data are generally more repeatable and less affected by equipment or operator variability. CPTs are generally faster and less expensive than SPTs for each exploration location, and CPTs provide continuous data. SPTs provide physical samples for visual classification and for index testing. CPTs are often used for initial site characterization. A more comprehensive site exploration program (including more CPTs, at least some SPTs, and other methods) can then be developed based on the results of the initial CPTs. When using the CPT, samples must also be obtained to verify soil type (by visual classification and index testing). Samples can be obtained using CPT push equipment, using SPTs, or by other methods. SPTs should be performed in general accordance with ASTM D 6066, which includes special provisions for seismic analyses in addition to the basic SPT procedures contained in ASTM D 1586. For high-hazard-potential dams, the hammer energy should be verified, and a qualified engineer or geologist should be assigned on a full-time basis to each drill rig to observe the testing procedures and to log the borings.

Fine refuse should be sufficiently characterized in the field to determine stratification, layering, distinction of sand-like and clay-like materials, and estimation of strength and associated properties. CPTs, in combination with recovery of samples (e.g., SPT samples), are recommended for addressing these issues at impoundment sites. Using both the SPT and CPT provides an opportunity for collecting redundant and complementary data to define layers and associated strengths of soft or loose deposits with a degree of resolution generally not achievable by relying solely on SPTs. However, there may be sites that, because of the fine refuse characteristics (e.g., uniformity of deposit, penetration resistance, etc.) or available detailed records of dam design and construction, can be adequately characterized by the SPT alone.

- Index testing – Whenever engineering property testing is performed, index testing (grain-size, Atterberg-limits, and specific-gravity) should be performed to allow comparison and interpretation of test results on different samples and to improve the understanding of the relationship between index properties and engineering properties of coal refuse. Grain-size analyses, hydrometer analyses, Atterberg-limits tests, and other index tests should be performed on samples that have not been air-dried or oven-dried. Wet preparation methods should be used.
- Undisturbed sampling – Obtaining high quality, undisturbed samples of sand-like material requires specialized procedures. Thin-walled, fixed-piston tube samplers, both mechanically actuated and hydraulically actuated, have been used successfully. A detailed procedure for using fixed-piston samplers is provided in Appendix 7C. Freezing of sandy material for either sampling or transportation has also been used. Freezing must be performed in a manner that allows the liquid water to escape the

sample as the freezing front advances. If liquid water becomes trapped, it will expand as it freezes and cause loosening of the sample.

- **Representative sampling** – Samples for laboratory testing must be representative of the layer being investigated. Therefore sufficient CPT and/or SPT data must be obtained to delineate material zones. Unsuccessful attempts to obtain undisturbed tube samples should be documented in order to confirm that the loosest material is being taken into account in the evaluation.
- **Variability and layering** – Variability is best evaluated based on CPT data and depositional history. Estimation of the depositional history includes consideration of all available information, including observations of the surface and documented or anecdotal information on operation of the structure. Undisturbed sampling and testing is not the best way to study variability and is most effectively performed after the variability of the deposit has been characterized.
- **Material zones** – Many of the analyses discussed in this chapter refer to zones of material. Zones should be identified based on consideration of depositional environment, grain size, plasticity, and penetration resistance (density and strength). Loose material should not be combined with medium or dense material in a single zone. CPT is often the most efficient method for defining the extent of loose zones. Further guidelines for site characterization are provided in Chapter 6.
- **Piezometric levels and degree of consolidation** – Soil properties are often estimated as a function of effective consolidation stress. Materials within tailings impoundments are not always fully consolidated under the current conditions of fill height and groundwater level. Therefore, to confirm estimates of effective consolidation stresses, subsurface exploration programs should include installation of piezometers for measurement of piezometric levels within various material zones at various depths within the impoundment. The piezocone is also valuable for measuring piezometric levels.
- **Laboratory testing on reconstituted samples** – Obtaining high-quality, undisturbed samples is often difficult, especially for materials with low plasticity. It would be easier to measure the steady-state strength of sand-like materials by reconstituting samples in the laboratory, starting at a very loose condition and consolidating them to the in-situ confining pressures. Unfortunately, there is little or no literature to document that reconstituted samples of fine coal refuse have the same void ratios or strengths as undisturbed samples with the same confining pressures. Anecdotal evidence for some natural soils and other mine tailings indicate that in some cases the reconstituted samples have significantly lower void ratios (and therefore higher steady state strengths) than undisturbed specimens at the same confining pressures, apparently either because of time effects (the time over which confining pressures are applied) or fabric effects (the particle structure is different in the lab and field). As a result, testing of reconstituted samples is generally not recommended without some verification that the consolidated laboratory samples have void ratios similar to the in-situ material. This might be a fruitful area for future research.

Commentary: For sand-like materials, use of reconstituted samples is recommended for developing the slope of the steady-state line in [Section 7.4.3.2.3](#) and for laboratory testing associated with the strain-based method of triggering analysis in [Section 7.4.2.3.1](#). However, these are exceptions to the general rule for using undisturbed samples. In the first case, in-situ strength is not being measured directly with the remolded samples; the slope of the steady state line is being measured. To obtain the in-situ, steady-state strength, undisturbed samples are needed. In the second case, samples are remolded and consolidated to match the in-situ void ratio (not

the in-situ confining pressure), and undisturbed samples are also needed for measurement of the in-situ void ratio.

- **Material Properties for Proposed Structures** – For design of a new dam, material properties may be based on supporting data for similar materials for existing facilities. Zones potentially susceptible to strength loss should be defined based on experience, available data from nearby sites, and published data for similar facilities. For slurry impoundments, consideration should be given to similarities in coal seams, mining and processing methods, and fine refuse deposition. The lower bound post-earthquake strength of $0.04 \sigma'_v$ is considered conservative for either loose sand-like or soft clay-like fine coal refuse, assuming the liquidity index is less than one (Table 7.1). As more testing and analysis of fine refuse becomes available, refinements to the $0.04 \sigma'_v$ relationship can be expected (initial published work is discussed in Section 7.4.3.2.3). Strengths estimated during design must be validated during construction by performing field investigations and obtaining samples of the actual materials. These data may lead to the need to modify the design of the facility.

7.4 SEISMIC STABILITY ANALYSES

7.4.1 General Discussion

Seismic instability may occur when the overall average post-earthquake shear strength is less than pre-earthquake shear strength in one or more zones of an embankment. The driving force of the stability failure is the static (gravity) weight of the embankment. For seismic instability to occur, three conditions must be met:

1. The earthquake shaking must be strong enough to trigger undrained strength loss in one or more zones of material.
2. The post-earthquake strengths must be less than the static driving shear stresses.
3. The amount of material that experiences strength loss must be sufficient to cause instability.

There are three general components to a seismic stability analysis:

1. Evaluation of whether the earthquake is strong enough to cause strength loss in one or more zones of the embankment or foundation. This is referred to as a triggering analysis.
2. Evaluation of the post-earthquake strengths in the various soil zones that may be susceptible to strength loss.
3. Performance of static, limit-equilibrium, slope-stability analyses using post-earthquake strengths for the materials in the embankment and foundation.

7.4.1.1 Triggering Analyses

In saturated, sand-like material, a small shear strain (1 percent or less) can trigger sudden strength decrease from S_{up} to S_{us} . In clay-like material, high shear strain (5 percent or more) is generally needed to cause some strength loss, and very high shear strain is generally needed to cause strength loss all the way to S_{us} . Highly sensitive clays may behave similarly to sand-like material in that strength loss may occur at low shear strains. Three general approaches to triggering analysis are discussed in Section 7.4.2, and are summarized as follows:

- **Pore-pressure-based approach** (Sections 7.4.2.1 and 7.4.2.2) – Uses a method developed for evaluating whether earthquake shaking will generate high excess pore

pressures as an index of whether the earthquake shaking will trigger strength loss in sand-like materials. This approach is not applicable to clay-like materials.

- **Strain-based approach** – For clay-like material (Section 7.4.2.3.1), this approach considers post-earthquake strength as a function of shear strain that occurs during the earthquake. For sand-like material (Section 7.4.2.3.2), this approach assumes that strength loss is triggered when the cyclic shear strain induced by the earthquake exceeds a critical value (i.e., the triggering shear strain).
- **Stress-based approach** (Section 7.4.2.3.3) – This approach assumes that strength loss is triggered when shear stresses exceed the undrained yield strength (the peak undrained strength). This approach is not applicable to clay-like materials.

It is important to note that for loose, saturated, sand-like material, moderate to large earthquakes will almost always be large enough to trigger strength loss. Therefore, triggering analyses should not be used to confirm the adequacy of a dam or embankment if the PGA at the base of the embankment is higher than 0.2g and the CSR (Section 7.4.2.2.1) in the zone of loose sand-like material is greater than 0.15. If the design earthquake causes a higher site PGA, then triggering of strength loss should simply be assumed for zones of loose, sand-like material with $CSR > 0.15$. The post-earthquake strength of the material in the loose zone should be assumed to be equal to S_{us} . A PGA of 0.2g and CSR of 0.15 are recommended guidance. In evaluating potential measures to improve the stability of a dam or embankment where the CSR in a zone exceeds 0.15, it may be useful to perform a triggering analysis to help assess whether alternative stabilization schemes that would reduce the CSR might ultimately improve the dam or embankment stability.

7.4.1.2 Evaluation of Post-Earthquake Strength

If the earthquake shaking triggers strength loss, the post earthquake strength of sand-like material will be the undrained, steady-state strength S_{us} , which is primarily a function of void ratio and is very sensitive to small changes in void ratio. The void ratio of sand-like material is primarily a function of the method of deposition. Even within a seemingly uniform layer, sand-like material deposited by water (including both natural sands and fine coal refuse) has significant variability in void ratio. As a result, multiple samples of sand-like material from the same zone or layer are likely to have varying values of S_{us} . Therefore, methods of evaluating S_{us} of sand-like materials for stability analyses should account for the potential variability within zones or layers.

In contrast, the void ratio of clay-like material is primarily a function of consolidation pressure and stress history. Furthermore, the peak-undrained strength and the steady-state (residual) strength in clay-like material is less sensitive to void ratio than in sand-like material. As a result, post-earthquake strengths within a zone are likely to be more uniform for clay-like material than for sand-like material.

Three general approaches to evaluating the post-earthquake strengths of materials that may be susceptible to strength loss are discussed in Section 7.4.3. The three approaches are:

1. Empirical correlations of SPT and/or CPT values with back-figured, post-earthquake strengths from flow slides may be used to estimate S_{us} for sand-like material (Section 7.4.3.1). These methods assume that the earthquake shaking triggered strength loss, so the post-earthquake strength is S_{us} .
2. Laboratory tests on high-quality samples from the field can be used to estimate post-earthquake strengths for both clay-like and sand-like material (Section 7.4.3.2).
3. Field vane-shear tests and CPTs can be used to measure S_{us} for clay-like material (Section 7.4.3.3). As discussed in Section 7.4.2.3.1, S_{us} is often a conservative low estimate of the actual post-earthquake strength for clay-like material.

7.4.1.3 Stability Analysis Using Post-Earthquake Strengths

A generalized approach presented as a series of steps for performing the triggering analyses, the post-earthquake strength evaluations, and the limit equilibrium stability computations is provided in [Section 7.4.4](#).

7.4.2 Triggering Analyses

7.4.2.1 Pore-Pressure-Based Method for Triggering of Strength Loss in Clay-Like Material

There is general agreement that highly plastic clays (with the exception of highly sensitive clays) are not susceptible to either significant pore-pressure buildup or strength loss due to earthquake shaking (Seed et al., 2003).

For clays that are not highly plastic, several criteria for pore-pressure buildup and susceptibility to strength loss due to earthquake shaking, based on Atterberg limits and percent clay content, have been proposed (Seed et al., 2003). However, while there is general agreement that susceptibility to strength loss decreases with increasing plasticity and increasing SPT or CPT resistance, there is no general agreement on specific criteria at the time of publication of this Manual.

Screening-level evaluations of the susceptibility of clay-like materials to strength loss, based on CPT and SPT data, are discussed in [Section 7.4.4.2](#). More detailed estimates of whether earthquake shaking is strong enough to trigger strength loss in clay-like material can be obtained by using the strain-based methods discussed in [Sections 7.4.2.3.1](#) and [7.4.3.2.2](#).

7.4.2.2 Pore-Pressure-Based Method for Triggering of Strength Loss in Sand-Like Material

This method is used for evaluating whether the design earthquake is large enough to cause (trigger) strength loss. For loose/contractive sand-like material, the earthquake shaking required to trigger strength loss is normally small, and triggering causes strength loss all the way to S_{us} . Therefore, as discussed in [Section 7.4.1](#), if the design peak ground acceleration (PGA) at the embankment site is larger than 0.2g and the CSR within the zone of loose sand-like material is greater than 0.15, then the triggering analysis described in the following paragraphs should not be performed, and triggering of strength loss should simply be assumed. The post-earthquake strength of the material in the loose zone should be assumed to be equal to S_{us} . In evaluating potential measures to improve the stability of a dam or embankment where the CSR in a zone exceeds 0.15, it may be useful to perform the triggering analysis to help determine whether alternative stabilization schemes that would reduce the CSR might ultimately improve the dam or embankment stability.

For sand-like materials, evaluating the potential for triggering of strength loss using pore-pressure-based methods is done using the “simplified method” first published by Seed and Idriss (1971). The method is referred to as “simplified” because it does not require cyclic laboratory testing or detailed analysis of site response to earthquake shaking. However, use of this method for coal refuse impoundments will often require a detailed analysis of site response. Additions and updates to the method have been published by numerous authors. A consensus on the state of practice for using the method was published by 21 technical practitioners (Youd et al., 2001).

Commentary: After Youd et al. (2001) was published, several investigators proposed refinements to various aspects of the analysis method. These include Seed et al. (2003) and others. These refinements can be considered for specific cases, or Youd et al. (2001) may be used directly.

The method was developed for evaluation of the potential for a zone of sand-like material to develop high (approaching 100 percent) excess pore pressures, but may also be used as an index of the susceptibility of the soil zone to lose strength.

The method is based on observations of high pore-pressure generation during earthquakes, as evidenced primarily by the appearance of sand boils, ground fissures, or lateral spreads at level or gently sloping sites and involves computations of cyclic stress ratio (*CSR*) and cyclic resistance ratio (*CRR*). *CSR* is a measure of the seismic “demand” on a soil layer. *CRR* is a measure of the capacity of the soil to resist pore-pressure increases during earthquake shaking.

The method was developed from case history data primarily from flat to gently-sloping sites underlain with Holocene (recent) alluvial or fluvial sediments at depths less than 50 ft. The method has been verified for, and is strictly applicable only to, these site conditions (Youd et al., 2001). However, the method is often extended to other site conditions with steeper slopes and deeper soils, such as coal refuse embankments, since no directly applicable performance history is available for such facilities.

The steps for evaluating the triggering of pore-pressure increase are:

1. For the location at which each value of either SPT $N_{1,60}$ or CPT q_{t1N} was obtained in zones of material that may be susceptible to strength loss, compute the cyclic stress ratio (*CSR*), which is the average cyclic shear stress caused by the design earthquake in the zone of material divided by the initial effective vertical stress in the zone of material (τ_{av}/σ'_{v0}). Although the method was developed based on average SPT or CPT values, it should be applied to all measured values for added conservatism and improved delineation of loose zones.
2. Estimate the cyclic resistance ratio (*CRR*) from various published plots that give *CRR* as a function of $N_{1,60}$ or q_{t1N} and fines content. Alternatively, *CRR* may be computed using spreadsheets or other computer programs based on equations that approximate the curves shown in the published plots.

Commentary: For some other analyses in this chapter, corrections for fines content are not recommended, but they should be considered for estimation of *CRR* based on $N_{1,60}$ or q_{t1N} values.

3. Compute the safety factor against triggering based on pore-pressure increase using *CSR*, *CRR*, and appropriate corrections for earthquake magnitude, overburden, and shear stress using the following relationship (Youd et al., 2001):

$$FS = (CRR_{7.5}/CSR) \times MSF \times K_{\sigma} \times K_{\alpha} \quad (7-1)$$

Methods for evaluating *CSR*, *CRR*, *MSF*, K_{σ} and K_{α} are discussed below.

4. If the safety factor against pore-pressure increase in a zone is greater than 1.4, then it can be assumed that the earthquake shaking will not be strong enough to trigger strength loss in that zone. For seismic stability analyses, the peak undrained strength S_{up} (but not more than the peak drained strength) may be used in that zone. If the safety factor (CRR/CSR) in a zone is less than 1.0, then triggering of strength loss should be assumed, and for seismic stability analyses, the undrained, steady-state (residual) strength S_{us} should be used in that zone. For safety factors between 1.0 and 1.4, triggering of strength loss is possible. Either assume that triggering of strength loss will occur, or perform more rigorous triggering analyses (strain-based or stress-based methods, as discussed in Section 7.4.2.3) to make a final evaluation of whether or not triggering occurs.

Commentary: The safety factor of 1.4 is recommended guidance and is intended to account for the strength loss that can be triggered even if the pore-pressure increase is substantially lower than 100 percent.

The paragraphs that follow discuss evaluation of CSR, evaluation of CRR, and correction factors for earthquake magnitude, overburden stress, and sloping ground.

7.4.2.2.1 Evaluation of Cyclic Stress Ratio (CSR)

The cyclic stress ratio (CSR) at a particular depth is given by:

$$CSR = \tau_{av} / \sigma'_{vo} \quad (7-2)$$

where:

$$\begin{aligned} \tau_{av} &= \text{average cyclic shear stress induced by the earthquake} = 0.65 \tau_{max} \text{ (force/length}^2\text{)} \\ \sigma'_{vo} &= \text{effective vertical overburden stress (force/length}^2\text{)} \end{aligned}$$

As discussed in the following text, computing τ_{av} in a zone of material requires a design earthquake PGA or a design-earthquake, acceleration time-history.

Three methods for computing CSR that are acceptable for various situations are:

1. CSR computation method 1 – The preferred method is to compute CSR by using 1D or 2D numerical site response software, such as SHAKE or QUAD4, that compute the variation in maximum shear stress τ_{max} with depth. The value of τ_{av} at the depth of interest should be taken from the site response analyses as $0.65 \tau_{max}$ at that depth. Using a one-dimensional (1D) or two-dimensional (2D) numerical site response analysis requires, as input to the analysis, an acceleration time-history for the design earthquake as well as dynamic properties (shear modulus and damping) for each material type. This method is appropriate for all sites.

Commentary: Important material properties used in performing the analysis are the shear modulus and damping. They can be estimated using index and classification data, or site-specific testing such as crosshole testing can be performed to measure shear wave velocity (to obtain the maximum shear modulus G_{max}). Laboratory testing including resonant-column testing and cyclic-triaxial testing can also be utilized. The resonant-column test measures dynamic soil properties at a lower range of shear strain than the cyclic-triaxial test. Dynamic properties of coal refuse materials are the subject of research in Kalinski and Phillips (2008) and Zeng and Goble (2008). Whether 1D or 2D site response analyses should be used depends on the specific conditions for which the triggering analysis is being performed (locations of potential slope stability failure surfaces, variability of materials, geometric complexity, and distance from the suspect zone to the exposed slope). For analysis of upstream failures of coal refuse impoundments, the potential failure surfaces are often relatively far from the downstream face, such that the simplifications associated with 1D analyses are acceptable. For analysis of downstream failures of coal refuse impoundments with wide coarse refuse stages, the potential failure surfaces generally pass through the coarse refuse stages and possibly thin zones of fine refuse. So even though the ground surface is sloping, this geometry can be reasonably modeled with a series of 1D analyses. For analysis of downstream failures of coal refuse impoundments with narrow coarse refuse stages, the potential failure surfaces pass through highly variable materials, and the sloping ground effects (downstream face) are more pronounced. Therefore 2D analyses should be used to model these more complex conditions.

2. CSR computation method 2 (for shallow, level-ground sites) – For conditions of nearly level ground, uniform deposits, and depths up to 75 feet, CSR can be computed from the following equation (Youd et al., 2001):

$$CSR = (\tau_{av}/\sigma'_{vo}) = 0.65 (a_{max}/g) (\sigma_{vo}/\sigma'_{vo}) r_d \quad (7-3)$$

where:

- a_{max} = maximum horizontal acceleration at the ground surface (e.g., top of embankment) (mass \times length/time²)
- g = acceleration of gravity (mass \times length/time²)
- σ_{vo} = total overburden stress (force/length²)
- σ'_{vo} = effective vertical overburden stress (force/length²)
- r_d = stress reduction coefficient (1.0 at the ground surface, decreasing with depth) (dimensionless)

Commentary:

- $\tau_{av} = 0.65 \tau_{max}$
- $\tau_{max} = \text{peak seismic shear stress at any depth} = (\sigma_{vo}) (a_{max}/g) (r_d)$
- $\tau_{max}/\sigma_{vo} = (a_{max}/g) (r_d)$

τ_{max} is the product of the total overburden stress at the depth in question σ_{vo} times the peak acceleration of the overburden mass above the depth in question $(a_{max}/g)(r_d)$. This is equivalent to saying that seismic shear force equals mass times seismic acceleration or seismic shear stress (force per square foot) equals total vertical stress (mass per square foot) times seismic acceleration.

The coefficient r_d accounts for the deformability of the overburden mass, which results in the seismic shear stress at depth being lower than the product of the total overburden stress σ_{vo} times the peak acceleration at the ground surface a_{max} . In other words, r_d represents the fact that the peak acceleration of the overburden mass $(a_{max}/g)(r_d)$ at depth is lower than the maximum acceleration at the ground surface, and thus there is a reduction of the ratio of peak seismic shear stress to total overburden stress (τ_{max}/σ_{vo}) with depth. Seed et al. (2003) present refinements for values of r_d for specific cases, or Youd et al. (2001) may be used directly.

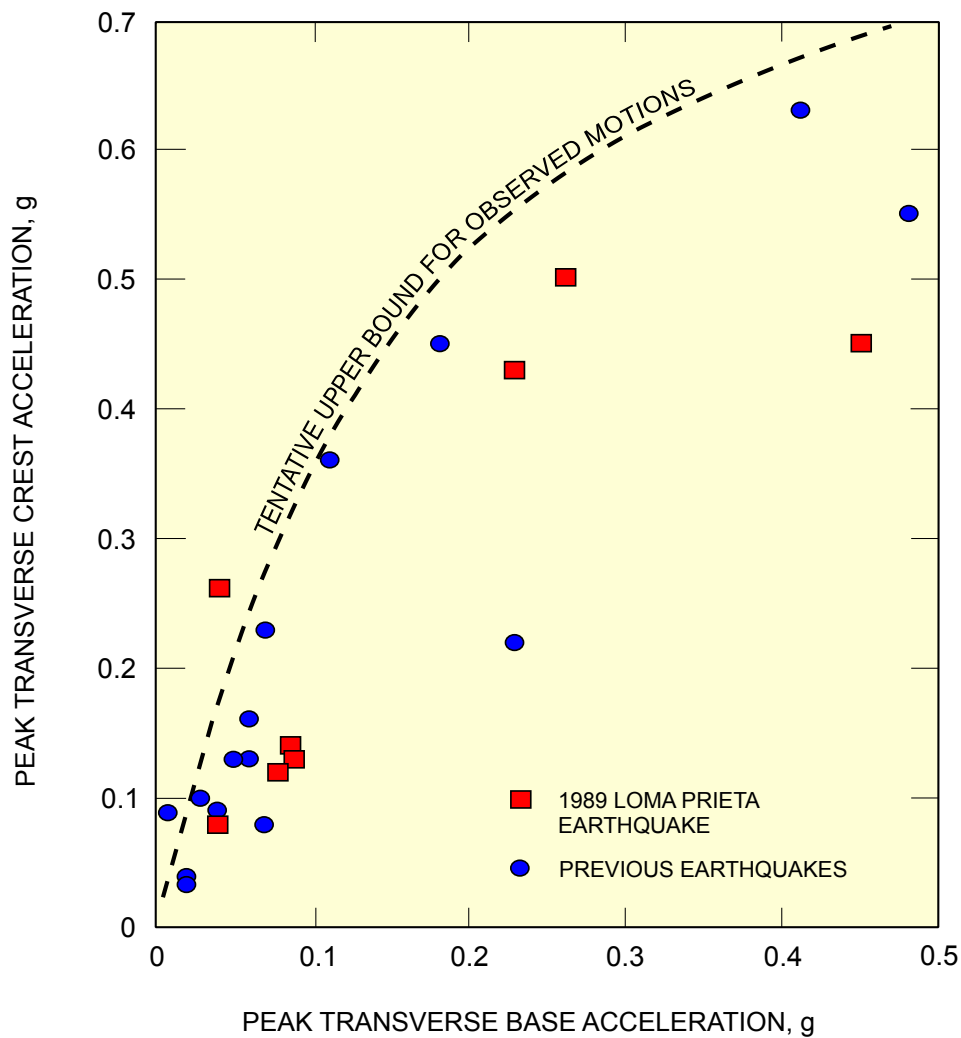
The computation of total overburden stress σ_{vo} should not include the weight of any free water that may exist above the ground surface. It is a relatively common error to include the weight of free water since it is part of the total overburden. However, it cannot be accelerated by the ground below, and thus it does not count as part of the mass being shaken.

3. **CSR computation method 3** – For depths greater than about 75 feet or for irregular and sloping ground conditions (i.e., for most coal refuse embankments), the following simplified method can, in certain cases, be used instead of Method 1. Method 3 can be used for cases where potential failure surfaces pass through relatively uniform materials, and the potential failure surfaces are relatively far from steep slopes. Examples are:
 - Upstream failures of coal refuse impoundments where the potential failure surfaces pass through reasonably uniform materials (no abrupt changes from loose or soft material to dense or hard material), and the failure surfaces are relatively far from the steep downstream slope.
 - Downstream failures of coal refuse impoundments with wide coarse refuse zones near the downstream slope, where the potential failure surfaces also pass through reasonably uniform materials.

Method 3 uses the same equation for CSR as Method 2. However, the stress reduction coefficient r_d used in that equation is only appropriate for level ground. Therefore, above the depth of interest, replace the product ($a_{max} r_d$) with the maximum acceleration of the overburden mass k_{max} . The value of k_{max} can be estimated from published relationships of the depth-dependent variation in maximum acceleration ratio (k_{max}/a_{max} versus y/h , where y is the depth below the top of the embankment and h is the embankment height). The “average of all data” line from Figure 7.4 can be used.

The maximum acceleration at the ground surface (top of embankment) a_{max} will normally be higher than the maximum acceleration at the ground surface at the base of the embankment (PGA). The value of a_{max} can be estimated from the PGA of the design earthquake at the base of the embankment using Figure 7.3.

Figures 7.3 and 7.4 were developed for conventional dams with an approximately triangular shape. Therefore, the results for Method 3 should be compared with the results of Method 2. If the results are significantly different, the more conservative value should be used, or an analysis using Method 1 should be performed.



(HARDER, 1991)

FIGURE 7.3 COMPARISON OF PEAK BASE AND CREST TRANSVERSE ACCELERATIONS MEASURED AT EARTH DAMS

Commentary: It should be noted that the ratios of maximum acceleration at the base of the embankment to maximum acceleration at the top of the embankment are different in Figures 7.3 and 7.4. That is because Figure 7.4 compares the maximum acceleration of the overburden mass above the base of the embankment to the maximum acceleration at the top of the embankment, while Figure 7.3 compares the maximum acceleration at the base of the embankment to the maximum acceleration at the top of the embankment. In other words, Figure 7.4 considers that, because the overburden mass is not rigid, the accelerations at different depths within the overburden mass will be different. Figure 7.4 looks at the average acceleration of the overburden mass at each time increment and then picks the maximum value k_{max} . In Figure 7.4, k_{max} acts at the base of the overburden mass, but represents the average acceleration of the mass above the base. In Figure 7.3, the peak transverse base acceleration is the acceleration at the specific depth corresponding to the bottom of the embankment.

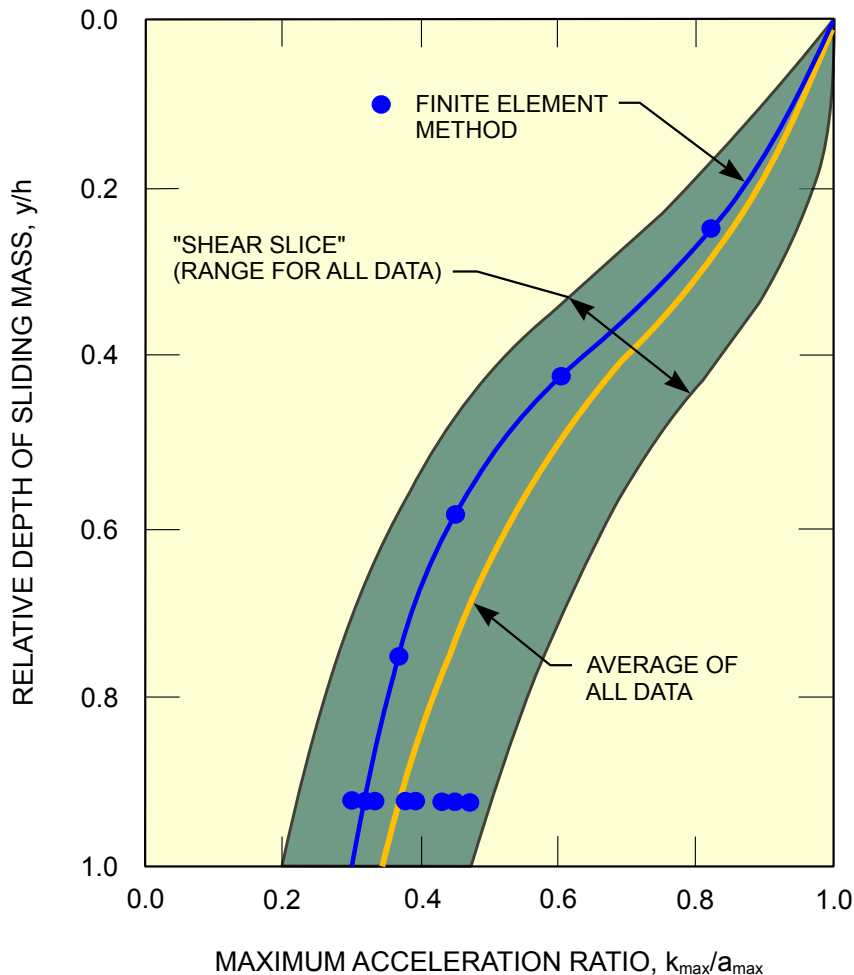


FIGURE 7.4 VARIATION OF MAXIMUM ACCELERATION RATIO WITH DEPTH OF SLIDING MASS

7.4.2.2.2 Evaluation of Cyclic Resistance Ratio (CRR)

The cyclic resistance ratio can be evaluated through the use of field test data including: (1) SPT data, (2) CPT data, and (3) shear-wave velocity (V_s) measurements. Procedures for computing CRR are described in Youd et al. (2001). It is good practice to obtain both SPT and CPT data. Shear-wave velocity data may also be helpful. A description of each of these approaches is provided in the following:

- CRR determined from SPT – Numerous plots have been published over the years showing CRR as a function of SPT blowcount $N_{1,60}$. The plot from Youd et al. (2001) is shown in Figure 7.5. The plot shows zones where data from case histories suggest

that significant pore-pressure increase will occur and zones where significant pore-pressure increase is unlikely to occur. The plot includes curves developed for soils with various percentages of fines. The curve for less than 5 percent fines is considered the basic penetration criterion for the simplified method described in Youd et al. (2001) and is thus referred to as the “SPT clean sand base curve.” Youd et al. (2001) describes ways to adjust $N_{1,60}$ to a clean sand value $N_{1,60(CS)}$. The curves are valid only for magnitude 7.5 earthquakes. Scaling factors to adjust for different magnitude earthquakes are discussed later.

Two corrections are normally made to the field blow count N . The first (C_N) is made to normalize N to an overburden pressure of 1 atmosphere (about 1 tsf or 100 kPa). The second (C_E) is made to normalize hammer energy to 60 percent of the energy generated by a 140-lb weight free-falling 30 inches. Other corrections less commonly made in practice include borehole diameter (C_B), rod length (C_R), and samplers with and without liners (C_S). Thus:

$$N_{1,60} = N \times C_N \times C_E \times C_B \times C_R \times C_S \quad (7-4)$$

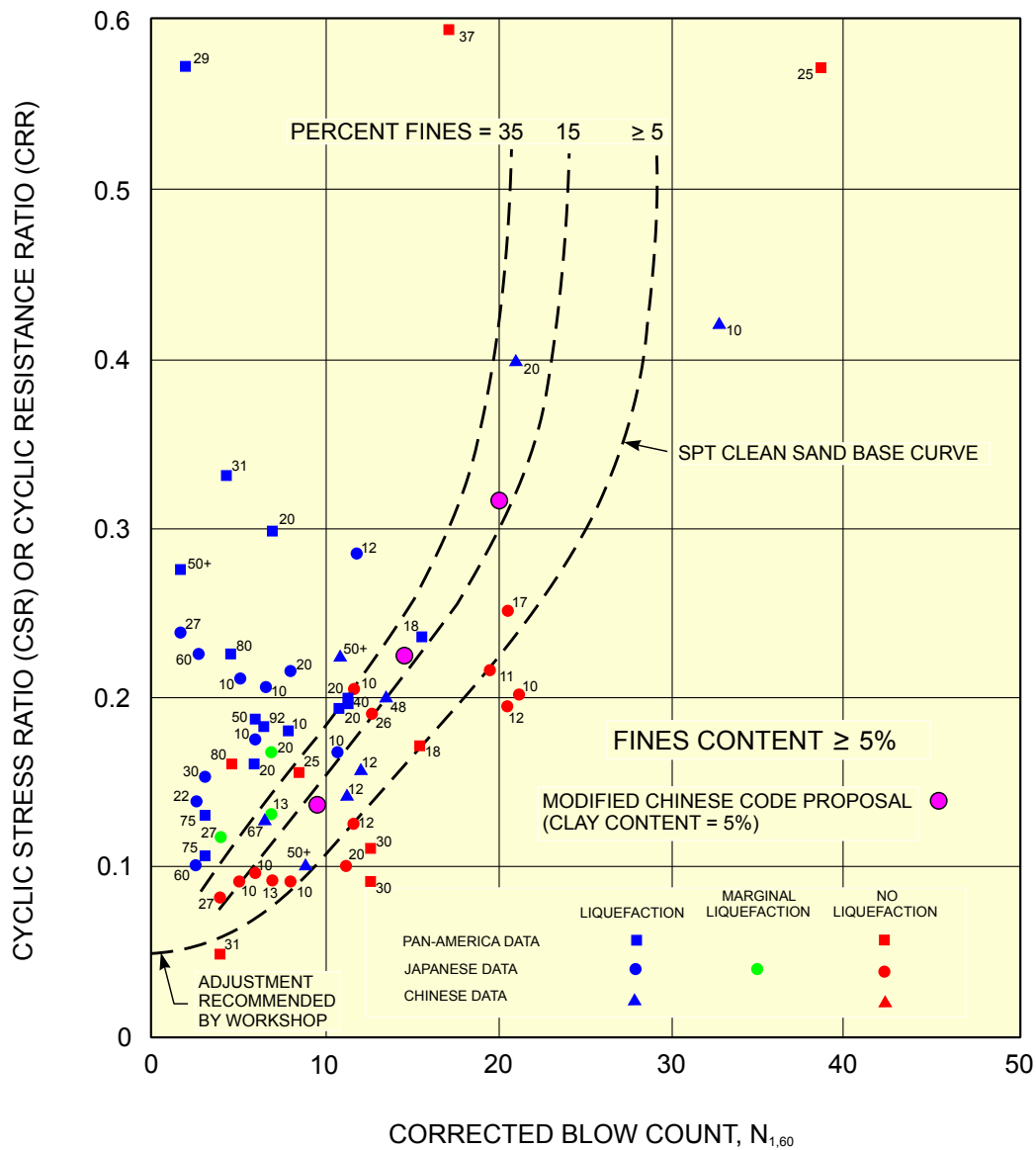
The correction factors are discussed in Youd et al. (2001), which notes that the correction for overburden (C_N) becomes highly uncertain for overburden pressures greater than 3 tsf.

The presence of gravel can interfere with the penetration of the SPT sampler and lead to higher penetration resistances. One way to correct for the presence of gravel in the SPT is to record the hammer blows for every inch of penetration (rather than the standard 6 inches) as proposed by Poulos in the 1970s and described in USBR (1989) and Seed et al. (2003).

- CRR determined from CPT – Robertson and Wride (1998) developed curves of CRR as a function of dimensionless CPT tip resistance ratio q_{t1N} , as shown in Figure 7.6. The figure shows zones where data from case histories suggest that significant pore-pressure increase will occur and zones where significant pore-pressure increase is unlikely to occur. The field CPT tip resistance q_t must be normalized to an overburden pressure of 1 atmosphere (about 1 tsf or 100 kPa) to obtain q_{t1N} and must be corrected to an equivalent clean sand value $q_{t1N(CS)}$. Equations and charts for normalizing q_t and correcting to an equivalent clean sand value are discussed in Youd et al. (2001) and updated by Robertson (2004), which also includes a discussion of using average CPT values in a layer versus using all measured values. An additional correction for thin soil layers can be made, if applicable (Youd et al., 2001). The references by Robertson and Wride (1998) and Youd et al. (2001) use the uncorrected tip resistance q_c whereas, more correctly, it should be q_t . For CPT in clean to silty sands, q_c and q_t are essentially the same and are often used interchangeably.

CPTs have the advantage that they are faster to perform and typically less expensive per test than SPTs, especially in deep, soft or loose deposits, and CPTs provide a continuous, more reliable profile of penetration resistance. CPTs are particularly useful for fine coal refuse. Physical samples of the material where CPTs are conducted should be obtained for purposes of description and laboratory testing.

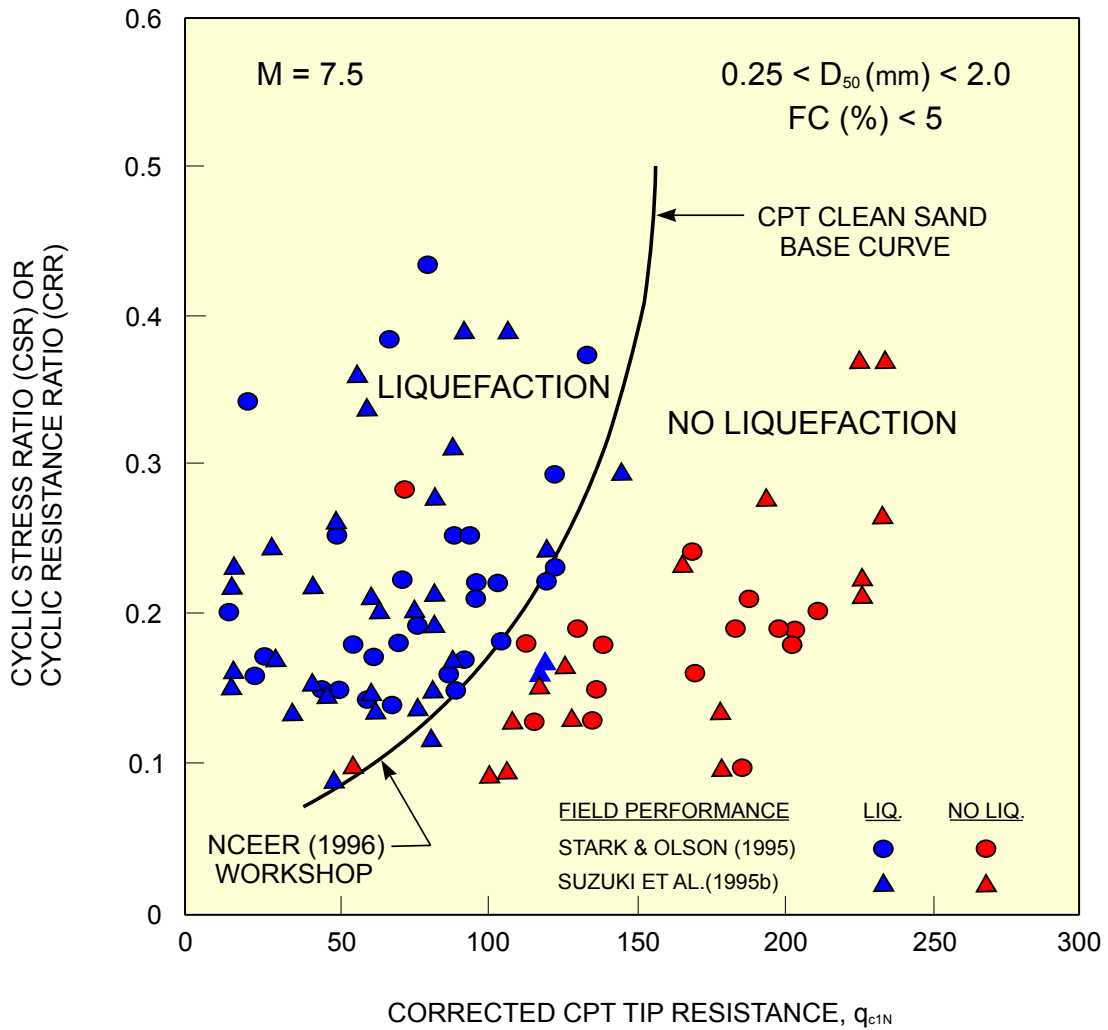
- CRR determined from shear-wave velocity – CRR criteria have been developed from field measurements of shear-wave velocity V_s . Shear-wave velocities can be measured



(ADAPTED FROM YOUND ET AL., 2001)

FIGURE 7.5 SPT CLEAN-SAND-BASED CURVE FOR MAGNITUDE 7.5 EARTHQUAKES WITH DATA FROM LIQUEFACTION CASE HISTORIES

using the seismic CPT (SCPT), crosshole testing, or other downhole or surface wave techniques. Crosshole testing is generally more accurate, but more expensive than seismic CPT. Potential advantages of using the shear-wave velocity are: (1) it is possible to obtain data in soils that are difficult to penetrate with CPT or SPT and (2) the shear wave velocity is directly related to small-strain shear modulus, which is a parameter required for estimating dynamic soil response. As discussed by Youd et al. (2001), concerns with the use of V_s include: (1) shear wave velocity measurements are made at small strains, whereas pore-pressure buildup and strength loss are medium to high strain phenomena and (2) thin, low shear-wave velocity layers may not be detected. V_s data, if obtained, should generally be used in conjunction with data from other methods. The shear-wave velocity obtained from the field should be normalized to a reference overburden pressure of one atmosphere. A recommended chart of CRR as a function of overburden-corrected shear wave velocity is provided in Youd et al. (2001).



(YOU D ET AL., 2001)

FIGURE 7.6 CALCULATION OF CRR FROM CPT DATA ALONG WITH EMPIRICAL LIQUEFACTION DATA FROM COMPILED CASE HISTORIES

7.4.2.2.3 Correction Factors for Earthquake Magnitude, High Overburden, Sloping Ground and Age of Deposit

The curves used to obtain *CRR* from SPT, CPT and V_s only apply to magnitude 7.5 earthquakes. Magnitude scaling factors (MSF) have been developed to adjust the curves to smaller or larger magnitudes. The recommendations by Youd et al. (2001) represent a wide consensus among experts in the field and are preferred at this time unless project-specific factors indicate that other recommendations should be used.

The “simplified” method was developed based on case history data from gently sloping sites (low static shear stress) and depths less than about 50 feet. Correction factors (K_σ and K_α) have been developed for extrapolating the method to higher overburden pressures and steeper slopes (higher static shear stress) than those encountered in the case histories. Youd et al. (2001) caution that using these correction factors requires specialized expertise, because the current bases for selecting specific values of the correction factors are limited. If used, the cyclic resistance ratio becomes:

$$CRR = (CRR_{7.5} \times MSF) K_\sigma K_\alpha \tag{7-5}$$

Recommendations for K_σ are provided in Youd et al. (2001).

Both Youd et al. (2001) and Seed et al. (2003) discuss the wide range of values that have been proposed for K_α and explain that there are no generally agreed upon recommendations. Seed et al. (2003) recommend that the K_α values proposed by Harder and Boulanger (1997) be used where the initial vertical effective overburden pressure is less than 3 tsf. Until a consensus is reached, K_α should be taken as 1.0 unless site-specific information (laboratory test data) indicates otherwise.

It has been noted that older deposits (both older reconstituted laboratory samples and geologically older natural soil deposits) are more resistant to pore-pressure increase. However, verified correction factors have not been developed. Since it is conservative to ignore age corrections, age corrections are not recommended at this time.

7.4.2.3 Strain-Based and Stress-Based Methods to Evaluate Triggering of Strength Loss

7.4.2.3.1 Clay-Like Material: Strain-Based Method for Triggering

Soft, clay-like materials may experience strength loss during an earthquake, but the strength loss is generally not as severe as with sand-like materials (Thiers and Seed, 1968; Castro, 2003; Boulanger and Idriss, 2004). This is because clay-like materials generally reach both peak undrained strength and S_{us} at much higher strains than sand-like materials, except for highly sensitive clays where the strain to peak undrained strength can be small.

Therefore, the term “triggering” can be somewhat misleading for clay-like material. It is more correct to say that the post-earthquake strength for clays is a function of the shear strain that occurs during the earthquake. The post-earthquake strength may be the peak undrained strength or it may be a reduced strength. The post-earthquake strength could be as low as S_{us} in highly sensitive clays, but for most clay-like material the post-earthquake strength will be higher than S_{us} . The reduced strength, while higher than S_{us} , may still be low enough to result in a flow slide.

There are three approaches to estimating the post-earthquake shear strength of clay-like material:

1. Conservatively assume that the post-earthquake strength is equal to S_{us} , and estimate S_{us} from laboratory or field testing, as discussed in [Sections 7.4.3.2.2](#) and [7.4.3.3](#).
2. Estimate the post-earthquake strength as a function of earthquake-induced shear strain, using the following procedure:

- Estimate the accumulated shear strain at points along critical failure surfaces in the embankment during the earthquake. The accumulated shear strains can be estimated using Newmark-type analyses (Section 7.5.4).

Commentary: This step of this method requires that a deformation analysis be performed as part of the evaluation of post-earthquake strength. A design earthquake motion (time history of acceleration) and dynamic soil properties (modulus and damping) are required for this step.

- Obtain a relationship of post-earthquake strength as a function of total strain based on laboratory testing or other correlations as discussed in Section 7.4.3.2.2.
- Use the computed total strains during the earthquake and the relationship of post-earthquake strength versus strain during the earthquake to estimate post-earthquake strength in each zone of clay-like material.

3. Estimate the post-earthquake strength based on the earthquake-induced, cyclic shear stress. This approach involves performing cyclic-undrained, shear-strength testing (that models the earthquake loading) on undisturbed samples of the clay-like material and then loading the samples monotonically to evaluate how much the cyclic loading degraded the peak strength. This method is discussed in more detail in [Section 7.4.3.2.2](#).

7.4.2.3.2 Sand-Like Material: Strain-Based Method for Triggering

The method described in the following text is used for evaluating whether the design earthquake will produce shear strains that are high enough to cause strength loss in a zone of sand-like material.

This method is only appropriate if the safety factor against triggering using the pore-pressure-based method (CRR/CSR) is between 1.0 and 1.4. If the safety factor is higher than 1.4, then triggering may be assumed to not occur. If the safety factor is less than 1.0, then triggering should be assumed. For safety factors between 1.0 and 1.4, the pore-pressure-based method indicates that triggering is likely, but this strain-based method may indicate that triggering will not occur.

As discussed in Section 7.4.1, if the design PGA is larger than 0.2g and the CSR in the loose zone is greater than 0.15, then the triggering analysis described in the following text should not be performed, and triggering of strength loss in the loose zone should simply be assumed. The post-earthquake strength of the material in the loose zone should be assumed to be equal to S_{us} . In evaluating potential measures to improve the stability of a dam or embankment where the CSR in a zone exceeds 0.15, it may be valuable to perform the triggering analysis to help assess whether alternative stabilization schemes that would reduce the CSR might ultimately improve the dam or embankment stability.

The discussion that follows is based primarily on Castro (1994), which should be consulted for further details. The steps in the method are:

1. Select one or more potential failure surfaces through the embankment. Estimate the total seismically-induced shear strain along the critical failure surfaces in the embankment during the earthquake. Failure surfaces that had the lowest safety factors in the post-earthquake stability analysis performed when triggering of loose material was assumed should be selected. The total shear strains include: (1) transient cyclic strains, which can be estimated by a 1D or 2D site-response analysis using SHAKE or QUAD4 and (2) accumulated strains, which can be estimated using Newmark-type analyses ([Section 7.5.4](#)) or numerical modeling ([Section 7.5.5](#)). To be conservative, the total seismically-induced shear strain should be computed by adding the maximum transient cyclic strain to the total accumulated strain.

If numerical modeling is used to estimate accumulated strain, the model output will include shear strains. If a Newmark-type analysis is used to estimate accumulated strains, the analysis will provide displacements. To convert displacements to shear strains, the thickness of the loose zone should be estimated, and the strains should be assumed to be uniform across the full thickness of the zone. In other words, the shear strain will be approximately equal to the displacement divided by the thickness of the zone. A Newmark-type analysis can be used instead of numerical modeling only for cases in which the loose zone is relatively thin compared to the overall failure mass.

Commentary: A design earthquake motion (time history of acceleration) is required for performing the deformation analysis required for this step.

2. The triggering shear strain of sand-like material is approximately equal to the shear strain at peak strength in undrained monotonic (non-cyclic) loading. However, for

the triggering analysis, conservatively assume that the triggering shear strain is equal to one-half the shear strain at peak strength in monotonic, strain-controlled undrained laboratory strength tests. (Shear strain is equal to 1.5 times the axial strain in triaxial tests.)

Perform undrained shear tests on samples consolidated anisotropically to stresses corresponding to the static anisotropic stresses along the potential failure plane through the embankment.

Undisturbed samples should normally not be used for this testing because of concern for densification during sampling, handling, and laboratory consolidation to the point that the samples are not as contractive in the laboratory as the in-situ material. Remolded samples should generally be used, attempting to bracket (after being anisotropically consolidated in the lab) void ratios (more correctly – relative densities) that reflect field conditions. Representative samples from the zone of interest should be mixed to obtain a batch of soil for remolded testing. The samples that are mixed should have similar grain size distribution. (As an example, clean sand material should not be mixed with material containing more than about 20 percent fines). Remolded samples can be prepared by moist tamping in multiple layers or by wet or dry pluviation. Pluviation may not be appropriate for silty samples because of the potential for material segregation by particle size.

Commentary: The strain to peak strength and the triggering strain vary with the degree of anisotropic consolidation. Therefore, to model field conditions, anisotropic consolidation is required for these tests. In contrast, for identical specimens consolidated to the same void ratio, the steady-state (residual) strength S_{us} measured in the laboratory will be the same for isotropically- and anisotropically-consolidated specimens. Therefore, for convenience, S_{us} testing is normally performed on isotropically-consolidated specimens, as discussed in [Section 7.4.3.2.3](#).

The recommendation to estimate the triggering shear strain as being equal to one-half the shear strain at peak undrained strength in a monotonic test is conservative. Being conservative at this step is appropriate because of: (1) the low shear strain required to reach peak undrained strength indicates a high potential for progressive failure and (2) the evaluation of seismically-induced shear strains is highly uncertain.

Instead of performing laboratory strength tests, the shear strain at peak undrained strength could be estimated as a function of the ratio of vertical to horizontal consolidation stress from published data for similar sand-like material (Castro 1994). The triggering shear strain would then be assumed to be equal to one-half the estimated shear strain at peak undrained strength. However, at this time, there is not adequate published data available to rely on, so either: (1) site-specific laboratory testing should be performed or (2) the triggering shear strain of the sand-like material can simply (conservatively) be assumed to be 0.25 percent. This recommended shear strain is a lower bound for the data presented in Castro (1994) for consolidation stress ratios typical of coal refuse impoundments.

3. If the total computed seismically-induced shear strain along the critical failure surface is less than the shear strain needed to trigger strength loss, as estimated from: (1) laboratory testing, (2) comparisons to published data on similar materials, or (3) simply taken as 0.25 percent, then strength loss will not be triggered. Use the peak undrained shear strength (or the drained strength, whichever is lower) in the stability analyses. If the total seismically-induced shear strain is greater than the triggering shear strain, use S_{us} in the stability analyses.

7.4.2.3.3 Sand-Like Material: Stress-Based Method for Triggering

This method is used to evaluate whether the design earthquake will produce shear stresses in a zone of sand-like material that are high enough to cause strength loss in that zone. The basic concept of the method is that strength loss will be triggered by earthquake shaking if the sum of the static (gravity) shear stresses along a potential failure surface plus the seismic shear stresses exceed the yield (peak) undrained strength $S_u(\text{yield})$.

This stress-based method for triggering is only appropriate if the safety factor (CRR/CSR) against triggering determined from the pore-pressure-based method is between 1.0 and 1.4. If the safety factor is greater than 1.4, then triggering can be assumed to not occur. If the safety factor is less than 1.0, then it should be assumed that triggering will occur. For safety factors between 1.0 and 1.4, the pore-pressure-based method indicates that triggering is likely, but this stress-based method may indicate that triggering will not occur.

As discussed in Section 7.4.1, if the design PGA is greater than 0.2g and the CSR is greater than 0.15, then the triggering analysis described in the following text should not be performed, and strength loss for loose sand-like material should simply be assumed. The post-earthquake strength of the material in the loose zone should be assumed equal to S_{us} . If evaluating potential measures to improve the stability of a dam or embankment where the CSR in a zone exceeds 0.15, it may be valuable to perform the triggering analysis to help assess whether alternative stabilization schemes that would reduce the CSR might ultimately improve the dam or embankment stability.

The methodology described in the following steps is based primarily on Olson and Stark (2003), which should be consulted for further details. The steps are:

1. Perform a slope stability analysis to estimate the static shear stress $\tau_{driving}$ in the loose zone of sand-like material. This is accomplished by varying the assumed undrained strength of the material in the zone until a safety factor of one is achieved. For denser soils, the peak drained or undrained strength should be used, as discussed in Section 7.4.4.3.
2. Divide the critical failure surface into 10 to 15 segments.
3. Compute the weighted average σ'_{vo} along the failure surface and calculate the average static shear stress ratio $\tau_{driving}/\sigma'_{vo}$.
4. Estimate the average seismic shear stress $\tau_{av, seismic}$ applied to each segment of the failure surface using a 1D or 2D site response analysis as provided by SHAKE or QUAD4. The value of $\tau_{av, seismic}$ for each segment of the failure surface can be taken as 0.65 times τ_{max} obtained from the site response analysis.
5. Estimate the value of $S_u(\text{yield})/\sigma'_{vo}$ from CPT or SPT data using the proposed equations in Olson and Stark (2003). The equations give a range of ratios based on SPT or CPT data. The median value of SPT or CPT data should be used for each zone, and the lower bound of Olson and Stark's equation should be used to compute the ratio of $S_u(\text{yield})/\sigma'_{vo}$.

Commentary: The equations are based on back-calculations of yield (peak) undrained strength from failure case histories where the failures were triggered by static, not seismic, loading. Therefore, the back-calculated strengths represent yield (peak) undrained strengths.

6. Compute values of $S_u(\text{yield})$ and $\tau_{driving}$ for each segment along the failure surface, based on the values of $S_u(\text{yield})/\sigma'_{vo}$ and $\tau_{driving}/\sigma'_{vo}$ (average) and the value of σ'_{vo} for each segment.

7. Compute the factor of safety against triggering for each segment as:

$$FS_{triggering} = S_{u(yield)} / (\tau_{driving} + \tau_{av, seismic}) \quad (7-6)$$

8. Assume that triggering of strength loss occurs for segments where $FS_{triggering}$ is less than or equal to 1.0. Assume that triggering of strength loss does not occur for segments where $FS_{triggering}$ is greater than 1.0.

7.4.3 Evaluation of Post-Earthquake Strength

7.4.3.1 Correlations of SPT and CPT with S_{us} of Sand-Like Material

Loose, sand-like refuse and sand-like natural soil may experience significant strength loss due to earthquake shaking, if the shaking is strong enough. The reduced strength is the undrained steady-state (residual) strength S_{usr} , which is often much lower than the peak undrained strength or the peak drained strength. Table 7.2 presents references for several correlations of S_{us} with SPT data ($N_{1,60}$) and CPT data (q_{t1}) for sand-like material.

The correlations are based on back-calculated values of S_{us} from actual flow slides and measured or estimated values of $N_{1,60}$ or q_{t1} . The correlations are generally limited to $N_{1,60}$ values (uncorrected for fines) less than about 12 or q_{t1} less than about 75 tsf because no flow slides have been reported for soils with higher penetration resistances. For higher values of $N_{1,60}$ and q_{t1} , the drained strength should be used because, as discussed in Section 7.4.4.2, the material is dilative.

The Seed and Harder (1990) plot (Figure 7.7) is probably the most well known of the S_{us} versus SPT or CPT correlations. The plot is an update of an earlier plot presented in Seed (1987). The 1990 plot includes a correction to increase $N_{1,60}$ values for silty materials to “equivalent clean sand” $N_{1,60(CS)}$ values. The correction varies from 1 to 5 blows per foot depending on the percent fines. However, no basis for this correction is provided in either the 1990 or 1987 paper.

TABLE 7.2 REFERENCES FOR CORRELATIONS OF S_{US} WITH SPT AND CPT DATA

Reference	Correlated Parameters
Seed (1987)	S_{us} vs. $N_{1,60}$
Davis, Castro and Poulos (1988)	S_{us} vs. $N_{1,60}$
Seed and Harder (1990)	S_{us} vs. $N_{1,60}$
Baziar and Dobry (1995)	S_{us} and S_{us}/σ'_v vs. $N_{1,60}$
Castro (1995)	S_{us} vs. $N_{1,60}$
Wride, McRoberts and Robertson (1999)	S_{us} and S_{us}/σ'_v vs. $N_{1,60}$
Yoshimine, Robertson and Wride (1999)	S_{us}/σ'_v vs. $q_{c1N(CS)}$
Olson and Stark (2002)	S_{us}/σ'_v vs. $N_{1,60}$ and q_{t1}
Idriss and Boulanger (2007)	S_{us} and S_{us}/σ'_v vs. $N_{1,60}$ and $q_{c1N(CS)}$

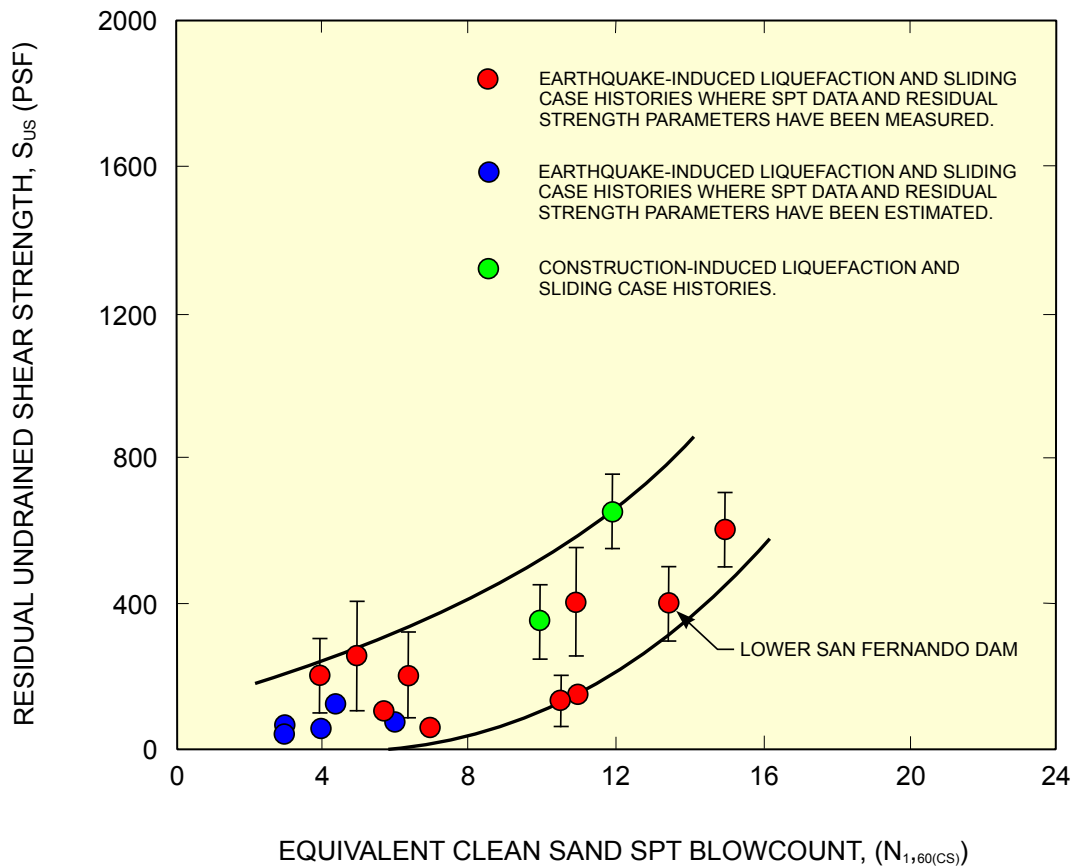
Note: S_{us} = Undrained steady state (residual) strength.

$N_{1,60}$ = Standard Penetration Test (SPT) N-value, normalized to an effective overburden stress of one atmosphere (typically 1 tsf) and normalized to a hammer efficiency of 60 percent.

S_{us}/σ'_v = Undrained steady state strength normalized to vertical effective stress.

$q_{c1N(CS)}$ = Cone Penetration Test (CPT) tip resistance normalized to a reference pressure of one atmosphere and corrected to an equivalent value for clean sand.

q_{t1} = CPT tip resistance normalized to an effective overburden stress of one atmosphere.



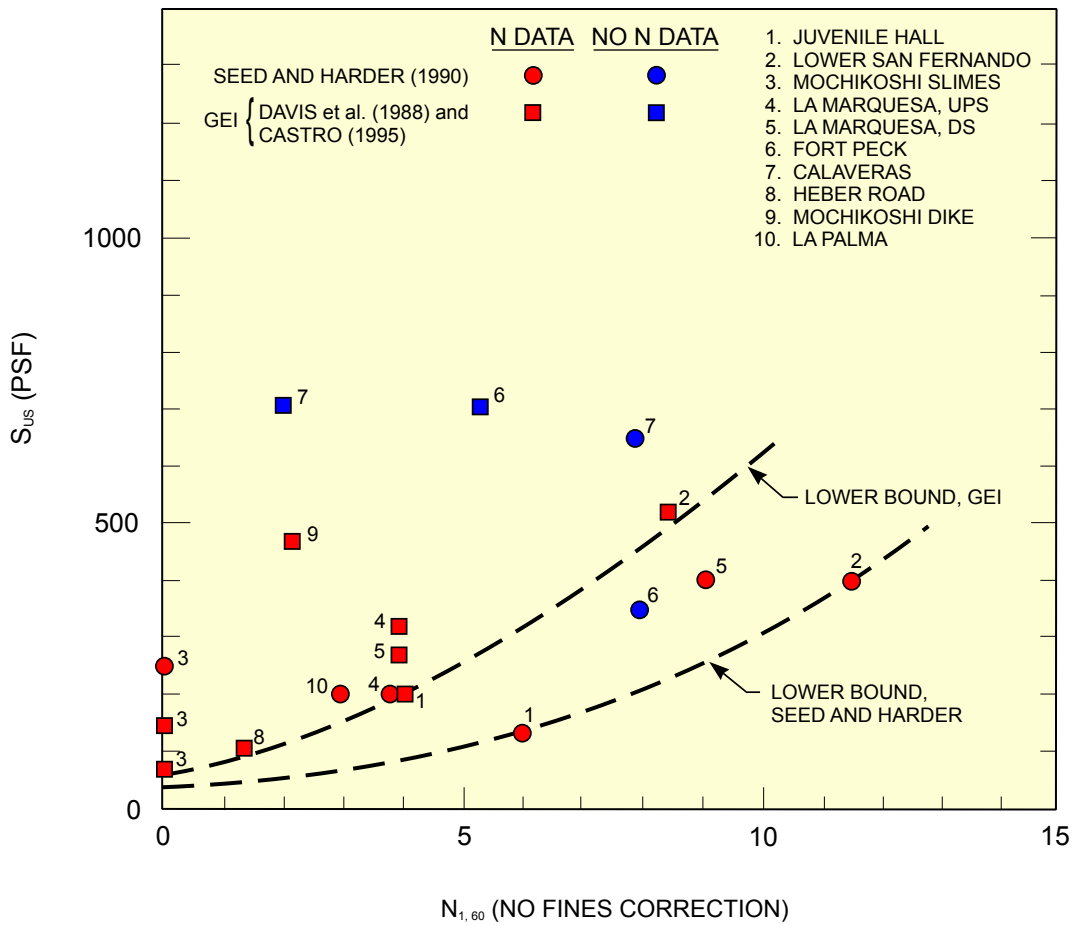
(ADAPTED FROM SEED AND HARDER, 1990)

FIGURE 7.7 S_{us} versus $N_{1,60(CS)}$

Castro (1995) re-evaluated several of the case histories in Seed and Harder (1990) for which detailed data were available. He also collected re-evaluations of some of the earlier case histories performed by Poulos (1988) and Davis et al. (1988). He referred to the re-evaluations collectively as the GEI data. Castro then replotted the Seed and Harder data points (without a fines correction) and compared them to the GEI data points. The resulting plot of representative $N_{1,60}$ values and back-figured S_{us} is shown in Figure 7.8. The original Seed and Harder (1990) lower-bound curve is somewhat lower than the Seed and Harder lower-bound curve shown in Castro (1995) because the original Seed and Harder curve included a fines correction while the Seed and Harder curve shown in Castro (1995) did not.

Correlations of S_{us}/σ'_v versus SPT and CPT data, back-calculated from case histories, are listed in Table 7.3. Olson and Stark (2002) re-evaluated the Seed and Harder (1990) data and added new case histories for development of plots of S_{us}/σ'_v versus both $N_{1,60}$ and q_{t1} . Olson and Stark did not include a fines correction to the $N_{1,60}$ values as Seed and Harder did. Olson and Stark's plot of S_{us}/σ'_v versus q_{t1} is shown as Figure 7.9. A reasonable lower bound of the Olson and Stark data is a ratio of S_{us}/σ'_v equal to 0.04, which is independent of SPT or CPT value.

Idriss and Boulanger (2007) re-evaluated the Seed and Harder case histories and the Olson and Stark case histories, and included the fines correction to the $N_{1,60}$ values as Seed and Harder did. Idriss and Boulanger recommended design curves for both S_{us} versus $N_{1,60(CS)}$ and S_{us}/σ'_v versus $N_{1,60(CS)}$. Idriss and Boulanger's design curve for S_{us} versus $N_{1,60(CS)}$ is in between the upper and lower bounds suggested by Seed and Harder in Figure 7.7.

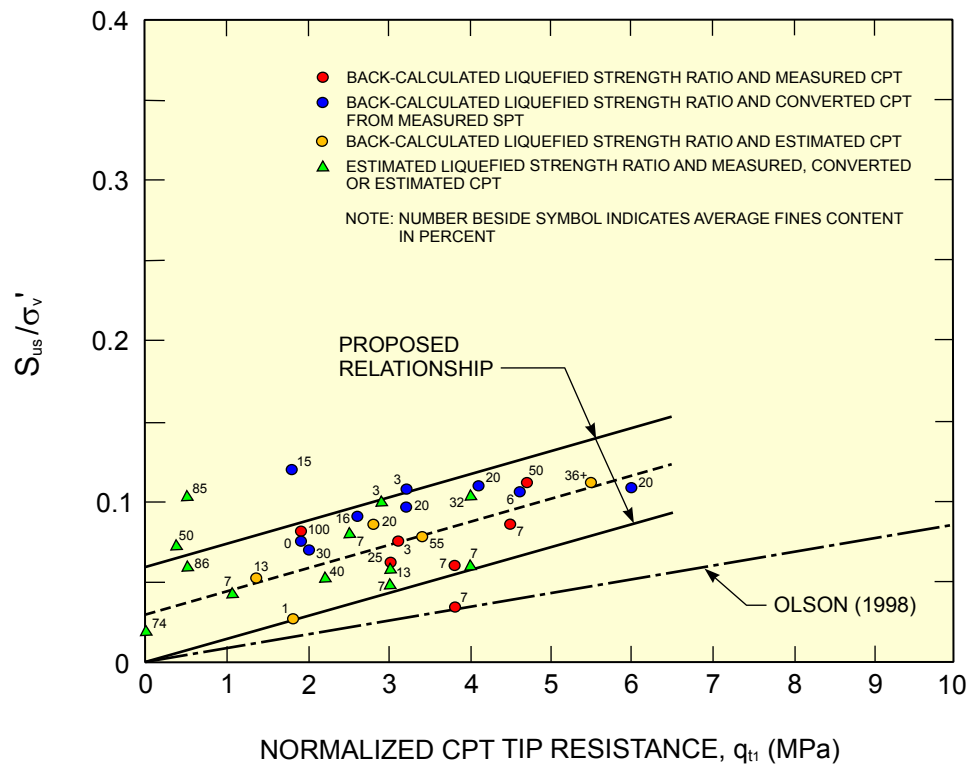


(CASTRO, 1995)

FIGURE 7.8 S_{us} versus $N_{1,60}$

TABLE 7.3 CORRELATIONS OF S_{US}/Σ'_V VERSUS SPT AND CPT DATA BACK-CALCULATED FROM CASE HISTORIES

Reference	Reported S_{us}/σ'_v	Types of Data and Materials
Baziar and Dobry (1995)	0.04 to 0.20	Back-calculated values from failure case histories for 9 sites with silty sand or sandy silt material (more than 10 percent fines). One of the 9 sites was identified as a tailings dam.
Yoshimine, Robertson and Wride (1999)	0.03 to 0.19	Back-calculated values from case histories involving multiple submarine slides at 3 sites. Materials were natural clean sand, silty sand, and sandy silt.
Olson and Stark (2002)	0.05 to 0.12 (proposed limits of ratios)	Back-calculated values from 33 failure case histories, including re-evaluation of the Baziar and Dobry sites. Four of the 33 sites were identified as tailings dams as compared to dams or slopes consisting of natural soils. Four of the 33 sites, including one of the tailings dam sites, had ratios of 0.02 to 0.04, outside their proposed boundary.
Idriss and Boulanger (2007)	0.05 to 0.22	Back-calculated values based on select case histories published by Seed (1987), Seed and Harder (1990), and Olson and Stark (2002) with adequate amount of in-situ measurements and reasonably complete geometric details (7 of the 35 case histories reviewed).



(ADAPTED FROM OLSON AND STARK, 2002)

FIGURE 7.9 S_{us}/σ'_v versus q_{t1}

Idriss and Boulanger's design curve for S_{us}/σ'_v versus $N_{1,60(CS)}$ is very close to the best fit line suggested by Olson and Stark in the range where $N_{1,60(CS)}$ is less than about 14. For $N_{1,60(CS)}$ values higher than about 12 to 14, which is beyond the range of the case history data, Idriss and Boulanger suggest two curves: one for the case where "void ratio redistribution effects" are negligible, and one for the case where void ratio redistribution effects may be significant. The difference between these two curves is discussed in the following commentary.

Commentary (Use of S_{us}/σ'_v Ratios): Using the ratios of S_{us}/σ'_v for confining pressures significantly higher than the confining pressures from the actual case histories may be unconservative. Twenty-eight of Olson and Stark's 33 case histories had mean σ'_v of 115 kPa or less. This corresponds to mean σ'_v of up to 2,400 psf or, for an assumed effective unit weight of 55 pcf, a mean depth of up to 45 feet. Using S_{us}/σ'_v ratios implies that increasing the confining pressure by a factor of 5, for example, would also increase S_{us} by a factor of 5. But laboratory testing has shown that the slope of the void ratio versus $\log S_{us}$ line is often steeper than the slope of the void ratio versus $\log \sigma'_v$ line. In other words, increasing the confining pressure by a factor of 5 often results in increasing S_{us} by a factor less than 5. So using the S_{us}/σ'_v ratios for high confining pressures may be unconservative. Therefore, recommended guidance is to consider only the lower-bound ratio of 0.04. The lower-bound ratio of $0.04 \sigma'_v$ is considered conservative enough that it is acceptable even at high confining pressures.

The lower bound ratio of 0.04 is applicable to non-plastic materials and to materials with a liquidity index (LI) of less than one. Materials with $LI > 1$ are unusual, but may have even lower values of S_{us} . At this time, the recommended lower bound value of S_{us} for soils with $LI > 1$ is 20 psf, but no higher than obtained with a strength ratio of 0.04, based on the judgment of the authors of this chapter.

The correlations of S_{us} with $N_{1,60}$ have uncertainty at high confining pressures because the correction factors used to correct N to N_1 to account for increasing confining pressure are highly uncertain at confining stresses

higher than about 2 tsf (Youd et al., 2001). However, the uncertainty of applying the S_{us} versus $N_{1,60}$ correlations at high confining stresses is less than the uncertainty of applying the correlations of SPT or CPT with S_{us}/σ'_v ratios.

Commentary (Void Ratio Redistribution): The phenomenon of void ratio redistribution is discussed in Section 7.4.5. It refers to the possibility that if a loose zone of sand-like material is overlain by an impervious zone, then earthquake shaking may cause pore water to migrate toward the interface of the two materials, which could result in the sand-like material becoming looser and therefore having a lower steady-state strength. There are no generally accepted methods for evaluating the potential for this to occur, and there is some controversy as to whether it actually occurs in the field at all.

The Idriss and Boulanger (2007) design curve for S_{us}/σ'_v versus $N_{1,60(CS)}$ splits at values of $N_{1,60(CS)}$ higher than about 12 to 14. For the case where void ratio redistribution effects are negligible, S_{us}/σ'_v increases rapidly as $N_{1,60(CS)}$ increases above 12 to 14. This is consistent with the fact that sand-like material with $N_{1,60(CS)}$ values higher than 12 to 14 tend to be dilative and not susceptible to strength loss (as discussed in more detail in Section 7.4.4.2.1). For the case where void ratio redistribution effects may be significant, S_{us}/σ'_v increases less quickly as $N_{1,60(CS)}$ increases. As Idriss and Boulanger explain, the curve for this case is largely conceptual, since there are no case history data at these $N_{1,60}$ values.

For the purposes of this Manual, and as discussed further in Section 7.4.5, specific evaluations for potential void-ratio redistribution effects are not required. As discussed in Section 7.4.4.3, the post-earthquake strength of sand-like material with $N_{1,60}$ greater than or equal to 15 may be based on the drained strength and not on correlations of S_{us} or S_{us}/σ'_v to $N_{1,60}$. However, if redistribution is a concern, the corresponding Idriss and Boulanger curve can be used.

For estimating S_{us} values of sand-like materials based on correlations to SPT and CPT data, the following three-step procedure is recommended:

1. For each zone of material, determine a representative value of $N_{1,60}$. In general, the representative value should be the median value. For this step, CPT data can be converted to $N_{1,60}$ using the relationships discussed in Section 6.4.3.7 (Lunne et al., 1997).
2. Use either the “Lower-Bound, GEI” curve or the “Lower-Bound, Seed and Harder” curve from the Castro (1995) plot (Figure 7.8) to obtain S_{us} as a function of representative value of $N_{1,60}$. Both curves can be extrapolated to values of $N_{1,60}$ as high as 14 by extending the curves along approximately straight lines. As discussed in Section 7.4.4.3, drained strength, rather than S_{us} , can be used for $N_{1,60}$ values of 15 or higher.
3. For each zone, if the resulting value of S_{us} is less than $0.04 \sigma'_v$, use $S_{us} = 0.04 \sigma'_v$ instead.

Commentary: As discussed in Section 7.4.1, S_{us} of sand-like material is very sensitive to small changes in void ratio. CPTs and SPTs are not sensitive to small changes in void ratio, and therefore correlations of CPT and SPT to S_{us} are expected to have large scatter, as shown in Figures 7.7, 7.8, and 7.9. The S_{us} versus SPT or CPT correlations provide conservative estimates of S_{us} . Generally S_{us} is not directly related to either $N_{1,60}$ or q_{t1} . The case histories used in these correlations are cases where S_{us} was low enough that a flow slide or significant deformations occurred. However, there were almost certainly other sites where $N_{1,60}$ or q_{t1} were similar, but flow slides or significant deformations did not occur because S_{us} was higher than obtained from the failure case histories. Cases where stability failure did not occur could provide lower-bound estimates of S_{us} (i.e., the minimum value of S_{us} needed to maintain stability), but these cases are not typically studied and would still provide only conservative estimates. Laboratory testing methods for estimating S_{us} may provide less conservative estimates of S_{us} .

7.4.3.2 Laboratory Testing for Measuring Post-Earthquake Strength for Clay-Like Material and S_{us} for Sand-Like Material

7.4.3.2.1 Laboratory Testing Issues

Soil fabric has been shown in the literature to affect the peak undrained strength of sand-like material. This often results in different peak undrained strengths for undisturbed samples versus reconstituted samples. However, initial soil fabric should not affect S_{us} , because S_{us} is measured at high strains after the soil fabric has become remolded. An example of this is presented in Castro, Seed, Keller, and Seed (1992). Samples of hydraulic sand fill prepared from slurry and by moist tamping had the same steady-state line.

There is extensive published research that shows that, for peak-undrained strength of clayey soils: S_u (triaxial compression) $>$ S_u (direct simple shear) $>$ S_u (triaxial extension). However, there are no data to suggest whether or not steady-state (residual) strength S_{us} varies with test type. The difficulty is that test methods other than triaxial compression can not generally be run to high enough strain levels to reach S_{us} before non-uniformities in the specimen become so large that the test data lose meaning. Triaxial extension tests experience necking at relatively low strains. Direct simple shear tests have significant stress non-uniformities (at all strains) because there are no vertical shear stresses (and therefore no horizontal shear stresses) at the outside edges of the specimen. Investigators who have tried to evaluate the effect of test type on measured S_{us} of sand-like material have encountered these difficulties, which make it difficult to identify S_{us} on stress-strain curves from tests other than triaxial compression.

It is reasonable that the peak strength varies with test type, because the peak strength is very much dependent on soil structure and therefore on the method of loading. For S_{us} , however, the initial soil structure has been lost (remolded) due to the high strain, so the method of loading should not be as significant. While there might be a difference in S_{us} for sand-like material related to the fact that the intermediate principal stress varies depending on the test type, this difference will be small compared to the variation in steady-state strength that one should expect for different samples from the same layer or zone of material. Expected in-situ strength variation was previously discussed in [Section 7.4.1](#).

For most clay-like material, S_{us} is such a conservative estimate of post-earthquake strength that minor differences that may or may not be a function of test type do not seem significant. In any event, the S_{us} value for clay-like soils cannot be measured using triaxial (compression or extension) or direct simple-shear tests, because the strain to S_{us} is so high. Testing of clay-like material to estimate post-earthquake strengths that are closer to S_{up} involves using cyclic loading followed by static loading, as discussed in [Section 7.4.3.2.2](#). For this testing procedure, differences in strength between triaxial compression and other test types should be small compared to the variation in strength one should expect for different samples from the same layer. However, one could, if desired, use direct simple-shear testing or correct the triaxial test strengths to equivalent direct simple-shear strengths using the information in Article 20 of Terzaghi, Peck, and Mesri (1996).

Based on the preceding discussion, the use of triaxial compression testing to estimate S_{us} for sand-like material, and to estimate post-earthquake strength for clay-like material, as discussed in Sections 7.4.3.2.2 and 7.4.3.2.3, is reasonable.

7.4.3.2.2 Laboratory Testing of Soft Clay-like Material to Measure Post-Earthquake Strength

As discussed in [Section 7.4.2.3.1](#), the post-earthquake strength for clay-like material is a function of the shear strains that occur during the earthquake. The post-earthquake strength may be the peak undrained strength S_{up} or it may be a reduced strength. The post-earthquake strength could possibly (but not likely) be as low as S_{us} .

A conservative estimate of post-earthquake strength for soft clay-like materials is to use S_{us} , which can be obtained by performing field vane-shear tests and/or CPTs, as described in [Section 7.4.3.3](#). A less conservative estimate can be obtained by performing laboratory testing to obtain an undrained strength that is appropriate based on considerations of accumulated strain and/or cyclic stress level. As discussed in [Section 7.4.4.3](#), the post-earthquake strength of stiff clay-like material can be taken as the peak-undrained strength.

If laboratory testing is performed, strain-controlled, undrained-triaxial (or perhaps undrained direct simple-shear) tests should be performed to measure: (1) the peak undrained strength, (2) the shear strain to peak undrained strength, and (3) the drop-off in shearing resistance with continued strain after peak. It should be remembered that shear strain in the triaxial test is 1.5 times the axial strain and that peak strength refers to the peak principal stress difference. Test specimens should be consolidated anisotropically to stresses that model in-situ conditions.

If the shear strain at peak strength is less than about 5 percent, or if the shearing resistance drops off significantly after peak, then either: (1) measure S_{us} (in the laboratory or the field) and use it as a conservative estimate of post-earthquake strength, (2) perform a series of laboratory tests with cyclic loading followed by monotonic loading to obtain a less conservative estimate of post-earthquake strength based on the strain that occurs during cyclic loading, or (3) perform a series of laboratory tests with cyclic loading followed by monotonic loading to obtain a less conservative estimate of post-earthquake strength based on the cyclic stress levels applied by the design earthquake. Details for these options are discussed in the following text. Note that the number of loading cycles in the cyclic loading sequence must be appropriate compared to the number of representative loading cycles associated with the design earthquake magnitude. Seed and Idriss (1982) correlated the number of representative loading cycles with earthquake magnitude (e.g., $M = 6.5$, $N = 10$; $M = 7.5$, $N = 15$; and $M = 8.5$, $N = 26$, where M is earthquake magnitude and N is the number of representative loading cycles).

If the shear strain at peak strength is more than 5 percent, and there is little drop-off in shearing resistance after peak, then options (1), (2), and (3) discussed in the preceding paragraph can be used. However, a simplified version of option (2) can also be used. If the seismically-induced shear strains, as described in Step 2a, are less than one-half the shear strain to peak strength in the monotonic (static) test, then the post-earthquake undrained strength can be assumed to be equal to the peak undrained strength S_{up} . This is based on previous testing of clay-like materials (Thiers and Seed, 1968; Castro and Christian, 1976; Castro, 2003).

The three options for evaluating the post-earthquake strength of clay-like material are:

1. Conservatively assume that the post-earthquake strength is S_{us} and measure S_{us} . To measure S_{us} in the field, CPT or field vane tests can be used, as discussed in [Section 7.4.3.3](#). To measure S_{us} in the laboratory, vane-shear tests can be used. The strain rate should be high to ensure that the sample is being sheared undrained and that the undrained S_{us} is being measured (see discussion of field vane-shear rates in [Section 6.4.3.8](#)). S_{us} cannot normally be reached for clay-like material (except highly sensitive clays) within the strain limitations of laboratory tests, other than possibly rotation shear. Since it is unlikely that the post-earthquake strength will be reduced to S_{us} except in highly sensitive clays, laboratory testing to measure S_{us} of clay-like material may not be needed in practice.
2. Measure the relationship between cyclic strain and post-earthquake strength. Anisotropically-consolidated, undrained-triaxial tests (or perhaps undrained, direct simple-shear tests, also consolidated with an initial shear stress), with cyclic loading followed by monotonic loading, can be used to obtain the relationship between accumulated shear strain during the earthquake and post-earthquake, undrained

strength. Accumulated strain is a measure of the effects of cyclic loading on the post-earthquake strength of clay-like material. After low accumulated strains, the post-earthquake strength will be close to the peak-undrained strength. After very high accumulated strains, the post-earthquake strength may be close to S_{us} . Instead of accumulated strain, peak strain could also be used as a measure of the effects of cyclic loading. However, the use of accumulated strains is recommended. A procedure for performing this type of testing is described in Castro (2003). The basic steps are:

- a. Select one or more potential failure surfaces through the embankment. Estimate the accumulated strains that develop due to earthquake shaking using either Newmark-type analyses (Section 7.5.4) or numerical modeling (Section 7.5.5). If numerical modeling is used to estimate accumulated strains, the model output will include shear strains. If a Newmark-type analysis is used to estimate accumulated strains, the analysis will compute displacements. To convert displacements to shear strains, the thickness of the loose zone must be estimated, and the strains should be assumed to be uniform across the full thickness of the zone. In other words, the accumulated shear strain will equal the displacement divided by the thickness of the zone. (A Newmark-type analysis can be used instead of numerical modeling only for cases in which the loose zone is relatively thin compared to the overall failure mass. CPT data are probably the best way of delineating the thickness of the loose zone. Another way to delineate the thickness of the loose zone, so that shear strain can be computed from displacement, is to identify the range of potential failure surfaces for which the safety factor is within perhaps 10 percent of the safety factor of the most critical failure surface. The thickness of the range of failure surfaces can be taken as the thickness of the loose zone.

Commentary: A design earthquake motion (time history of acceleration) and dynamic soil properties (modulus and damping) are required for performing the deformation analysis required for this step.

- b. Perform a series of tests on undisturbed specimens consolidated anisotropically to in-situ stresses. First apply cyclic stresses to each specimen, and measure the accumulated strains. Then, without allowing for dissipation of the pore pressures generated by the cyclic loading, apply monotonic loading to each specimen to measure the peak strength. Perform tests at various cyclic stresses to bracket the accumulated strains indicated by the deformation analysis. The cyclic loading portion of the test should be load-controlled, and the monotonic loading portion of the test should be strain-controlled.
- c. Plot the value of peak undrained strength under monotonic loading versus the accumulated strain during loading. There should be a trend of constant monotonic peak strength for small accumulated strains and then decreasing monotonic strength for higher accumulated strains. (In the example in Castro (2003), post-earthquake strength was plotted against maximum cyclic strain instead of accumulated strain, but the concept is the same. The monotonic strength began to decrease for cyclic shear strains exceeding about 7.5 percent.)
- d. Select the post-earthquake strength as the value of monotonic strength that corresponds to the estimated accumulated shear strain from the de-

formation analysis. For clay-like materials, 80 to 100 percent of the peak-undrained strength should be used, as discussed in [Section 7.4.4.3](#).

3. Measure the effect of cyclic loading on post-earthquake strength – This approach involves performing cyclic undrained shear strength testing on undisturbed samples of the clay-like material, which are consolidated anisotropically to stresses that model the more critical in-situ conditions (i.e., higher anisotropic stress ratio for materials along the critical potential failure zone). The samples should be cyclically loaded for a conservative number (not less than 20) of cycles, while bracketing a conservative range of cyclic stress or *CSR* based on the design earthquake. (Cyclic stress or *CSR* for the design earthquake can be obtained from 1D or 2D site response analyses, as described in [Section 7.4.2.2.1](#), Method 1.) The samples should then be subject to undrained monotonic loading to measure the range in post-cycling S_u for the range of *CSR*.

The intent is to test clay-like samples at the higher end of the in-situ anisotropic stress ratio, to a conservative number of cycles (not less than 20 cycles) of loading and a conservative range of *CSR*, not to obtain a unique relationship between cyclic loading and S_u , but only to bracket a post-earthquake S_u (often higher than S_{us}) that can be applied in post-earthquake limit equilibrium analyses. This approach might be helpful in instances where undrained triaxial or direct simple-shear monotonic tests indicate a shear strain at peak strength somewhat less than 5 percent, but the post-peak drop-off in shearing resistance is not dramatic or particularly significant. It may also be helpful when such testing indicates a shear strain at peak strength greater than 5 percent, but the post-peak behavior and/or the perceived sensitivity of the clay-like material warrants more direct evaluation of the undrained strength behavior following cyclic loading.

For material that is clay-like, or that borders between sand-like and clay-like behavior, laboratory testing of undisturbed samples of the site-specific materials, as described above, should be considered. The laboratory testing might be monotonic testing to obtain just S_{up} and strain to S_{up} , or (for critical structures) cyclic loading followed by monotonic testing to obtain the relationship between seismically-induced shear strain and post-earthquake strength. If quality undisturbed samples of site-specific materials can not practically be obtained, then testing of carefully reconstituted samples of the site-specific materials should be considered. However, data from reconstituted samples should only be used if they can be compared to data from at least some undisturbed samples or a thorough base of in-situ and laboratory test data, to confirm that the reconstituted samples are representative of and/or bracket in-situ conditions.

For proposed new facilities, where material for testing is not available, undisturbed or carefully reconstituted samples of similar materials from other facilities can be used. Once a significant base of testing of fine coal refuse is built up, then it may be possible to estimate strength reduction based on correlations with previous testing. Provisions should be made to confirm soil properties of proposed facilities by performing testing as the facility is constructed.

7.4.3.2.3 Laboratory Testing of Sand-like Material to Measure S_{us}

In loose sand-like material, if the earthquake shaking triggers strength loss, then the post-earthquake strength will be equal to the undrained steady state (residual) strengths S_{us} . Estimates of S_{us} for sand-like material should first be made based on correlations with SPT and/or CPT data, as discussed in [Section 7.4.3.1](#). If desired, laboratory testing to measure S_{us} can also be performed. Laboratory testing, while complex, often results in less conservative estimates of S_{us} than the SPT and CPT correlations. If laboratory testing to measure S_{us} is planned, the designer should make the parties responsible for obtaining, transporting, and testing the samples fully aware of the methods to be followed. For example, since S_{us} is highly sensitive to void ratio, high quality undisturbed samples are required and changes in void ratio must be tracked during material sampling, trans-

portation, and testing. Failure to follow the testing guidance may bring laboratory measured values of S_{us} into question. The designer should consider discussing the approach and methods with MSHA prior to initiating sampling and testing.

The discussion that follows is based primarily on Poulos, Castro, and France (1985), which should be consulted for further details. In addition, Castro, Seed, Keller, and Seed (1992) discuss application of this laboratory testing method to the 1971 slide at the Lower San Fernando Dam. Additional information is provided in [Appendices 7A, 7B, and 7C](#) of this Manual.

At this time, an upper bound is recommended for the values of undrained steady state (residual) strength S_{us} obtained from laboratory testing of sand-like material. That upper bound is an envelope based on the median $N_{1,60}$ value of the loose layer being tested, as indicated in [Table 7.4](#). The purpose of the upper bound is to make sure that unreasonably high values of S_{us} based on laboratory testing of sand-like material are not proposed.

TABLE 7.4 UPPER-BOUND VALUES OF S_{US} FOR CORRESPONDING VALUES OF $N_{1,60}$

$N_{1,60}$	Maximum Allowable Value of S_{us} Based on Laboratory Testing
0	200 psf
5	500 psf
10	1100 psf
14	1700 psf

Some basic concepts associated with laboratory testing for measuring S_{us} of sand-like material are:

1. The undrained steady state (residual) strength S_{us} is equal to the undrained strength at high strains, after the initial structure or fabric of the material has been fully remolded.
2. S_{us} is very sensitive to void ratio and to minor changes in grain-size distribution. As discussed in [Section 7.4.1](#), deposits of sand-like material have inherent variations in both. Therefore, multiple samples from the same layer or zone are expected to have varying values of S_{us} .
3. Strain-controlled, undrained triaxial compression tests with pore-pressure measurement are typically used. Experience has shown that isotropic and anisotropic consolidation in the triaxial cell yield the same values of S_{us} . Figure 9 in Castro et al., (1992) provides a good example. Isotropic consolidation is commonly used for simplicity.
4. At strains beyond about 20 percent in the triaxial test, non-uniformities in specimen stress and strain become significant.
5. S_{us} is obtained from the triaxial test, as shown in the following. Note that these equations are derived from the Mohr-Coulomb failure envelope in [Appendix 7A](#).

$$q_s = (\sigma_{1s} - \sigma_{3s})/2, \text{ where } q_s \text{ is one-half the principal stress difference at steady state}$$

$$\sin \phi'_s = q_s / (\sigma'_{3s} + q_s), \text{ where } \phi'_s \text{ is the effective stress friction angle at steady state}$$

$$S_{us} = q_s \cos \phi'_s$$

6. For different samples of a given material (all with exactly the same grain-size distribution), S_{us} is a function only of void ratio. The relationship between void ratio and

S_{us} for a given soil, with S_{us} plotted on a log scale, is referred to as the steady-state line (Figure 7.10).

7. Since S_{us} and σ'_{3s} are related by ϕ'_s (Appendix 7A), the steady-state line can be plotted as either void ratio versus S_{us} or void ratio versus σ'_{3s} . Plotting void ratio versus σ'_{3s} makes it possible to plot the state of the sample before and after consolidation in the triaxial cell, as well as at steady state.
8. It has been shown experimentally that similar materials with the same grain shape and mineralogy, but slightly different grain-size distributions, will have steady-state lines that are parallel but not coincident. Examples are provided in Figures 3, 4, and 5 of Poulos, Castro, and France (1985).
9. High quality undisturbed samples are used to measure S_{us} of in-situ material. Because of unavoidable densification that occurs during sampling, handling, and especially during consolidation in the triaxial cell, S_{us} measured in the laboratory will be higher than the in-situ S_{us} . Correcting the value of S_{us} measured in the laboratory back to the in-situ S_{us} for a given sample requires two things. First, careful measurements must be made during sampling, handling, and testing to measure the total change in void ratio from the in-situ condition to the laboratory-consolidated condition. Second, the slope of the steady-state line must be measured.

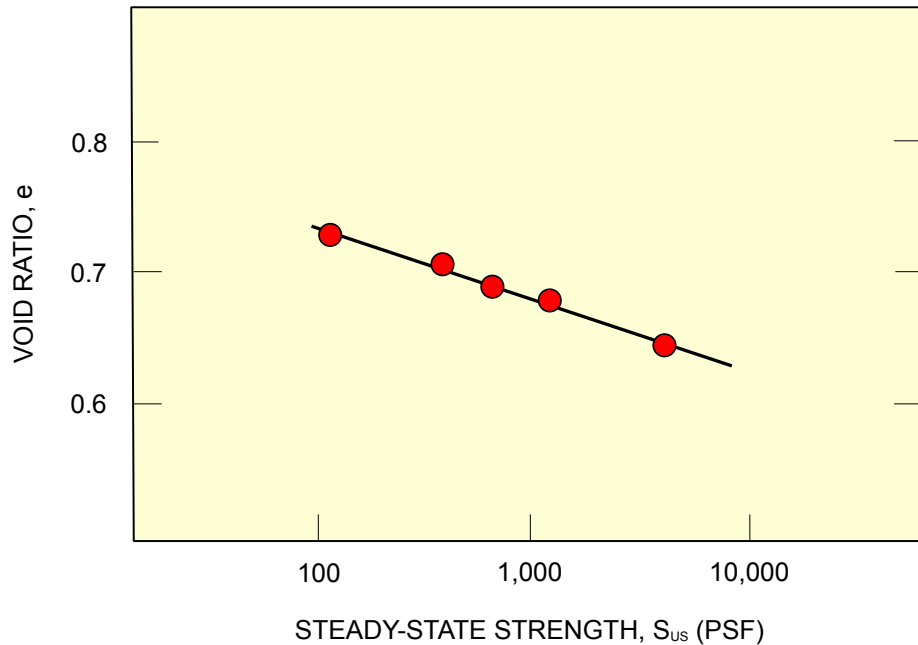


FIGURE 7.10 STEADY-STATE LINE

The basic procedural steps in a steady-state (residual) strength laboratory testing program for sand-like material are provided in the following list (for each zone of interest). Detailed procedures are presented in Appendix 7B.

1. Identify the zone of loose material based on SPT, CPT, and/or other desired field methods. Obtain enough disturbed or undisturbed samples from which a batch mix can be created that will contain enough soil for at least 5 tests to measure the slope of the steady-state line. Obtain enough high quality undisturbed samples to perform at least 8 tests on undisturbed samples from each zone of interest to measure the in-situ S_{us} . A detailed sampling procedure that has been used with fixed-piston sampling to record sample densification during sampling is provided in Appendix 7C.

2. Perform grain-size, hydrometer, specific-gravity, and (if the material has any plasticity) Atterberg-limits tests on material from the batch mix. Also perform grain-size tests on the trimmings from all undisturbed samples used to measure the in-situ S_{us} .
3. To measure the slope of the steady-state line, prepare at least 5 very loose uniform specimens from the batch mix for triaxial testing. Moist tamping in 10 layers has worked well for 3-inch-diameter by 7-inch-tall specimens. Isotropically consolidate the specimens to varying consolidation pressures such that a range of final void ratios is obtained. Carefully measure the volume of the sample in the triaxial cell after saturation but before beginning consolidation. This is typically done by applying a small vacuum to the sample so that it will maintain its shape with no cell pressure applied. After measuring the sample volume, carefully keep track of all volume change during consolidation. Shear the samples in undrained strain-controlled compression, and measure S_{us} at high strains. (See testing Note 2 below for how to identify whether S_{us} has been reached.) After the test, oven dry the entire tested sample to measure its water content. Using the water content and the specific gravity of the material, compute the void ratio during shear. Then plot the void ratio during shear versus S_{us} for each test. All the tests should plot close to a straight-line fit of the data (Figure 7.10). This is the steady-state line for the batch mix.
4. Set up, saturate, and consolidate each undisturbed sample. Measure the sample volume before consolidation and volume changes during consolidation, as discussed in the previous step. Shear each undisturbed sample in undrained, strain-controlled compression and measure S_{us} at high strains. After the test, oven dry the entire tested sample to measure its water content and dry weight. Alternatively, measure the entire wet weight, then use half the sample for water content measurement and half the sample for grain-size and/or specific-gravity testing. For fine coal refuse, a specific gravity measurement must be performed for each undisturbed test sample. Using the water content, the dry weight, and the specific gravity of the material compute the void ratio of the sample during undrained shear (Appendix 7B). The measured value of S_{us} corresponds to the void ratio during undrained shear in the triaxial cell. To estimate the in-situ value of S_{us} for that sample, first plot the result of the test on a diagram of S_{us} versus void ratio. Then draw a line upward and to the left from that data point, parallel to the steady-state line measured for the batch mix. Where the line drawn reaches the in-situ void ratio, select the value of in-situ S_{us} (Figure 7.11). Refer to Appendix 7B for detailed procedures for measuring the as-tested and in-situ void ratios of each sample.
5. The eight or more tests on undisturbed samples will result in a range of estimated in-situ values of S_{us} . Select a design value of S_{us} that is lower than two-thirds of the estimated in-situ values and higher than one third of the values. The appropriate total number of tests that should be performed for each zone depends primarily on the variability of that zone. An example is shown in Figure 7.12. As shown in the figure, one should not expect the as-tested S_{us} values from the undisturbed samples to plot on a straight line of void ratio versus $\log S_{us}$, because slight variability in grain-size distribution from sample to sample may result in significant variability in the vertical position, but not the slope of the correlation of S_{us} versus void ratio.

Some notes on testing include the following:

1. Accuracy in measuring void ratio is critical to proper measurement of S_{us} . Appendices 7B and 7C discuss the required precision of various measurements in the field and laboratory. A given error in void ratio will result in a higher error in S_{us} for mate-

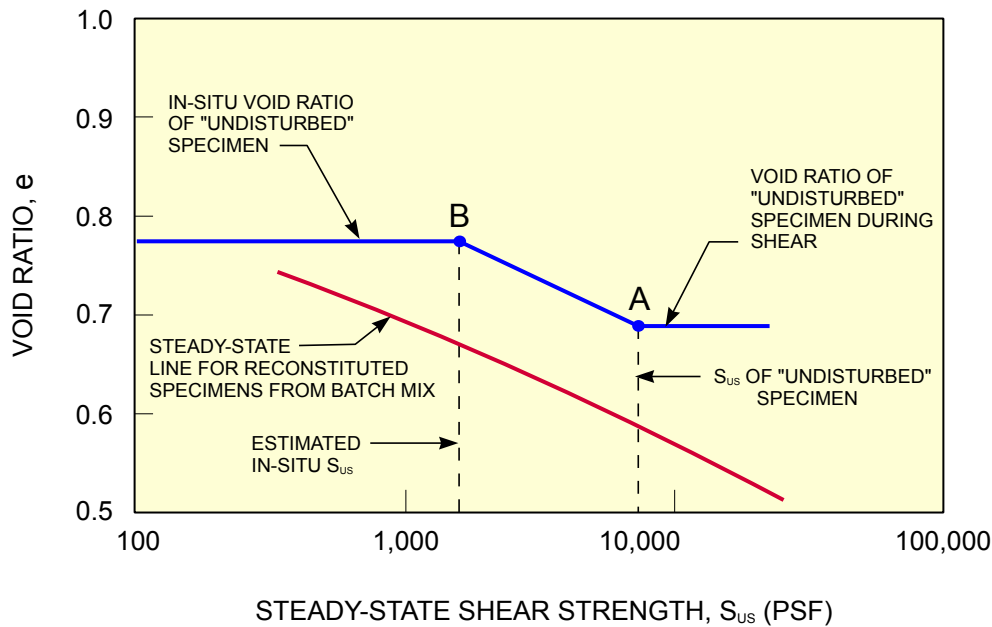


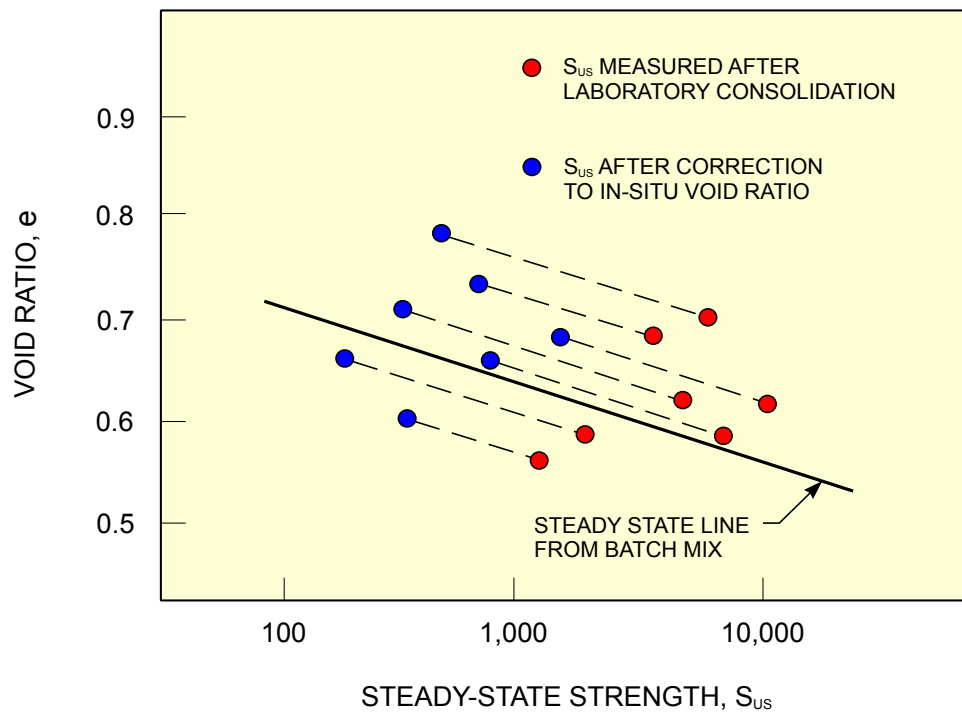
FIGURE 7.11 METHOD FOR CORRECTING LABORATORY S_{us} TO IN-SITU S_{us}

rials with relatively flat steady-state lines. In other words, materials with low slopes of the steady-state line (low values of $\Delta e / \Delta \log S_{us}$), are more sensitive to errors in the measurement of void ratio.

The range of slopes of steady-state lines ($\Delta e / \Delta \log S_{us}$) for coal refuse reported for seven sites in West Virginia and one site in Kentucky was 0.090 to 0.140 (personal communication, GEI, 2007). For the flattest slope of 0.090 (the most sensitive case), errors in void ratio measurement would lead to errors in S_{us} , as shown in Table 7.5. As discussed in Appendix 7B, void ratios at the various steps of sampling and testing should be computed to the nearest 0.001. The goal is that the computed in-situ and as-tested void ratios should be correct to within 0.010. The resulting values of S_{us} should then be correct to within 30 percent, as indicated in Table 7.5.

- When looking at a stress-strain curve to identify whether the steady state has been reached, curves for contractive samples are more definitive than curves for dilative samples. Contractive samples will typically exhibit peak strength at small strains followed by a drop-off in strength and a flattening out at the steady state within the strain limits of the triaxial test. Dilative samples, on the other hand, typically show a gradually increasing strength and may not reach steady state within the strain limits of the test. Also, dilative samples are more likely to develop failure planes during shear, meaning that steady state is reached only within the thin failure zone where the void ratio is unknown. Therefore, contractive samples are preferred.

For an undisturbed sample with a given void ratio, consolidating the sample to a higher effective confining stress before undrained shear is likely to make the sample more contractive during undrained shear, as explained further in the commentary that follows. Contractive samples tend to have stress-strain curves that are more definitive for interpretation of S_{us} , as explained in the previous paragraph. Therefore, it is often good practice to consolidate the sample to a high confining pressure before undrained shear. The disadvantage is that consolidating the sample to a high confining pressure also decreases the void ratio of the sample in the test and requires a bigger correction to obtain the in-situ value of S_{us} .


 FIGURE 7.12 INTERPRETATION OF LABORATORY S_{us} TESTING

It is not necessary to consolidate the sample to stresses that model in situ conditions. This is because the steady-state strength is the strength at high strains and is not affected by stress history. Therefore, isotropic consolidation is normally used.

Commentary: Consolidated samples that plot well to the right of the steady-state line will be contractive, as shown in Figure 6 of Poulos et al. (1985). Experience with laboratory testing tells us that the $e - \log \sigma'_3$ consolidation curve is usually slightly flatter than the steady-state line (plotted as e versus $\log \sigma'_3$ per item 7 on page 7-46). Therefore, increasing the consolidation stress tends to move the sample further to the right compared to the steady-state line, and the sample tends to become more contractive.

At the steady state, both the principal stress difference and σ'_3 should be constant with strain.

 TABLE 7.5 ERROR IN VOID RATIO AND CORRESPONDING PERCENT ERROR IN S_{us}

Error in void ratio (Δe)	$\Delta \log S_{us}^{(1)}$	$S_{us}(\text{measured})/S_{us}(\text{actual})^{(2)}$	Error in S_{us} (%)
0.005	0.0555	1.14	14
0.010	0.1111	1.29	29
-0.005	-0.0555	0.88	12
-0.010	-0.1111	0.77	23

Note: 1. $\Delta \log S_{us} = \Delta e / 0.090 = [\log S_{us}(\text{measured})] - [\log S_{us}(\text{actual})] = \log [S_{us}(\text{measured}) / S_{us}(\text{actual})]$

2. $S_{us}(\text{measured}) / S_{us}(\text{actual}) = 10^{(\Delta \log S_{us})}$

3. It is helpful to plot the compression curves ($e - \log \sigma'_3$) along with the values at steady state. Especially for the samples tested from the batch mix to measure the steady-state line, these plots will help determine what consolidation stresses are needed to achieve contractive samples at desired void ratios. (Figure 7.13)
4. Published data for coal refuse, based on laboratory testing as described above, include: (1) a reported range of 0.06 to 0.27 for S_{us}/σ'_v and (2) a reported slope of the steady-state line $\Delta e/\Delta \log S_{us}$ in the range of 0.11 to 0.13 based on laboratory testing of 34 undisturbed samples (PI in the range of 0 to 12) of fine coal refuse from five West Virginia sites (Genes et al., 2000). Also, reported slopes of the steady-state line $\Delta e/\Delta \log S_{us}$ for one site in West Virginia and one site in Kentucky were found to be 0.09 and 0.14 (GEI, 2007).

Because the preceding parameters are based on limited data and a wide range of ratios, the data should be used carefully. Also, as discussed in Section 7.4.3.1, using the ratios of S_{us}/σ'_v for confining pressures significantly higher than the confining pressures from the actual samples may be unconservative. However, if values of S_{us} are measured using laboratory testing of site-specific materials or comparable deposits at comparable confining pressures, then the site-specific ratios may be valuable for adjusting the measured S_{us} values for other portions of the embankment, or for future construction stages (Genes et al., 2000).

Over time, if a database of strength ratios for fine coal refuse is developed, it should become possible to use these ratios with more confidence.

Estimation of strengths using strength ratios requires an estimate of the consolidation pressure. One should not make the assumption a priori that the soils are normally consolidated without obtaining confirming data and monitoring. In areas where fine coal refuse will serve as the foundation for embankment construction, the design plan should include provisions for monitoring pore pressures and, if significant upstream construction is planned, controlling the rate of construction to mitigate excess pore pressure development and/or reducing the likelihood that significant zones of fine refuse will be under consolidated as construction proceeds. When evaluating existing embankments, piezometer data should be obtained to allow estimation of effective consolidation stresses. Also, pore-pressure-dissipation tests performed with the piezocone at various depths are an effective

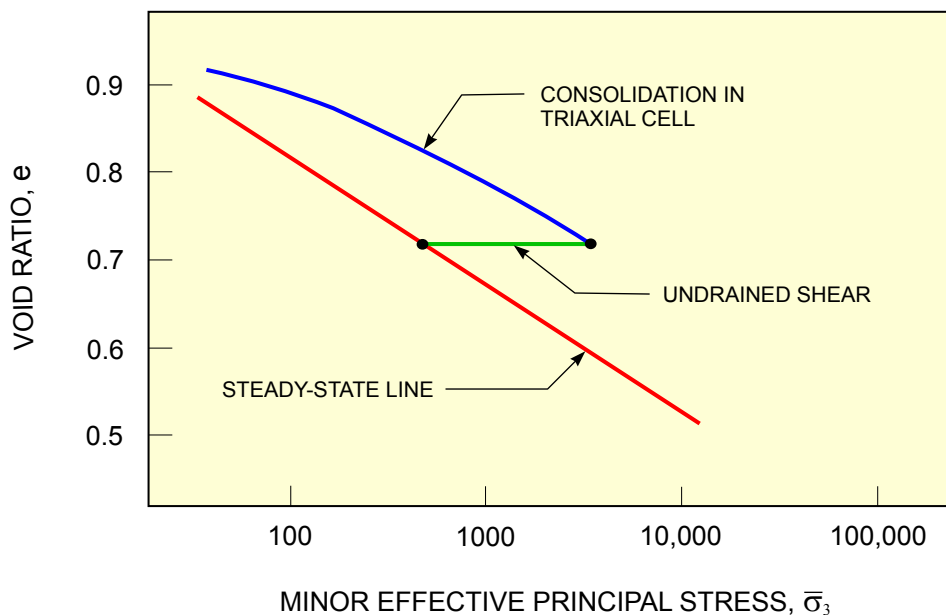


FIGURE 7.13 CONSOLIDATION CURVE AND STEADY-STATE LINE

way of obtaining the pore-pressure profile at a given location. Consolidation tests on undisturbed samples of clayey layers can also be used to determine the current consolidation stresses on the clayey layer and adjacent more sandy layers.

7.4.3.3 Field testing to Measure S_{us} of Soft Clay-Like Material

Field vane-shear testing can be used to estimate S_{us} of clay-like material. For the field vane measurements to be valid, they must be performed to high enough strains to reach S_{us} and must be performed quickly to be confident that the material is being sheared undrained. Recommended vane shear testing procedures are provided in Chapter 6, Section 6.4.3.8. It is a good idea to pair field vane-shear tests with CPTs, to confirm that the field vane is being performed in a layer of clay-like material.

CPT sleeve friction measurements can also be used for estimating S_{us} of clay-like material (Lunne et al., 1997), although comparison field vane tests are recommended because the CPT sleeve friction is less reliable in sensitive clays. CPTs should be performed with pore-pressure measurements to confirm that the pore-pressure response indicates undrained shear. Lack of elevated pore-pressure response may indicate that the material is behaving as drained rather than undrained.

Commentary: For most clay-like materials the post-earthquake strength will be higher than S_{us} . Therefore, using S_{us} as an estimate of post-earthquake strength may be overly conservative. Laboratory methods of estimating post-earthquake strength of clays, as discussed in Section 7.4.3.2.2, may provide less conservative estimates of post-earthquake strength.

As a lower bound, clay-like material with a liquidity index of less than 1.0 can be considered to have a post-earthquake strength of $0.04 \sigma'_v$. If the liquidity index is greater than or equal to one, a lower bound post-earthquake strength of 20 psf, but no higher than $0.04 \sigma'_v$, may be used. These values are guidance based on the judgment of the authors. Clay-like materials with a liquidity index less than 1.0 are unlikely to lose strength all the way to S_{us} due to earthquake shaking. A reduction in undrained strength for these materials from a pre-earthquake peak strength of $0.2 \sigma'_v$ (a value within the representative range for natural clays) to a post-earthquake strength of $0.04 \sigma'_v$ is considered conservative. Clay-like material with a liquidity index of 1.0 or higher may act like a “quick” clay with a very low remolded or post-earthquake strength. Therefore, a lower bound of just 20 psf, but no higher than $0.04 \sigma'_v$, is considered appropriate.

7.4.4 Analysis Steps

Engineers use various methods for evaluating triggering and post-earthquake strength. Engineers also perform these evaluations and the related limit-equilibrium, slope-stability analyses in varying sequences. The following steps represent a generalized approach that can be adjusted for individual projects. Reference should be made to the flow chart in Figures 7.1a, 7.1b and 7.1c.

7.4.4.1 Step 1 - Define Embankment Geometry

Define the geometry of the embankment and of the material zones within the embankment. Identify zones of clay-like versus sand-like materials.

7.4.4.2 Step 2 - Screen for Potential Strength Loss

Review the subsurface conditions at the embankment to evaluate whether any zones have the potential for strength loss due to earthquake shaking.

7.4.4.2.1 Sand-Like Material

For this initial screening step, saturated to nearly-saturated, sand-like materials with $N_{1,60}$ values less than 15, or q_{t1} values less than 75 tsf, should be considered potentially susceptible to strength loss.

Commentary: The screening criteria that sand-like materials with $N_{1,60}$ values greater than 15 or q_{t1} values greater than 75 tsf are not susceptible to strength loss are based on case-history data from large earthquakes indicating that flow slides have only occurred where $N_{1,60}$ values were 13 or lower (Seed and Harder, 1990; Castro, 1995; Wride et al., 1999) and q_{c1} values were less than 65 tsf (Olson and Stark, 2002). Olson and Stark (2003) present curves showing dilative versus contractive behavior for sands. The boundary for dilative versus contractive in terms of $N_{1,60}$ values varies from 10 to 15. The boundary in terms of q_{c1} values varies from 65 to 85. Also, Seed (1979) presents data showing that sands with relative densities higher than about 50 percent or N_1 values higher than about 15 have limited strain potential and therefore may experience cyclic mobility but not strength loss, even though pore pressures may have reached 100 percent.

Many experts agree that a fines correction might be reasonable in this screening analysis for sand-like material. That is, a silty sand may be less likely to be contractive than a clean sand with the same N -value. However, the data to support this are sparse and vague. Therefore, a fines correction should not be applied here unless additional data is published in the future that can justify it.

It is interesting to note that the curves presented in Youd et al. (2001) indicate that “liquefaction” may occur during large earthquakes in sand-like material having $N_{1,60}$ values as high as 30, and q_{c1N} values as high as 150. This is because, in Youd et al. (2001), “liquefaction” refers to increases in pore pressure but not necessarily to strength loss. As stated in the introduction to Youd et al. (2001): “In moderately dense to dense materials, liquefaction leads to transient softening and increased cyclic shear strains, but a tendency to dilate during shear inhibits major strength loss and large ground deformations.” (The term “increased cyclic shear strains” is referred to herein as cyclic mobility.) In other words, moderately dense to dense sand-like materials ($N_{1,60}$ values higher than 15 or q_{t1} values higher than 75 tsf) may experience high excess pore pressures and cyclic mobility, but they will not experience strength loss.

The criterion that sand-like materials with $N_{1,60}$ values greater than 15, or q_{t1} values greater than 75 tsf, be considered not susceptible to strength loss is a conservative criterion. Many materials with $N_{1,60}$ values less than 15, or q_{t1} values less than 75 tsf, will be dilative and not susceptible to strength loss. Therefore, if almost all $N_{1,60}$ values exceed 13 and the mean $N_{1,60}$ value exceeds 15 within a zone, or almost all q_{t1} values exceed 65 tsf and the mean q_{t1} value exceeds 75 tsf within a zone, then the zone can be considered not susceptible to strength loss.

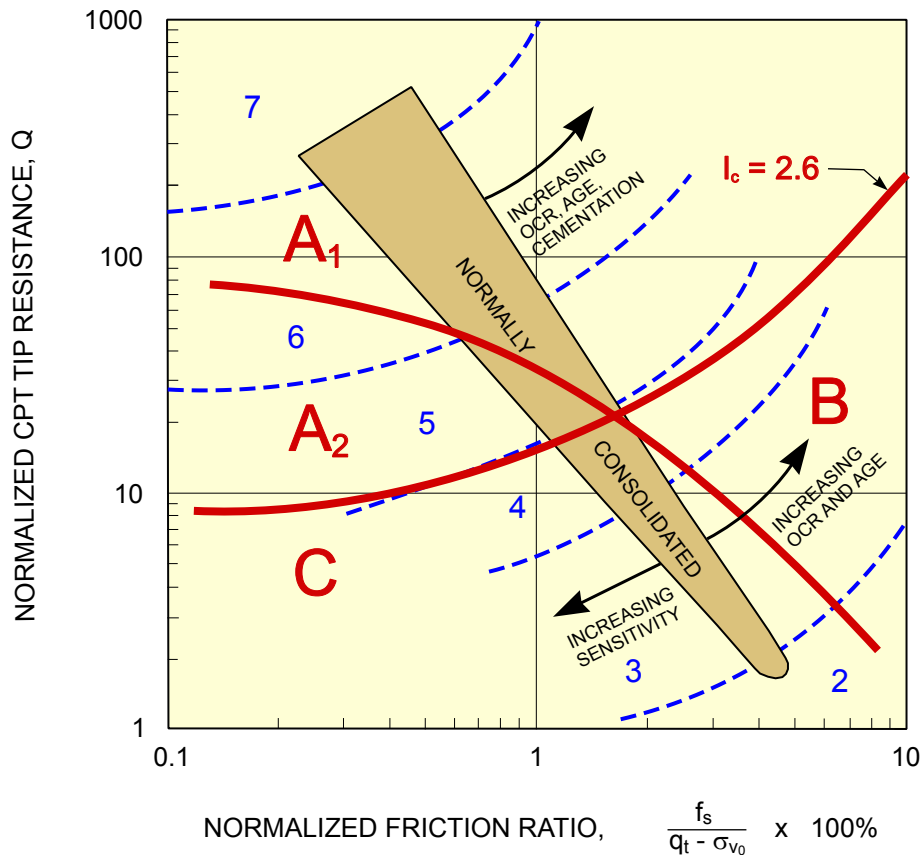
Conservative criteria and conservative engineering judgments are appropriate and intended at this step for three reasons: (1) little if any of the data supporting these criteria are based on coal refuse materials (although, considering that coal refuse particles are more compressible than natural soil particles, one might expect these criteria to be even more conservative, because the compressibility of the coal refuse may mean that SPT and CPT values are lower for coal refuse than for natural soils at the same void ratio), (2) there is some uncertainty in the overburden corrections used to convert measured field values to $N_{1,60}$ and q_{t1} values, and (3) no further analysis is recommended for materials that satisfy these criteria.

Thorough site-specific field and laboratory testing should ultimately yield data other than $N_{1,60}$ and q_{t1} to better evaluate whether sand-like materials at a site are or are not susceptible to strength loss. If in-situ and laboratory test data are available during the initial screening phase, it should also be used in classifying sand-like zones as susceptible or not susceptible to strength loss.

7.4.4.2.2 Clay-Like Material

For this initial screening step, clay-like material may be screened for zones with potential for significant strength loss based on CPT data, as shown in Figure 7.14 (Robertson, 2008). This figure is a slightly more conservative version of a similar figure presented in Robertson and Wride (1998). In this figure, Q is equivalent to q_{c1N} and F is the friction ratio. Computation of both Q and F is discussed in Youd et al. (2001). CPT data in Zone B indicate clay-like material for which significant strength loss is unlikely. CPT data in Zone C indicate potentially highly sensitive clay-like material for which significant strength loss can occur (Zones A1 and A2 indicate sand-like material). If CPT data are not avail-

able, then SPT data can be used along with Atterberg limits to confirm that the material is clay-like. $N > 6$ corresponds to Zone B and $N < 6$ corresponds to zone C. For this screening step, the N -values of the clay-like material should be corrected for hammer efficiency per Youd et al. (2001), but should not be corrected for overburden pressure. Overburden pressure corrections are applicable only to sand-like material, not clay-like material. Undrained strength data, if available, can also be used. Peak undrained strength of 1500 psf or higher corresponds to Zone B, and peak undrained strength less than 1,500 psf corresponds to zone C.



- NOTE: 1. VALUES OF Q AND F ARE COMPUTED FROM CPT DATA AT THE DEPTHS OF INTEREST, AS DESCRIBED IN YOU D ET AL. (2001).
2. CPT DATA THAT PLOT IN ZONES A₁ AND A₂ INDICATE MATERIAL THAT IS NOT CONSIDERED CLAY-LIKE, SO THIS SCREENING METHOD IS NOT APPLICABLE.
3. CPT DATA THAT PLOT IN ZONE B INDICATE CLAY-LIKE MATERIAL THAT IS NOT SUSCEPTIBLE TO STRENGTH LOSS.
4. CPT DATA THAT PLOT IN ZONE C INDICATE CLAY-LIKE MATERIAL THAT MAY BE SUSCEPTIBLE TO STRENGTH LOSS.
5. NUMBERED ZONES SEPARATED BY DASHED BLUE LINES ARE FOR REFERENCE ONLY AND ARE A GUIDE TO SOIL TYPES, AS DESCRIBED IN YOU D ET AL. (2001). FOR EXAMPLE, DATA IN ZONE 3 INDICATE SILTY CLAY TO CLAY WHILE DATA IN ZONE 6 INDICATE CLEAN SAND TO SILTY SAND. THE LINE SEPARATING SAND-LIKE FROM CLAY-LIKE MATERIAL CORRESPONDS TO A SOIL BEHAVIOR TYPE INDEX (I_c) OF 2.6, AS ALSO DESCRIBED IN YOU D ET AL. (2001).

(ADAPTED FROM ROBERTSON, 2008; © 2008 NRC CANADA OR ITS LICENSORS; REPRODUCED WITH PERMISSION.)

FIGURE 7.14 USE OF CPT DATA TO SCREEN CLAY-LIKE MATERIAL

Commentary: These screening criteria for clay-like material are recommended guidance. No generally accepted screening criteria for susceptibility to strength loss were found in the literature. Selection of these criteria is based on the authors' judgment and experience, and considering published data from sites where liquefaction (strength loss or excess pore pressure) was observed in soils with significant fines content.

In applying these criteria, CPT data are considered the most reliable, laboratory strength data the next most reliable, and SPT data the least reliable.

7.4.4.2.3 Screening Results

If no zones within the embankment or foundation are susceptible to strength loss, then the seismic stability of the embankment is acceptable (assuming, of course, that the static stability has been analyzed and is acceptable, including cases where undrained strengths are considered). No further analyses of seismic stability are needed. The next step is to evaluate seismic deformations.

If one or more zones within the embankment or foundation are susceptible to strength loss, then further analyses should be performed as discussed in Step 3, which follows.

7.4.4.3 Step 3 - Define Post-Earthquake Strengths for Limit Equilibrium Stability Analyses

Stability analyses are typically performed using 2D limit-equilibrium, slope-stability software for one or more potentially critical cross sections of the embankment. The stability analyses should be static analyses using post-earthquake strengths. Analyses should be performed for both potential upstream and potential downstream failures.

Upstream failures may or may not pose a risk of uncontrolled release, depending on whether the location of the critical surface leaves adequate freeboard and crest width in place. Guidelines for deciding whether potential upstream failures pose a safety hazard are discussed in Sections 6.6.4.1 and 6.6.4.3.

Values of post-earthquake strength for various zones of the embankment should be selected as discussed in the following:

- Dense sand-like materials ($N_{1,60} > 15$ and $q_{t1} > 75$ tsf) such as compacted coarse refuse and dense sand-like natural soils tend to be dilative when they are sheared. That is, the undrained strength tends to be higher than the drained strength. Also, these materials do not experience strength loss due to earthquake shaking. For post-earthquake stability analysis, one cannot be certain whether the material will act as if it is drained or undrained, and the negative pore pressures required to mobilize a higher strength may not develop because they cause cavitation. Therefore, it is reasonable and conservative to use the drained strength for these materials, as discussed in Chapter 6.
- Stiff clay-like materials (SPT $N > 6$ and CPT data in Zone B) tend to have high shear strain up to the peak undrained strength and limited drop-off in shearing resistance after the peak, so they should not experience significant strength loss due to earthquake shaking. Unlike dense sand-like materials, stiff clay-like materials should act as undrained during the most critical earthquake and post-earthquake period. For these materials, 80 to 100 percent of the peak undrained strength should be used.

Commentary: Available data indicate that the cyclic stresses and strains caused by earthquakes are unlikely to cause significant strength reduction in stiff clays. However, some practitioners have commonly used 80 percent of the peak undrained strength for clays that are subject to significant seismic loading, presumably to account for possible strength degradation and other factors. Therefore, although it is perhaps overly conservative, the 80-percent value is recommended in areas of moderate to high seismic hazard potential. Use of 100 percent of the peak undrained strength is reasonable in areas of low seismic hazard potential and when applying a factor of safety of 1.5 in initial post-earthquake stability evaluations to classify the structure and foundation (Figure 7.1a, Boxes 5 and 6).

- For loose saturated sand-like material, as in most fine coal refuse impoundments, strength should be selected based on the results of triggering analyses, and S_{us} estimates should be made in accordance with the previous sections of this chapter. If triggering of strength loss is assumed or computed to occur, use S_{us} . If triggering is assumed or computed to not occur, use the peak undrained strength, but no higher than the drained strength. The S_{up} values for sand-like materials can be obtained from published data such as Castro (2003) and Olson and Stark (2003). Alternatively, the S_{up} values can be obtained from the testing on remolded samples performed as part of the testing program described in Section 7.4.3.2.3. Tests on remolded samples with values of steady-state strength and confining pressure similar to in-situ samples can be considered representative of in-situ conditions.

Drained strengths for these materials can be used if they are clearly determined to be unsaturated (saturation ratio less than 80 percent), and it can be demonstrated that they will remain unsaturated. (When the degree of saturation is higher than 80 percent, strength loss is still possible for loose, sand-like material.) Materials above the phreatic surface should not necessarily be assumed to be unsaturated. Materials above the phreatic surface may be saturated or close to saturated, particularly if the water level was previously higher than the current phreatic surface.

- For soft or sensitive clay-like material (SPT $N < 6$ or CPT data in Zone C), strength should be selected based on the results of strength-loss estimates made in accordance with Sections 7.4.2.3.1, 7.4.3.2.2, and 7.4.3.3. If triggering (significant strain during the earthquake) is assumed or computed to occur, use a value lower than S_{up} , but probably not as low as S_{us} . (If the zones of this material are relatively small and probably not significant to the seismic stability, then S_{us} can be used as the post-earthquake strength even though it is probably overly conservative. For highly sensitive clays, S_{us} may be the appropriate post-earthquake strength.) If triggering (significant strain during the earthquake) is computed to not occur, use 80 percent of S_{up} . S_{up} for clay-like material can be obtained from CPT data, field vane shear testing, or laboratory testing. S_{up} for borderline material can be obtained from CPT data (if the push is undrained based on pore-pressure response) or from laboratory testing or possibly from field vane-shear tests performed at high strain rates.

Coal refuse impoundments tend to be stratified. Variations in post-earthquake undrained strengths may be more significant than variations in drained strengths. Therefore, post-earthquake strengths should be selected conservatively. For zones of mixed coarse and fine refuse (such as the lower portion of an upstream stage), use strength properties weighted toward the properties of the overlying coarse refuse zone or the underlying fine refuse zone, based on the prevalence and extent of each zone, the index properties of each zone, and a realistic estimation of the upstream embankment cross section (based on subsurface conditions and past experience with displacement of fines during upstream construction pushouts).

Commentary: *Strain compatibility is not an issue for these stability analyses, because the strengths used all represent reasonably conservative estimates of the undrained strength that the soil might have at high strains (5 percent to 10 percent). As discussed previously, the recommended strengths are:*

- Loose sand-like material – Undrained steady-state (residual) strength. This is the lowest resistance that the material can have at any strain beyond a few percent.
- Dense sand-like material – Drained strength. The undrained stress strain curve of a dense, dilative, sand-like material increases steadily with strain with no drop-off at high strain. For these materials, the drained strength is a conservative estimate of the undrained resistance at any strain beyond a few percent.

- *Soft clay-like material* (SPT $N < 6$ or CPT data in Zone C) – Either: (1) the undrained steady state (residual) strength as a very conservative estimate of the available strength, (2) the post-earthquake peak strength estimated from cyclic tests followed by monotonic (static) tests, or (3) 80 percent of the peak-undrained strength. But option 2 or 3 can only be used if the clay-like material has a broad peak to the stress-strain curve, with no rapid drop-off in resistance after peak, which is the case for most clay-like material. So, the strength selected for use should be appropriate for a wide range of strain.
- *Stiff clay-like material* (SPT $N > 6$ and CPT data in Zone B) – 80 to 100 percent of undrained peak strength. The undrained stress-strain curve of stiff clay-like material reaches nearly its peak strength at a few percent strain and then levels off or increases slowly with strain with no drop-off at high strain. So, again, the strength used is appropriate for a wide range of strain. As discussed above, the 80-percent value is recommended in areas of moderate to high seismic-hazard potential. Use of 100 percent of the peak-undrained strength is reasonable in areas of low seismic-hazard potential, and when applying a factor of safety of 1.5 in initial post-earthquake stability evaluations to classify the structure and foundation (Figure 7.1a, Boxes 5 and 6).

7.4.4.4 Step 4 - Perform Initial Stability Analysis

First perform an initial, conservative, post-earthquake stability analysis. This initial stability analysis is performed with the assumption that the earthquake shaking is strong enough that soils potentially susceptible to strength loss do in fact experience strength loss.

Use S_{us} for sand-like material in zones of the embankment that, based on the screening analysis in Section 7.4.4.2, have low N-values and CPT values and may therefore be susceptible to strength loss. For this analysis, S_{us} for sand-like materials can be conservatively estimated from correlations with SPT and/or CPT data (Section 7.4.3.1). Also, the post-earthquake strength of clay-like material considered not susceptible to significant strength loss (Zone B on the CPT chart or $N > 6$) can be estimated as 80 to 100 percent of S_{up} , as discussed in Section 7.4.4.3. The post-earthquake strength of clays considered potentially susceptible to significant strength loss should be taken as an estimated value of S_{us} . S_{up} and S_{us} for clays can be estimated from CPT data, field vane shear data, or laboratory data (Chapter 6 and Section 7.4.3.3).

The slope stability analysis is a total-stress analysis using undrained strength, which is a function of the pre-earthquake consolidation stress. The location of the phreatic surface affects the pre-earthquake consolidation stresses and thus the undrained strength. The estimated location of the phreatic surface at the time of the earthquake should be used in the stability analysis. Elevated pore pressures caused by earthquake shaking need not be considered.

If these initial stability analyses (for various potential upstream and downstream failure surfaces) indicate a minimum safety factor of at least 1.2, then seismic stability is considered acceptable, and the next step is to perform a deformation analysis.

If the minimum safety factor is below 1.2, then the embankment geometry should be modified to make the factor of safety acceptable, or else more sophisticated (and less conservative) evaluations of post-earthquake shear strength and triggering, as subsequently discussed, may be appropriate. If the safety factors are very low, then it may be clear at this initial stage that some modification to the embankment design is needed. It is often useful to vary the assumed values of S_{us} in the zones potentially susceptible to strength loss to find the values of S_{us} that would be needed to obtain a safety factor against instability of 1.2, and then judge if the materials in question could possess such strengths before undertaking more detailed evaluations of S_{us} .

Commentary: A safety factor of 1.2 is recommended for this analysis because, even though the shear strengths selected for this analysis are fairly conservative, there may be significant uncertainties in the geometry of the embankment and the various zones within the embankment and foundation.

7.4.4.5 Optional Step 5 - Perform More Detailed Evaluation of S_{us} for Sand-Like Material

Obtain representative high quality undisturbed samples of sand-like material in zones that may experience strength loss (Section 7.4.4.2). Perform a laboratory steady-state shear strength testing program involving monotonic undrained tests on both undisturbed and reconstituted specimens (Section 7.4.3.2.3) to obtain better estimates of S_{us} .

Re-run the limit equilibrium stability analyses using the better estimates of S_{us} . If the minimum safety factor is at least 1.2, then the seismic stability of the embankment is acceptable, and seismic deformations should be evaluated next.

Commentary: The preceding discussion refers to laboratory testing to measure S_{us} for sand-like material. Performing this testing before undertaking triggering analyses should be considered, because the measured values of S_{us} might result in satisfactory seismic stability, and thus triggering would not be an issue. Also, the S_{us} testing will give information on stress-strain behavior, including strain at peak-undrained strength, which may be used in the triggering analysis. However, this step involves complex sampling and testing, and it can be deferred until after a triggering analysis is performed. This step can also be skipped entirely, especially if the post-earthquake strength of sand-like materials was not a significant factor in the initial stability analyses.

7.4.4.6 Optional Step 6 - Perform Triggering Analysis

If the minimum safety factor is still less than 1.2 after a more detailed evaluation of S_{us} , then for loose sand-like material, consider performing a triggering analysis, as discussed in Section 7.4.2, to evaluate whether the earthquake is large enough to trigger strength loss in the critical zones.

For sand-like materials, triggering analyses should only be performed if the design earthquake is relatively small. If the design earthquake produces a peak ground acceleration at the embankment site of more than 0.2g and causes a cyclic stress ratio (CSR) within the zone of interest of more than 0.15, then triggering of strength loss in sand-like material potentially susceptible to strength loss should simply be assumed.

If triggering analyses are performed for sand-like materials, the pore-pressure-based method, as discussed in Section 7.4.2.1 (Youd et al., 2001) should be performed first. If the safety factor against triggering using the pore-pressure-based method (CRR/CSR) is higher than 1.4, then triggering can be assumed to not occur. If the safety factor is less than 1.0, then triggering of strength loss should be assumed. For safety factors of between 1.0 and 1.4 calculated using the pore-pressure-based method, triggering of strength loss is possible. Either assume that triggering of strength loss will occur, or perform more rigorous triggering analyses (strain-based or stress-based methods as discussed in Section 7.4.2.3) to make a final evaluation of whether or not triggering occurs.

For clay-like material, a strain-based triggering analysis (possibly involving laboratory testing with cyclic loading followed by monotonic loading as discussed in Section 7.4.3.2.2) can be performed to evaluate whether the earthquake shaking is strong enough to trigger a decrease in S_{up} and to determine what the decrease will be.

If strength loss is not triggered in one or more of the zones that had previously been assumed to experience strength loss, then re-run the stability analysis using the appropriate, higher strength in those zones as discussed in Step 3, Section 7.4.4.3. If the safety factor is at least 1.2, then the seismic stability is acceptable, and seismic deformations should be evaluated next.

If the safety factors are still less than 1.2, then the embankment is not seismically stable. Additional investigations should be performed to better characterize the geometry and materials in the embankment or the embankment must be redesigned or modified.

7.4.5 Comments on Methods for Evaluating Triggering and Strength

All of the methods described in this chapter require special expertise, and should only be applied by geotechnical engineers with experience in seismic stability and deformation analyses.

Laboratory steady-state (residual) strength testing programs provide site-specific values of S_{us} that are often less conservative than the values obtained from empirical correlations with SPT and CPT data, but these testing programs require sophisticated undisturbed sampling and laboratory testing.

Strain-based triggering analyses require sophisticated laboratory testing and sophisticated analyses of shear strains induced by the design earthquake for evaluation of whether the earthquake shaking is strong enough to cause strength loss down to S_{us} . Thus, steady-state laboratory programs and strain-based triggering analyses are normally performed only for large embankments where the additional testing and analysis costs are relatively small compared to the cost of redesigning or modifying the embankment.

If contractive zones of material are confined by overlying layers of material with low hydraulic conductivity, then drainage of excess pore water generated by earthquake shaking can be impeded. There is some indication from centrifuge model tests that this may result in migration of pore water toward the overlying low-hydraulic-conductivity layer, with consequent redistribution of void ratio and loosening of the material near the interface with the low-hydraulic-conductivity layer. This in turn reduces the post-earthquake strength of the material near the interface. This mechanism was suggested by Whitman in the 1980s. Recent work on the subject includes Malvick et al. (2006) and Naesgaard et al. (2005). There are currently (2008) no generally accepted methods for analyzing this potential mechanism, and therefore it need not be directly considered in stability analyses at this time. A method for including the potential effects of void ratio redistribution on post-earthquake strength has been proposed by Idriss and Boulanger (2007). As discussed in [Section 7.4.3.1](#), this method can be used for sand-like material with $N_{1,60} > 15$ if one has a concern for the possibility of void-ratio redistribution (contractive zones overlain by lower-hydraulic-conductivity materials that would impede dissipation of excess pore-water pressure). In such a case drainage provisions (such as wick drains, as discussed in [Section 6.6.3.3](#)) could be incorporated. The need for such drainage provisions for dissipation of pore pressure in fine coal refuse at a slurry impoundment could be assessed based on pore-pressure monitoring during upstream construction.

Commentary: Pore-water migration and void-ratio redistribution (which may or may not actually occur outside laboratory centrifuge tests) are not considered in either laboratory testing or SPT/CPT methods for estimating post-earthquake strength. The laboratory testing relates to pre-earthquake void ratios. If there is pore-water migration, the relationship of void ratio to strength obtained from the laboratory testing would allow one to quantify the effects of a given amount of void ratio change (assuming that one day we will have methods to estimate to what extent, if any, pore-water migration takes place). SPT and CPT data also reflect pre-earthquake conditions. One cannot expect that SPT or CPT data will be able to predict whether or not, and to what extent, pore-water migration might take place, and what impact the pore-water migration might have on post-earthquake strength.

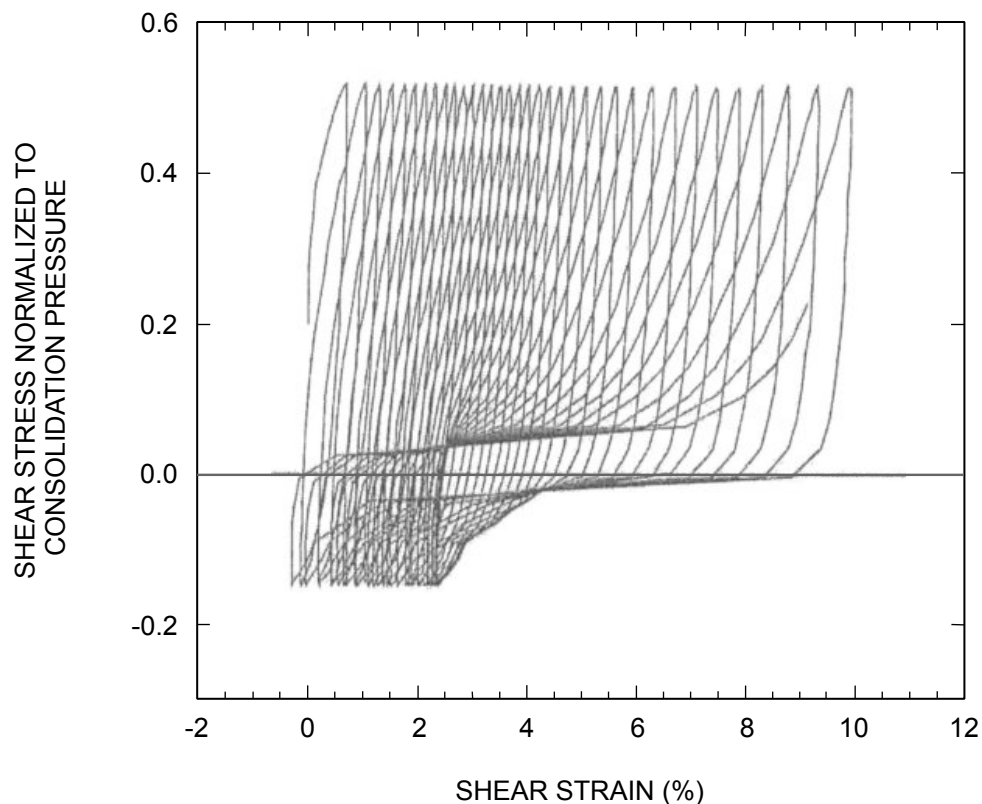
At the present time (2008), it is debatable whether pore-water migration did or did not occur for the case histories used to develop the relationships between SPT/CPT data and post-earthquake strength. For example, extensive investigations of the Lower San Fernando Dam slide indicate that the characteristics of the slide can be explained without assuming pore-water migration (Castro, Seed, Keller, and Seed, 1992).

7.5 SEISMIC DEFORMATION ANALYSES

7.5.1 General Discussion

The procedures described in Sections 7.5.2 through 7.5.6 are appropriate for sites where seismic stability has been shown to be adequate based on analyses discussed in the previous sections of this chapter. Even if the seismic stability is adequate, a dam or embankment will deform during earthquake shaking because of the development of accumulated strains along a potential sliding surface due to the superposition of seismic and static (driving) shear stresses. Two mechanisms for developing accumulated strains should be considered:

- **Yielding mechanism** – When seismic accelerations in an embankment are high enough, total shear stresses (static plus cyclic) along a potential failure surface may tend to exceed the available shear strength. The soil along the potential failure surface yields during short earthquake time increments when the total shear stress tends to exceed the available shear strength. Another way of saying this is that the soil along the potential failure surface yields during the short time increments of the earthquake when accelerations are higher than the acceleration that can be transmitted by the soil. This mechanism can occur in both sand-like and clay-like material. The resulting deformations can be evaluated using Newmark-type analyses.
- **Ratcheting mechanism** – As shown in [Figure 7.15](#), cyclic stress-strain curves are softer in loading than in unloading. When there is a static shear stress, repeated cyclic loading will result in accumulated strains (deformations) in the direction of the static shear stress, even if the available shear strength is not exceeded. These ratcheting accumulated strains (deformations) are generally significant only if cyclic mobil-



(SEED ET AL., 2003)

FIGURE 7.15 CYCLIC STRESS-STRAIN CURVE DEMONSTRATING RACHETING MECHANISM

ity occurs. If the cyclic loading involves stress reversal (i.e., the cyclic shear stress exceeds the static consolidation shear stress), and if enough cycles of loading occur that pore pressures approach 100 percent, then the cyclic stress-strain curve will develop an S-shape, and the cyclic strains will become significant. This type of cyclic stress-strain behavior is referred to as cyclic mobility. If there is no static shear stress, then cyclic mobility will not cause significant accumulated strain. Similarly, if there is a static shear stress, but cyclic mobility does not occur, then accumulated strains will generally be insignificant. To evaluate whether a material will develop cyclic mobility due to earthquake shaking, the Youd et al. (2001) procedure should be used to evaluate whether excess pore pressures will approach 100 percent. For the purpose of deformation analyses, a safety factor (CRR/CSR) of 1.0 or less should be considered to result in cyclic mobility.

For both the yielding and ratcheting mechanisms, the deformations are driven by the earthquake shaking. Therefore, the magnitude of the deformations is related to the intensity of the earthquake. This is in contrast to seismic instability, where the instability failure may be triggered by the earthquake shaking, but the instability failure is driven by the static (gravity) weight of the embankment.

Deformations may involve the embankment crest and both the upstream and downstream embankment slopes. Deformations along the upstream slope may or may not pose a risk of uncontrolled release, depending on whether the location and magnitude of the potential movement leaves adequate freeboard and crest width in place. Guidelines for deciding whether potential upstream slope movements pose a safety hazard are discussed in Sections 6.6.4.1 and 6.6.4.3. If these guidelines are met, detailed deformation analyses may not be required (i.e., if deformation screening or simplified analysis indicates acceptable performance for potential sliding masses that include the crest or provide overall dam freeboard and integrity, then detailed analyses may not be needed for other potential sliding masses that do not affect the integrity of the dam). While this point may also apply to potential movements on the downstream slope, the deformation, strain and stability of the remaining embankment should be evaluated considering both undrained and drained strength conditions and the potential for progressive failure.

***Commentary:** If seismic stability and deformation screening or simplified analysis demonstrate that a substantive portion of the embankment and crest would be preserved and would be sufficient to preclude a release from the impoundment (although other portions of the embankment might be compromised), then detailed deformation analysis to assess the significance of other zones that might be subject to cyclic mobility may not be warranted. This judgment should be based on the site-specific cross-section and material properties with careful consideration of: (1) the presence, extent and depth of zones of potential cyclic mobility and (2) mitigating factors that would limit large deformations or otherwise provide support for the adjoining embankment (e.g., the configuration of the upstream slope and impoundment might restrict the amount of displacement that could be expected, thus providing some remaining confinement and support to preserve a substantial portion of the foundation and embankment).*

Limit-equilibrium slope stability analyses, employing post-earthquake strengths, might be useful in identifying the foundation-embankment zone most prone to significant deformation and in judging what portion of the foundation and embankment would remain to preclude a release from the impoundment. For broader dams and broader upstream embankment stages, limit-equilibrium analyses with post-earthquake strengths may be adequate to justify that sufficient embankment breadth, crest width and freeboard would remain such that detailed deformation analyses are not warranted. However, for narrower dams and narrower upstream embankment stages founded on significant zones subject to potential cyclic mobility, the initiation and progression of excessive deformation and breaching of the crest may be a concern, and detailed deformation analyses are likely to be unavoidable. The distinction between “broader” and “narrower” dams and embankments is not definitive, but

professional judgments can be supported by the margin of safety suggested by the static and seismic (post-earthquake) stability analyses, considering potential failure surfaces within portions of the embankment-foundation that are anticipated to be preserved (e.g., factors of safety much greater than the minimum recommended values of 1.5 and 1.2, respectively) and supported by a limited extent of potential failure reflected by surfaces with low factor of safety (e.g., near the recommended minimum). Generally, to justify such judgment, potential failure surfaces with a low factor of safety should be limited in extent relative to the entire embankment breadth.

7.5.2 Preliminary Screening

If the site is in a low seismic-hazard area, which is defined in Section 7.7.3.7 as an area where the National Seismic Hazard Map of the United States (Frankel et al., 2002) indicates that the PGA with a return period in 2,500 years is less than or equal to 0.10g, and if the seismically-induced, pore-pressure buildup does not approach 100 percent (which could lead to cyclic mobility), then deformations will be small enough that no further evaluation of deformations is required. As noted in Section 7.5.1, all deformation evaluations, including this preliminary screening, are applicable only if the embankment has first been determined to be seismically stable. Therefore, for preliminary screening, the following steps can be followed, as indicated in the flow chart in Figure 7.1c:

1. Is this a structure-foundation system for which no deformation analysis at all is required (e.g., structures of the type indicated in Figure 7.1a, Box 1)? If the answer is "Yes," then no seismic deformation analysis is required. If the answer is "No," then continue to Step 2.
2. If the site is in an area of low seismic hazard potential (as defined in Section 7.7.3.7), then continue to Step 3. If the site is in an area of higher seismic hazard area, then skip to Step 5.
3. In sand-like materials, evaluate the potential for pore-pressure increase using the methods discussed in Section 7.4.2.2 (Youd et al., 2001). If the safety factor against 100 percent pore-pressure increase in any zone (*CRR/CSR*) is greater than 1.0, then cyclic mobility will not develop in that zone. For clay-like materials, confirm the safety factor from the static stability analysis using post-earthquake strengths. If the safety factor is greater than 1.2, then significant deformations in zones of clay-like material are unlikely.
4. If the analyses in Step 3 do not indicate cyclic mobility in sand-like material and the analyses in Step 3 indicate high safety factors for static stability in clay-like material, and if the site is in a low-seismic-hazard-potential area, then deformations will be small enough that no further evaluation of deformations is required.

Commentary: These criteria are intended to be conservative and represent recommended guidance based on experience with deformation analyses.

5. If the criteria in Step 3 are not met, or if the site is not in an area of low seismic hazard potential, then permanent deformations should be evaluated, as described in Sections 7.5.3 through 7.5.6, which follow.

7.5.3 Pseudo-Static Procedure for Screening

A relatively simple pseudo-static procedure (Hynes-Griffin and Franklin, 1984) can be used for screening of seismically-induced deformations. This procedure is applicable only if all of the following conditions are met:

- Design earthquake of magnitude less than 8 ($M < 8$).
- No significant zones susceptible to strength loss, as determined during the seismic

stability analyses (Sections 7.4.2 or 7.4.4.2).

- Small displacements (less than 3 feet) are not significant to the performance of the dam or embankment.

For this procedure, limit-equilibrium slope-stability analyses are performed with a pseudo-static seismic coefficient of one-half the PGA determined at the base of the embankment. For clay-like material, 80 percent of the peak undrained shear strength should be used. For sand-like material, 80 percent of the peak undrained shear strength, but no higher than 80 percent of the drained strength should be used. If the factor of safety is greater than 1.0 (based upon a thorough scope of geotechnical investigation or a high confidence level in material characterizations) or greater than 1.2 (based upon a moderate geotechnical investigation or less certain material characterization), then the deformations can be assumed to be less than 3 feet.

Commentary: Hynes-Griffin and Franklin (1984) suggested that a safety factor of 1.0 is adequate for assuming deformations would be less than 3 feet. The 1.2 safety factor has been added for cases where there is limited confidence in the site characterization. The method was developed based solely on earthquake records from the 1971 San Fernando earthquake. However, it is considered acceptable to apply the method to eastern as well as western sites. This screening analysis applies to any height of embankment. The height is taken into account indirectly by the pseudo-static limit-equilibrium analysis.

7.5.4 Newmark-Type Analysis (No Cyclic Mobility)

This method of analysis addresses the yielding mechanism of strain accumulation discussed in Section 7.5.1. In these Newmark-type analyses (Newmark, 1965), deformations are analyzed by considering movements of a sliding mass over a sliding surface caused by yielding of the soil at its available strength. The basic assumption is that movement (or yielding) occurs when the sum of the static plus the seismic shear stresses along the sliding surface reaches the value of the available shear strength. Thus, the acceleration that can be transmitted to the sliding mass is limited to a value referred to as the yield acceleration.

A Newmark-type analysis is not appropriate for very large deformations because it is based on the assumption that the embankment geometry is the same before and after the earthquake.

The basic steps are as follows:

1. For a given sliding mass, perform a pseudo-static stability analysis to determine the horizontal acceleration that produces a safety factor of one. This is the yield acceleration k_y , and it has the units of gravity. Critical sliding masses may be selected by searching for the most critical mass (critical sliding surface) while varying the pseudo-static horizontal acceleration until a safety factor of one is achieved. The estimated location of the phreatic surface at the time of the earthquake should be used. Elevated pore pressures caused by earthquake shaking need not be considered. The material strengths for the pseudo-static stability analyses should be the available undrained strengths determined as indicated in Sections 7.4.1 through 7.4.3 and 7.4.4.3. In general, the following strengths should be used:
 - Loose sand-like material – Undrained peak strength S_{up} or undrained steady-state (residual) strength S_{us} depending on results of triggering analysis
 - Dense sand-like material – Peak undrained strength S_{up} but no higher than peak drained strength S_{dp}
 - Soft to medium clay-like material – 80 percent of S_{up}
 - Stiff clay-like material – 80 percent of S_{up} or 80 percent of the post-earthquake strength determined as per Section 7.4.3

Commentary: The use of 80 percent of S_{up} instead of 100 percent of S_{up} for stiff clay-like materials in Newmark deformation analyses is based on a recommendation in Makdisi and Seed (1978). The recommendation accounts for the fact that some deformation accumulates when the peak stresses exceed about 80 percent of S_{up} . The Newmark analysis assumes that there is no deformation until the selected strength is reached. The 80-percent value results in some computed deformation when stresses exceed 80 percent of peak.

2. Define a time history of average acceleration of the sliding mass $k(t)$ during the design earthquake. Values of $k(t)$ are in units of gravity. The maximum value of $k(t)$ is referred to as $k(max)$. One- or two-dimensional computer programs such as SHAKE, FLUSH, or QUAD4 can be used to compute $k(t)$ by modeling the propagation of the earthquake motion from bedrock to the zone of interest. The $k(t)$ time history is not the same as the acceleration time history output by SHAKE (or other programs) at the elevation of the base of the sliding mass. Rather, to obtain $k(t)$, one should take the time history of seismic shear stress output by the computer program at the base of the sliding mass and divide it by the total overburden pressure at that elevation (acceleration equals force/mass or stress/pressure). In this way, $k(t)$ will represent the average acceleration of the sliding mass and not the acceleration of individual layers or elements at the base of the sliding mass. Note that the total overburden pressure must not include the overburden stress caused by any free water above the ground level.

Commentary: In SHAKE, or other programs, potential yielding of the soil is ignored, so the computed accelerations, $k(t)$ can be higher than the yield acceleration. The analysis is said to be decoupled because it separates the computations of accelerations and the computations of deformations due to yielding, when in fact they occur simultaneously. However, comparisons with more rigorous coupled methods indicate that generally the uncoupled method is satisfactory. Wartman et al. (2004) conclude that uncoupled analyses are satisfactory for cases where the predominant frequency of the motion is at least 1.3 times the natural frequency of the soil mass, which is generally the case for earthquake shaking of dams and embankments.

3. During time intervals that $k(t)$ exceeds k_y , displacements are initiated. Displacements continue even after $k(t)$ becomes less than k_y , until the velocity of the mass becomes zero. Compute the total displacement of the sliding mass by double-integrating the portion of the $k(t)$ curve above and below k_y for time intervals where velocity is greater than zero (Figure 7.16).
4. If performing one-dimensional analyses at different points along the potential failure surface to compute $k(t)$, then the resulting displacements must be combined in order to estimate the displacement of the overall potential failure wedge. A method for combining the computed displacements is presented in Appendix 7D.

The deformations computed using a Newmark-type analyses are appropriate only if there is no significant softening (loss of stiffness) of the soil caused by cyclic mobility, as described in the second bullet point (ratcheting mechanism) in Section 7.5.1. This is because the Newmark-type analyses are based on the assumption that no displacements are initiated during time intervals when $k(t)$ is less than k_y , but significant displacements could occur during those time intervals if cyclic mobility and resulting accumulated strains are occurring.

Commentary: Newmark-type analyses should generally not be used if cyclic mobility is expected (i.e., if $CRR/CSR \leq 1.0$). Newmark-type analyses are based upon the assumption that there is no deformation when the sum of static plus seismic shear stresses is less than the available shear strength. But if cyclic mobility occurs, then significant deformations may occur due to the ratcheting mechanism described in Section 7.5.1

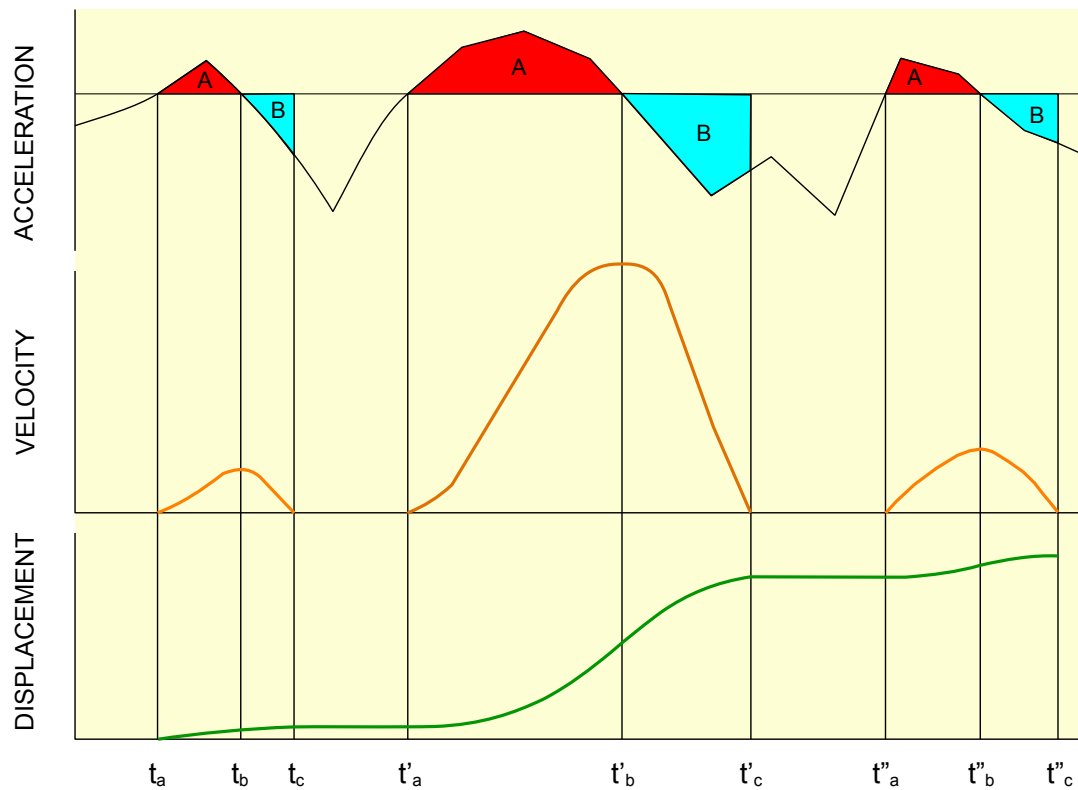


FIGURE 7.16 DOUBLE INTEGRATION TO OBTAIN DISPLACEMENT

even when the sum of the shear stresses is less than the available strength. Therefore, if cyclic mobility occurs, the Newmark-type analyses will under-predict deformations. In areas of low seismic hazard potential, the earthquake shaking may not be high enough to cause cyclic mobility. For small earthquakes, CRR/CSR may be greater than 1, such that Newmark-type analyses may be valid even for cases of upstream construction with loose sand-like material.

A simplified procedure for evaluating embankment deformations using the Newmark method was developed by Makdisi and Seed (1978). The method provides estimates of embankment deformations if the following information is known or a representative range of values can be established:

- The natural period of the embankment
- The maximum crest acceleration due to earthquake shaking
- The earthquake magnitude

The method was developed for embankments in the range of 100 to 200 feet high with a natural period ranging between 0.26 seconds and 5.22 seconds, based on several western earthquake records with magnitudes of about 6.5 to 8.25. A simplified formula for estimating the natural period of the embankment ($T = 2.6 H/V_s$ where H is the height of the embankment and V_s is the representative shear-wave velocity) is provided in Makdisi and Seed (1977). This simplified formula for the natural period is applicable to embankments with a cross section that is approximately triangular and therefore may not be applicable to non-trapezoidal coal refuse embankments. For embankment configurations that deviate from a triangular cross section, a range in natural period may be preferable to an approximate single value. Because of the limited range of conditions upon which it was based, the Makdisi and Seed method is not considered appropriate for evaluation of significant- or high-haz-

ard-potential coal refuse impoundments unless the embankment under consideration approximates a triangular configuration or more conservative configuration (with respect to seismically-induced deformation) and is founded on materials that are not susceptible to cyclic mobility.

7.5.5 Numerical Modeling with No Cyclic Mobility

If stress reversal and cyclic mobility are not likely (i.e., if $CRR/CSR > 1.0$, as discussed in [Section 7.5.1](#)), then Newmark analyses may be used. An alternative to Newmark analyses for this case is computer modeling based on finite-element or finite-difference analyses.

With finite-element modeling, the cross section of the structure is divided into a grid of discrete (finite) elements that connect to each other at node points. The elements are assigned material properties such as unit weight, Poisson's ratio, and stress-strain properties. Loads (forces) are applied at the node points, and displacements at the node points are computed by solving the stiffness matrix for the assembly of finite elements. Strains and stresses within elements are computed based on the displacements at the node points and the material properties.

With finite-difference modeling, the cross section of the structure is divided into a grid of lumped masses that interact with each other in accordance with constitutive equations based on the material properties. The displacements resulting from forces applied to the lumped masses in the grid are computed by solving the equations of motion (force equals mass times acceleration) at sequential time steps.

One of the key issues is assigning appropriate material properties (especially stress-strain properties) to the elements. Various non-linear soil models have been developed that, when used properly, can reasonably model material behavior when cyclic mobility does not occur. The soil models can be complex, and using them without fully understanding them can lead to errors. The results of the analyses are often sensitive to relatively minor variations in the parameters used to define the stress-strain properties. Checking the sensitivity by varying the parameters is an important part of the analysis. It is also important to check the model output to be sure that the pattern of stresses and strains across the cross section of the structure appears reasonable.

7.5.6 Numerical Modeling Considering Cyclic Mobility

If stress reversal and cyclic mobility are likely, (i.e., if $CRR/CSR < 1.0$) then the evaluation of deformations becomes highly uncertain, and Newmark analyses ([Section 7.5.4](#)) are not appropriate. Finite-element or finite-difference numerical models can be used, but the stress-strain models must have special provisions to account for cyclic mobility. These models are particularly complex because they model the S-shaped, stress-strain curve associated with cyclic mobility (very low stiffness at low to moderate strains followed by dilation and increasing stiffness at high strains). An example of such a stress-strain model is presented in Byrne et al. (2004). It is particularly important to check the output of these analyses for sensitivity to modeling parameters and for reasonableness. The U.S. Army Corps of Engineers demonstrated a procedure using commercially available finite-difference software (FLAC) and a modified version of the UBSAND model (Byrne et al., 2004) to conduct a deformation analysis for a dam in California, including comparison of the results with somewhat more simplified methods (Perlea et al., 2009).

Cyclic mobility is most likely to be a concern for cases of upstream construction in areas of medium to high seismic risk. Deformation analyses of complex embankment-foundation configurations and situations where significant zones of the structure are subject to cyclic mobility require experience with numerical analysis techniques (e.g., finite element and finite difference) and soil behavior constitutive models. An experienced user of the selected modeling software for deformation analyses should be involved in the modeling and/or validation of the results.

7.5.7 Acceptable Deformations

Once estimates of deformation have been made, the question arises as to what values of deformation are considered acceptable and what values are considered excessive. For embankments that do not retain liquids, fine coal refuse, or similar materials, deformations are not normally a problem so long as the embankment is stable. For dams or embankments that do retain liquids, fine coal refuse, or similar materials, deformations should be small enough that:

- Freeboard is not significantly compromised.
- Cracking through the dam, which affects the integrity of the dam for retaining liquids or might allow a release of material, does not occur.
- Appurtenant structures that affect dam safety are not severely damaged.
- Affected structures can be repaired before they might deteriorate further and pose a greater hazard.

The following are generally considered acceptable:

- Downstream analyses – Computed displacements or deformations less than 25 percent of the available freeboard and less than 3 feet.
- Upstream analyses – Computed displacements or deformations less than 25 percent of the available freeboard and less than 6 feet.

7.6 EMBANKMENT MODIFICATIONS FOR IMPROVING STABILITY OR RESISTANCE TO DEFORMATIONS

Measures to improve the seismic stability and the resistance to deformations of new and existing facilities can be grouped into the following general categories:

- Changes to embankment geometry (e.g., flatter slopes, buttressing, wider coarse refuse zone)
- Drainage control measures (including both internal and surface drainage)
- Soil/refuse improvement or reinforcement
- Increased freeboard

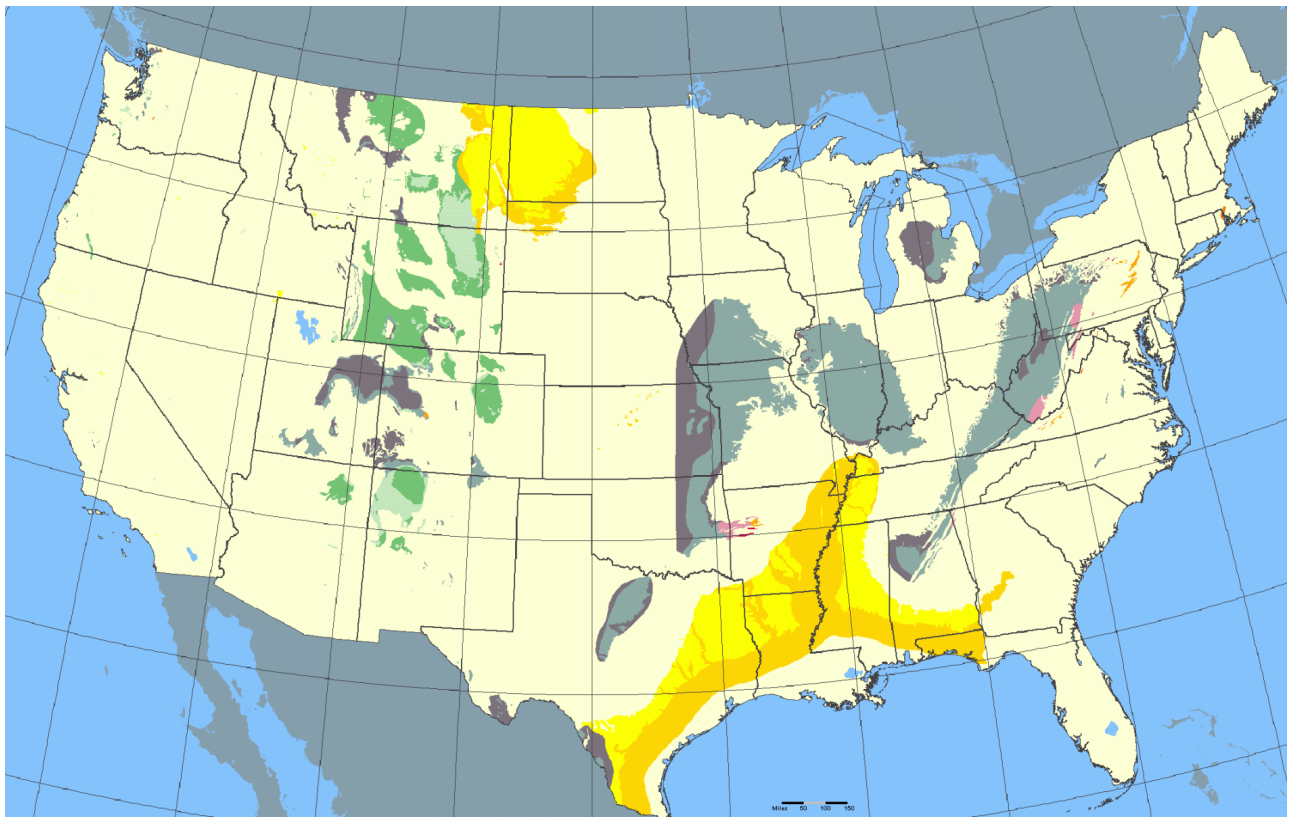
These measures are discussed in Chapter 6.

7.7 SEISMIC HAZARD ASSESSMENT (SEISMICITY)








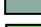


The purpose of a seismic hazard assessment is to estimate the appropriate design earthquake(s) for a site in terms of earthquake magnitude (M) and peak ground acceleration (PGA) and, when needed, to define representative time histories of ground motions.

This discussion of recommended procedures for deriving the seismic hazard is intended to be applicable in the U.S. where coal is mined. [Figure 7.17](#) shows the various regions where anthracite, bituminous and lignite coals are mined. Although the greatest amount of coal production is from the western U.S., the type of coal processing in that region does not typically require the construction of tailings dams for coal refuse. Accordingly, the procedures defined to derive seismic hazard place emphasis on eastern U.S. conditions, which are different from the western U.S. in many respects, as discussed in [Section 7.7.1](#).

Anthracite coal is mined in eastern Pennsylvania. Bituminous coal deposits in the eastern U.S. are found in the Appalachian, Illinois, Michigan, and the Western Interior Basins, with some bituminous coal also found within the Gulf Coast lignite deposits ([Figure 7.17](#)). These sources, primarily anthra-



LEGEND

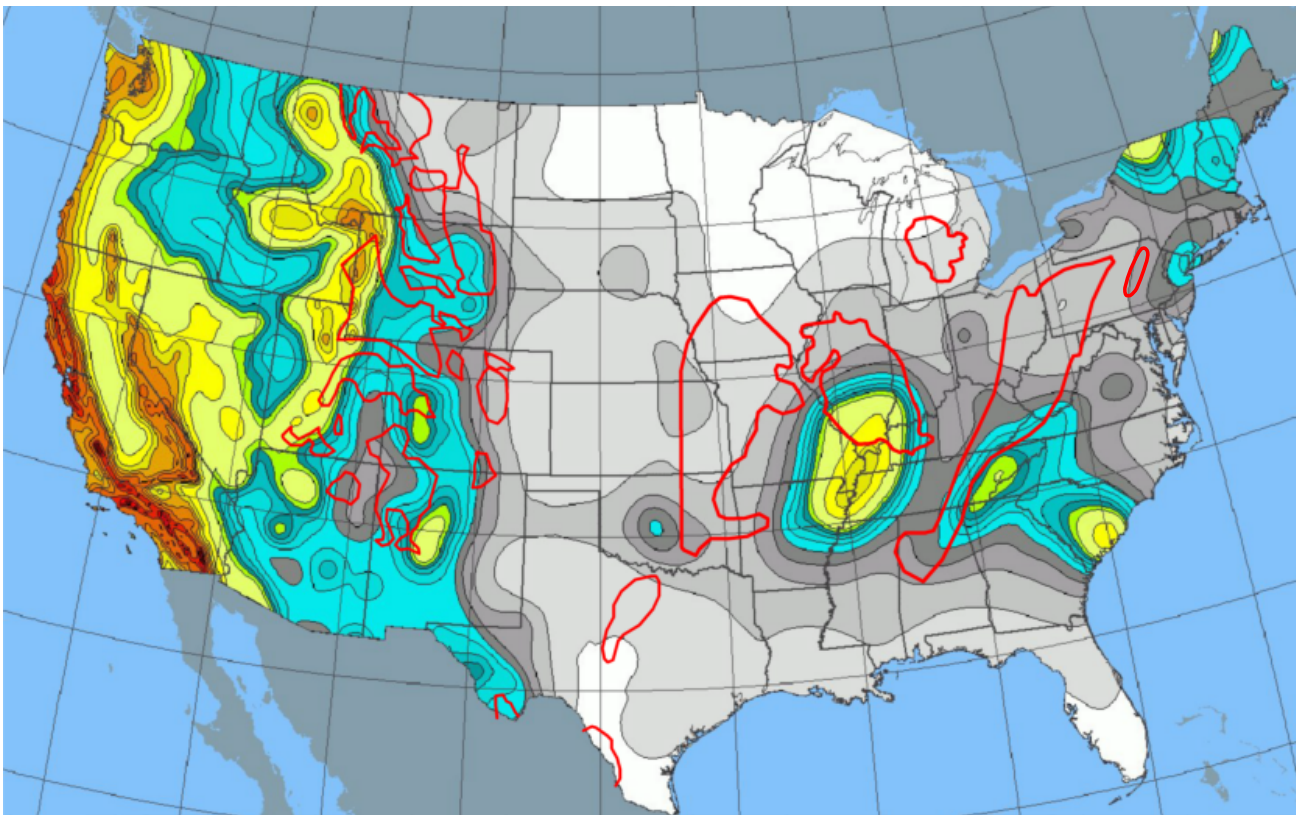
	ANTHRACITE/OTHER USES
	ANTHRACITE/POTENTIALLY MINABLE
	LIGNITE/OTHER USES
	LIGNITE/POTENTIALLY MINABLE
	LOW VOLATILITY BITUMINOUS/OTHER USES
	LOW VOLATILITY BITUMINOUS/POTENTIALLY MINABLE
	MEDIUM AND HIGH VOLATILITY BITUMINOUS/OTHER USES
	MEDIUM AND HIGH VOLATILITY BITUMINOUS/POTENTIALLY MINABLE
	SUB-BITUMINOUS/OTHER USES
	SUB-BITUMINOUS/POTENTIALLY MINABLE

NOTE: IMAGE WAS OBTAINED FROM THE USGS "NATIONAL ATLAS" WEB SITE AND WAS COMPILED BY THE USGS EASTERN ENERGY RESOURCES TEAM (EERT).

FIGURE 7.17 LOCATION OF U.S. COAL RESOURCES

cite in eastern Pennsylvania and bituminous in the Appalachian and Illinois Basins, are where coal needs to be processed and where coal refuse impoundments are required. Within these large areas, the seismic hazard is not uniform and can range from being nearly insignificant to an important design consideration.

The U.S. Geological Survey (USGS) has prepared national seismic hazard maps based on probabilistic analyses that define the variation of seismic hazard throughout the conterminous U.S., Alaska, Hawaii, Puerto Rico and the U.S. Virgin Islands, among other regions. Figures 7.18 and 7.19 present USGS seismic hazard maps respectively for the PGA with a 10 percent and 2 percent probability of exceedance in 50 years (~500 year and ~2,500-year return periods, respectively) in the conterminous U.S. Surface or near-surface active faults are the main sources of seismic hazard in the western U.S., whereas the eastern U.S. coal fields are affected primarily by three less-well-defined seismic sources: the New Madrid Seismic Zone, the Eastern Tennessee Seismic Zone, and the Charleston, South Carolina Seismic Zone (Figure 7.20). The coal fields with the most significant seismic hazard



LEGEND

PEAK HORIZONTAL GROUND ACCELERATION
IN % g WITH A 10% PROBABILITY OF
EXCEEDANCE IN A 50-YEAR PERIOD

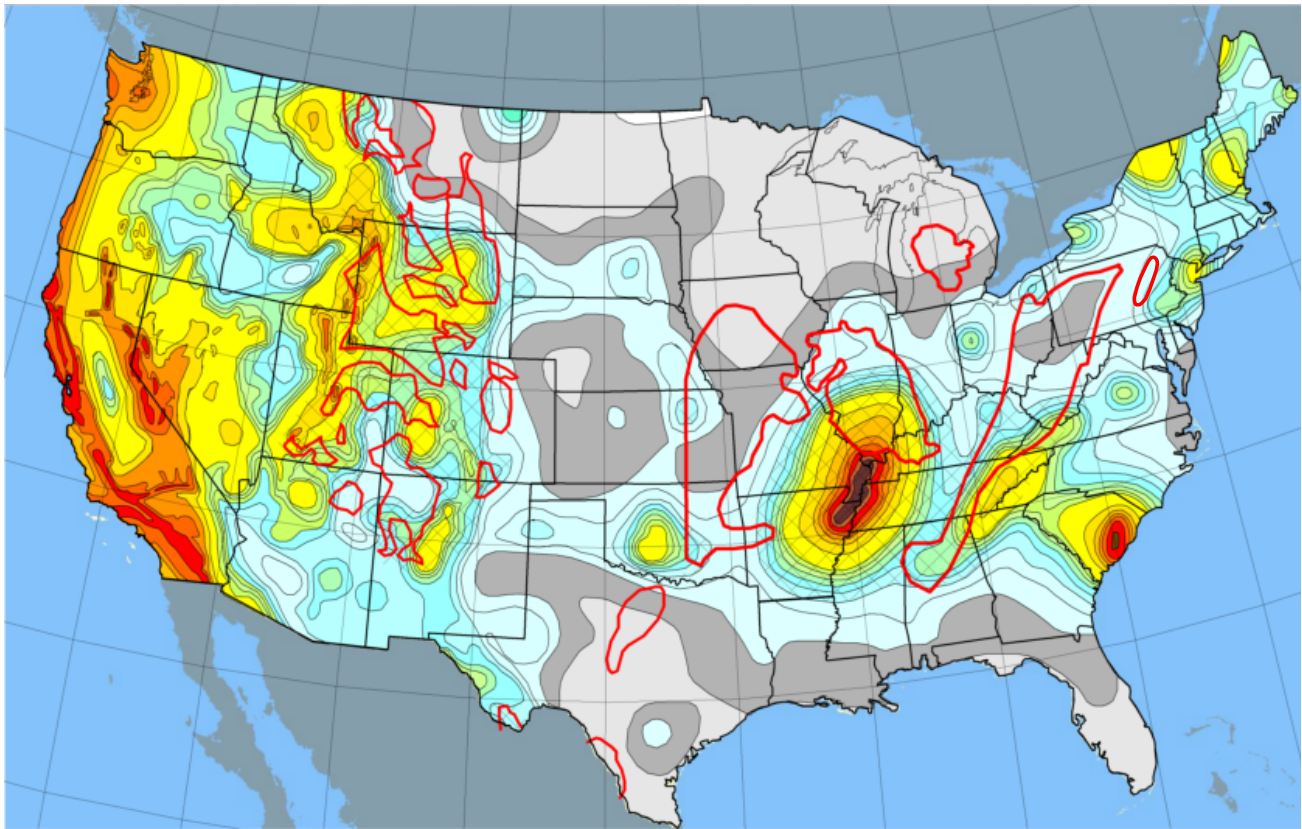
	20		5
	15		4
	10		3
	9		2
	8		1
	7		0
	6		

- NOTE: 1. IMAGE WAS OBTAINED FROM THE USGS "NATIONAL ATLAS" WEB SITE AND WAS COMPILED BY THE USGS GEOLOGIC HAZARDS TEAM.
2. ANTHRACITE AND BITUMINOUS COAL FIELDS ARE DENOTED BY RED BORDERS.

FIGURE 7.18 SEISMIC HAZARD MAP OF THE U.S. WITH OVERLAY OF MAIN BITUMINOUS COAL FIELDS

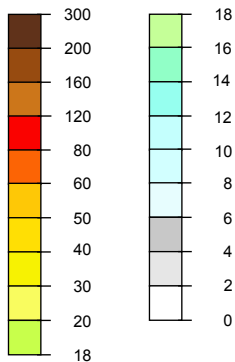
in the eastern U.S. are those in the southern half of the Illinois Basin. Portions of the coal fields in the southern Appalachians have moderate hazard. The Michigan and Western Interior Basins have very low hazard.

Seismic evaluation of coal refuse facilities and embankment dams requires the estimation of at least two ground motion parameters (earthquake magnitude and PGA). Another factor that needs to be considered in association with these two parameters is frequency content. Earthquake magnitude is critical because of the general relationship of magnitude and duration, as well as the strength of ground motion and related parameters such as frequency content, attenuation characteristics, etc. In essence, the larger the earthquake magnitude, the longer the earthquake, which implies that the soil will have to resist a greater number of ground-motion cycles of greater magnitude. Magnitude is not the only consideration in evaluating earthquake duration, as variations in fault mechanism, distance from the source, and local geologic conditions also contribute to duration, but acceptable practice is to consider



LEGEND

PEAK HORIZONTAL GROUND ACCELERATION IN % g WITH 2% PROBABILITY OF EXCEEDANCE IN A 50-YEAR PERIOD (2475-YEAR RETURN PERIOD).

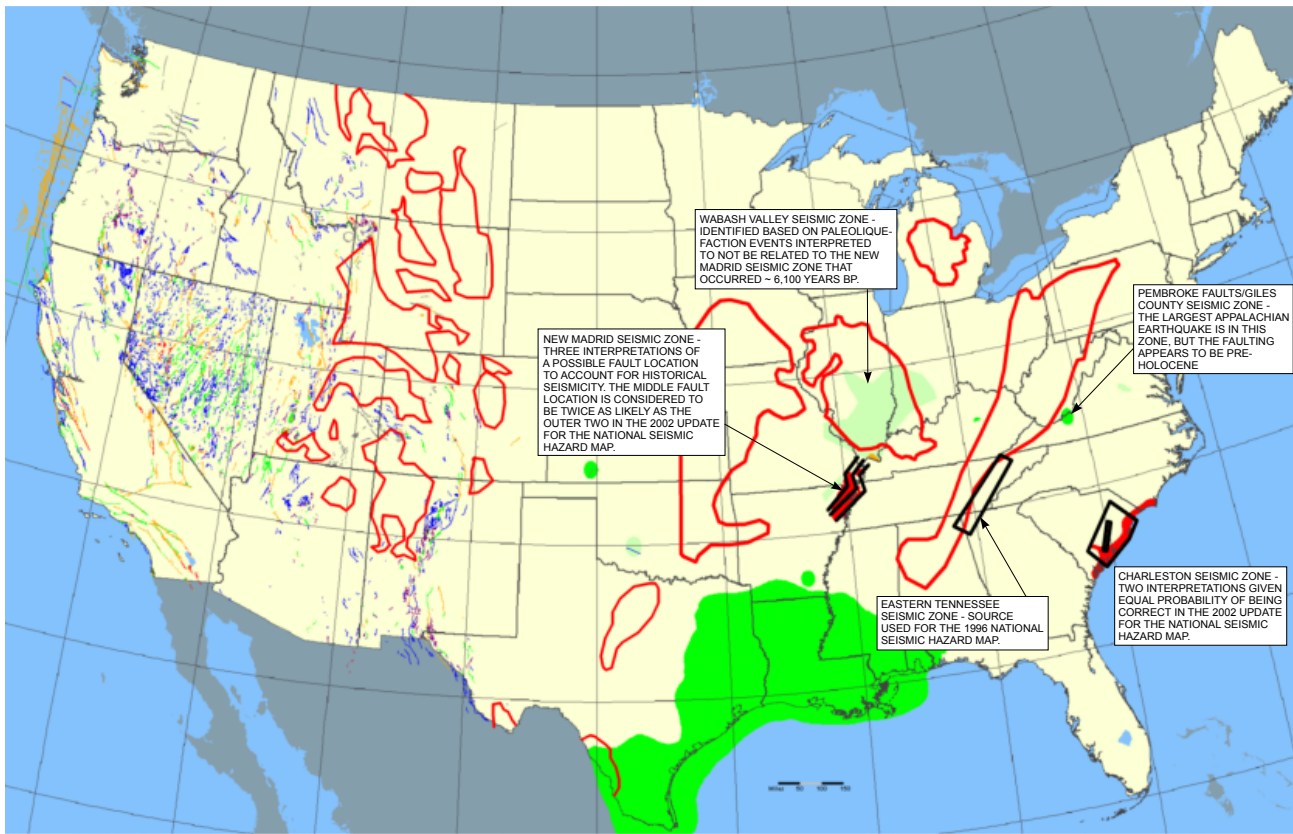


ZONE WHERE COMPLETE DSHA OR PSHA IS REQUIRED FOR EVALUATION OF SEISMIC HAZARD. BY INFERENCE, A SIMPLIFIED EVALUATION OF SEISMIC HAZARD IS PERMISSIBLE IN ALL OTHER AREAS.

- NOTE: 1. IMAGE REDRAWN FROM 2002 HAZARD MAP FOR A 2% PROBABILITY OF EXCEEDANCE IN 50 YEARS FROM THE USGS "NATIONAL ATLAS" WEB SITE.
 2. ANTHRACITE AND BITUMINOUS COAL FIELDS ARE DENOTED BY RED BORDERS.

FIGURE 7.19 ILLUSTRATION OF MODERATE- TO HIGH-HAZARD REGION

duration as a function of magnitude (Youd et al., 2001). PGA is the most commonly used parameter to define the strength of ground motion, but its significance also depends on frequency content. The actual seismic hazard will depend on the combination of duration and ground motion strength. With respect to dams and embankments, a single cycle of high PGA at a high frequency (in the range of 0.25 to 0.45g at a predominant frequency of 25 Hz) will likely not be as significant as a larger number of cycles of lower acceleration (in the range of 0.10 to 0.15g at 1 Hz). The reason for this is that for a dam to be significantly excited by earthquake ground motion, some portion of the ground motion must be close to the predominant frequency of the dam. A simple method for estimating the predominant frequency of an embankment based on height and shear-wave velocity of the embankment materials is provided by Makdisi and Seed (1977). For a typical coal refuse dam ranging in height from 100 to 400 feet and with



LEGEND

AGE OF QUATERNARY FAULTING

- HISTORIC
- HOLOCENE (< 15,000 YEARS AGO)
- LATE QUATERNARY (< 130,000 YEARS AGO)
- MID-LATE QUATERNARY (< 750,000 YEARS AGO)
- QUATERNARY (< 1.6 MILLION YEARS AGO)
- POSSIBLY OLDER THAN QUATERNARY
- OBSERVED EVIDENCE OF PALEOLIQUEFACTION

- NOTE: 1. IMAGE WAS OBTAINED FROM THE USGS "NATIONAL ATLAS" WEB SITE AND WAS COMPILED BY THE USGS GEOLOGIC HAZARDS TEAM.
2. BITUMINOUS COAL FIELDS ARE DENOTED BY RED BORDERS.

FIGURE 7.20 QUATERNARY FAULTS AND SIGNIFICANT SEISMIC SOURCES WITH OVERLAY OF MAIN BITUMINOUS COAL FIELDS

average shear wave velocities ranging from 500 to 1,600 ft/sec, the predominant frequency for the first mode of vibration could range from about 0.5 to 6 Hz. Accordingly, coal refuse dams are more likely to be affected by low-frequency ground motion, implying that more than one earthquake source may need to be considered in order to fully characterize the seismic hazard at a given site.

FEMA (2005b) defines the following design earthquakes:

- Maximum Credible Earthquake (MCE) – The MCE is the largest earthquake magnitude that could occur along a recognized fault or within a particular seismotectonic province or source area under the current tectonic framework.
- Maximum Design Earthquake (MDE) or Safety Evaluation Earthquake (SEE) – This is the earthquake that produces the maximum level of ground motion for which a structure is to be designed or evaluated. The MDE or SEE can be set equal to the MCE or to a design earthquake less than the MCE, depending on the circum-

stances. Factors to consider in establishing the size of MDE or SEE are the hazard potential classification of the dam (FEMA 2004a), criticality of the project function (water supply, recreation, flood control, protection of the environment, etc.), and the turnaround time to restore the facility to operability. In general, the associated performance requirement for the MDE or SEE is that the project performs without catastrophic failure (such as uncontrolled release of a reservoir) although significant damage or economic loss may be experienced. If the dam contains a critical water supply reservoir, the expected damage should be limited to an extent that allows the project to be restored to operation within an acceptable timeframe.

- **Operating Basis Earthquake (OBE)** – The OBE is an earthquake that produces ground motions at the site that can reasonably be expected to occur within the service life of the project. The associated performance requirement is that the project functions with little or no damage and without interruption of function. The purpose of the OBE is to protect against economic losses from damage or loss of service. Therefore, the return period for the OBE may be based on economic considerations.

Coal refuse impoundments and other mining dams often have significant or high hazard potential, and recommendations for selection of the MDE and seismic hazard assessment are presented in [Table 7.6](#). To protect site operational personnel, the public and the environment, it is necessary to design coal refuse impoundments having high hazard potential so that catastrophic failure does not occur. This is normally accomplished by considering the MCE when developing the design earthquake. The MCE might be represented by more than one earthquake event (i.e., from near-field and far-field sources) for which the structure should fail catastrophically. For coal refuse impoundments and dams having significant hazard potential, some federal dam safety agencies are giving consideration to events with return periods of the order of 2,500 years for design earthquakes. Further guidance on return-period criteria for significant- and high-hazard-potential dams is anticipated in the future from federal dam safety agencies.

Although the OBE does not typically govern the safe design of a coal refuse impoundment, it is still recommended that an OBE be defined on the basis of its probability of occurrence during the life of the dam. A 500-year (or more precisely 475-year) return period is consistent with the basis for defining an OBE in some conventional building codes and corresponds to one of the hazard maps published by the USGS (corresponding to a 10-percent probability of non-exceedance event for a 50-year lifetime), as shown on [Figure 7.18](#). The OBE earthquake parameters should be used to check the reasonableness of the design MCE. It is expected that the MCE will be a remote event with a PGA substantially higher than the OBE.

7.7.1 Analytical Procedures

Two approaches, probabilistic seismic hazard analysis (PSHA) and deterministic seismic hazard analysis (DSHA), are commonly applied to estimation of earthquake ground motions at a site. Fundamentally, only a DSHA can be used to estimate the Maximum Credible Earthquake (MCE). In PSHA, an MDE is associated with a return period far beyond the life span of the structure and is associated with a very low probability of occurrence.

7.7.1.1 Deterministic Seismic Hazard Analysis (DSHA)

The basic steps in a DSHA are as follows:

1. Develop a seismotectonic model. Review and summarize the basic geology and tectonics of a region surrounding the site (approximately 322-km radius) with particular attention to specific seismic sources, both area sources (provinces) and linear

TABLE 7.6 MDE AND SEISMIC HAZARD ASSESSMENT RECOMMENDATIONS

Dam Hazard Potential Classification	Maximum Design Earthquake (MDE)	Seismic Hazard Assessment	
		Low-Seismic-Hazard-Potential Area ⁽¹⁾	Moderate- to High-Seismic-Hazard-Potential Area ⁽¹⁾
High Hazard Potential	MCE ⁽²⁾	Simplified Minimum EQ and Simplified Design Ground Motion ⁽³⁾ or Site-specific DSHA ⁽²⁾ supported by PSHA ⁽⁴⁾	Site-specific DSHA ⁽²⁾ supported by PSHA ⁽⁴⁾
Significant Hazard Potential	MDE ~ 2500 return period ⁽⁵⁾	USGS EQ Hazard Maps or Site-specific PSHA	USGS EQ Hazard Maps or Site-specific PSHA

- Note:
1. Low-seismic-hazard-potential areas, as defined in this Manual, are distinguished using the USGS Earthquake Hazard Maps for a return period of 2,500 years with a $PGA \leq 0.1g$ and $M \leq 5.5$. All other areas are considered moderate- to high-seismic-hazard-potential areas.
 2. The Maximum Credible Earthquake (MCE) derived on the basis of a DSHA, as described in Section 7.7.1.1, is recommended as the MDE for high-hazard-potential dams based on FEMA (2005b). If a PSHA is used to establish the MDE for a high-hazard-potential facility, the designer should be able to demonstrate that the probability of occurrence is very remote (the actual return period may be a function of the seismic hazard area and tectonic conditions).
 3. See Section 7.7.3.7 for Simplified Design Ground Motion and Simplified Minimum Earthquake (EQ) description.
 4. The results of a Probabilistic Seismic Hazard Assessment (PSHA) can aid in demonstrating that the probability of catastrophic failure is very remote and in deciding whether mean, or mean-plus-one standard deviation or greater estimates of ground motion, would be justified for the MDE from the deterministic ground motion analysis to achieve an acceptably low probability of exceedance (FEMA, 2005b).
 5. For a significant-hazard-potential facility, the designer should be able to demonstrate that the probability of catastrophic failure is remote. The actual return period may be a function of the seismic-hazard area and tectonic conditions (e.g., consideration of a return period of the order of 2,500 years may be reasonable for low-seismic-hazard areas).

sources (faults). Note that a 332-km (200-mile) potential radius of influence has been chosen in order to account for the susceptibility of fine tailings to liquefaction effects from large, distant earthquakes.

2. Conduct a review of the seismic history of the site's region; locate the epicenters of all significant earthquakes and plot these earthquakes on a map that shows magnitude values.
3. Relate these epicenters to the mapped sources defined in Step 1.
4. Based on the results of Step 3, postulate a group of conceivable MCEs by selecting the most severe earthquake within or along each source that could be larger than the largest historical earthquake and "move" each earthquake to the point on the respective source nearest to the site.
5. Derive the ground motion at the site in terms of PGA on the basis of regionally applicable attenuation functions (i.e., relationships that allow the estimation of ground motion parameters at the site as a function of earthquake magnitude, source-to-site distance, and soil conditions at the site).
6. From the various PGAs obtained in Step 5 for the group of conceivable MCEs from Step 4 (applying the minimum distances from source-to-site), determine the most severe ground motion and classify this motion as the MCE. In the case of dams and embankments, the most severe earthquake event is not simply a function of the site-specific PGA, so it might not be apparent that a single event controls. A distant,

large-magnitude earthquake might not be associated with a PGA as high as for a smaller magnitude, nearer event, but such a distant earthquake could pose a greater threat because of its greater energy content and potential to induce more cycles of significant vibrations around the natural damped frequency of vibration of the structure-foundation system. Consequently, an examination of representative ground motions for more than one event might be necessary (Step 7).

7. Associate the MCE ground motion(s) to time history(ies) of ground motion consistent with the magnitude of the source and, with lesser emphasis, the calculated PGA from that source.

The ground conditions for which the selected attenuation functions in Step 5 are applicable require consideration when determining where on or in the ground the derived ground motion should be applied in site-specific dynamic analyses of the structure-foundation system. For example, some attenuation functions are only applicable to site conditions characterized by firm rock and thin, very stiff soil. Hence, the derived ground motion at a site with less stiff or thicker soil overburden should be applied at the top of rock, rather than at the ground surface. Depending on the site conditions, this derivation of ground motion at the top of relatively soft ground could be accomplished using the SHAKE program (Schnabel et al., 1972) or other similar approach as further discussed in [Section 7.4.2.2.1](#) and [7.5](#).

7.7.1.2 Probabilistic Seismic Hazard Analysis (PSHA)

A PSHA requires the same basic input as the DSHA in terms of the definition of seismotectonic models and attenuation functions to characterize site ground motion. However, the results from PSHA and DSHA are fundamentally different. PSHA addresses the chance of a given level of ground motion being exceeded from all possible earthquakes.

The methodology used for the PSHA is well established in the literature (Cornell, 1968; McGuire, 1976; McGuire, 1978). PSHA is the methodology used by the USGS to derive the seismic hazard of the United States, and details of the procedures followed are described by Frankel et al. (1996). Calculation of the seismic hazard requires specification of the same inputs as required for the DSHA, except with the additional requirement that the uncertainties associated with each input need to be quantified:

- Source geometry – the geographic description of the seismic sources in the region of influence around the site. A seismic source is a portion of the earth associated with a tectonic fault or (if individual faults cannot be identified) with an area/province of homogeneous seismicity. Source geometry determines the probability distribution of distance R from the earthquake to the site $f_R(r)$.
- Seismicity – the rate of occurrence ν and the magnitude distribution $f_M(m)$ of earthquakes within each seismic source.
- Attenuation functions – the definition of attenuation functions is the same as with the DSHA, except that it is important to define the uncertainty of each possible function.

One consideration related to uncertainties with each input is how to weight the events within a seismic source and weight the influence of a source. The USGS report, “Documentation for the 2002 Update of the National Seismic Hazard Maps,” prepared by Frankel et al. (2002), explains the data, evaluations, judgments and assumptions behind their PSHAs for different regions.

Mathematically, the calculation of whether the annual probability $\lambda Y > y$ the ground-motion characteristic parameter Y , expressed in terms of peak ground acceleration PGA or spectral acceleration S_a for various frequencies of vibration, exceeds level y involves the summation, over seismic sources that may pose a threat to the site, of the following relationship:

$$\lambda Y > y = \sum_{i=1}^N v_i \left\{ \int_{r_{min}}^{r_{max}} \int_{m_l}^{m_u} P[Y > y | m, r] f_{M,R}(m, r) dm dr \right\}_i \quad (7-7)$$

where:

- N = number of the nearby seismic sources, including both line sources (i.e., active faults) and area sources
- v_i = annual mean rate of occurrence of earthquakes generated by source i with magnitudes between m_l and m_u
- r_{min} = minimum source-to-site distance for source i
- r_{max} = maximum source-to-site distance for source i
- m_l = lower-bound values of magnitude for source i
- m_u = upper-bound values of magnitude for source i

and:

- $P[Y > y | m, r]$ is the conditional probability that the site may be struck by a ground motion with parameter $Y > y$ generated by an earthquake of magnitude $M = m$ with epicenter in source i at distance $R = r$ from the site.
- $f_{M,R}(m, r)$ is the joint probability density function of magnitude M and distance R for source i

Hence the expression within brackets in Equation 7-7 is the probability that at the site an earthquake with parameter $Y > y$ will occur because a seismic event of magnitude m ($m_l \leq m \leq m_u$) originated anywhere in source i .

Ground motion at the site is modelled by an attenuation function, which is a mathematical equation that defines the relationship between the ground-motion parameter Y , earthquake magnitude, source-to-site distance and local soil condition at the site. The attenuation function is used to compute the conditional probability in the integrand of Equation 7-7. Note that the USGS hazard maps are for a “firm-rock site condition, where the shear-wave velocity averaged over the top 30 meters (V_{s30}) is 760 meters per second (boundary of NEHRP site classes B and C).” On a practical level, this means that the USGS has not tried to model site-specific conditions. If there are site-specific conditions that need to be accounted for, an extra step in the analysis is required.

If a scalar parameter such as peak ground acceleration (PGA) is chosen, the repetition of these calculations for different values of the threshold level y allows the construction of the seismic hazard curve for the site (a plot of annual probability of exceedance, or return period, versus the parameter level). If the parameter of the ground motion is expressed in terms of spectral acceleration, $S_a(f, \xi)$, a family of seismic hazard curves for the site can be evaluated for various values of f and ξ (f is the frequency and ξ is the percentage of the critical damping). These results based on spectral ordinates can also be rearranged in order to obtain Uniform Hazard Spectra (UHS) (McGuire, 1974), which represent the response spectra whose ordinates are associated with the same probabilities of exceedance at the site. These methods that make use of spectral quantities include those that employ only a high-frequency parameter such as PGA.

7.7.1.3 DSHA versus PSHA

Regardless of whether seismic hazard is defined by a DSHA or PSHA methodology, the results still have some degree of uncertainty. The advantage of PSHA is that it can incorporate a range of uncer-

tainties inherent in the seismotectonic model, occurrence frequency, and ground-motion attenuation relationships, that is not possible with a DSHA approach. However, PSHA has some significant limitations, especially in terms of selecting ground motion parameters that can be considered representative of a maximum credible event (MCE). A discussion of the limitations of the PSHA approach for defining the seismic input for critical facilities is presented by Krinitzsky (1995).

Selection of the design ground motion parameters from a PSHA is complex because there are infinite points (choices) on the hazard curve. It is not practical to pick a point from a hazard curve and be able to relate it to the ground motion representing a reasonable worst case. Furthermore, the ground motion derived from PSHA does not have a clear physical meaning (Wang et al., 2003), because the total hazard (total annual frequency of exceedance) at a site is the sum of the individual hazards (annual frequency of exceedance) and is not associated with any individual earthquake, but potentially many earthquakes. For example, on the 2002 USGS national seismic hazard maps, the total seismic hazard in Chicago, Illinois was derived from a series of earthquakes with magnitudes ranging from 5.0 to 8.0 at distances ranging from 0 to 500 km (Harmsen et al., 1999). Therefore, it can be difficult to identify from the results of a PSHA a specific earthquake that represents a worst case scenario.

Although the earthquake magnitude and PGA are not physically related, the USGS Earthquake Hazards Program now provides probability mapping for earthquake magnitude (Moment Magnitude M within 50 km of a site as discussed in [Section 7.7.2.5](#)) as well as PGA, which allows for definition of a local earthquake event by M and PGA for a selected return period or probability. (The USGS provides maps of PGA for return periods up to a 2,475-year event, although the PGA for a 4,975-year return period can be computed on the basis of available site-specific deaggregations.) The use of the USGS hazard mapping to arrive at these parameters does not provide any specific insight to the controlling source and earthquake event, or a representative ground motion, but should provide a reasonable set of design parameters for lower seismic hazard sites for a given return period or probability, as each variable would be statistically represented by the maximum mean value. Then actual ground motion records for locations within 50 km of past earthquakes of magnitude “ M ” not less than the design M can be adopted in design, in lieu of attempting to identify the controlling source earthquakes and to derive attenuated ground motions from each of those events.

The primary advantage of the DSHA approach in terms of defining the seismic hazard for a structure like a dam or embankment is that it deduces a particular seismic scenario, consisting of the postulated occurrence of an earthquake of a specified size at a specified location upon which a ground-motion-hazard evaluation is based. A DSHA approach provides ground-motion parameters from those earthquakes that have the most significant impacts. This is particularly advantageous for seismic design and analysis of dams and embankments.

As noted previously, the design basis for high-hazard-potential dams and impounding embankments is generally the MCE. Fundamentally, probability is not a consideration for the MCE, except as verification that the MCE is an extremely remote event. Previous designs for some coal refuse impoundments in some areas of the northern Appalachian and Illinois Basins have associated a 10,000-year return period with a MCE event, absent a detailed site-specific study or the availability of a detailed study from a similarly critical nearby structure/facility. This return period is at the upper end of typical recommendations (USCOLD, 1999). [Table 7.6](#) presents recommendations for the seismic hazard assessment (and design earthquake), and the subsequent sections of this chapter describe development of the design ground motion based on a DSHA, which yields an earthquake magnitude, peak horizontal ground acceleration, and associated time histories/response spectra. The procedures presented herein include verification that the design earthquake is an extremely remote event, through comparison with published return periods or results of a PSHA. If a designer elects to base the design for a high-hazard-potential dam on a PSHA, the return period should be established such that the

MDE can be equated to the controlling MCE, as cited in FEMA (2005b). Further PSHA guidance on return-period criteria for significant- and high-hazard-potential dams is anticipated in the future from federal dam safety agencies.

7.7.2 Seismotectonic Modeling

Most seismotectonic studies and publications focus on the western U.S. where there is a relative abundance of data and observations. The seismotectonic modeling of the central and eastern U.S. requires that the differences between the eastern and western U.S. be appreciated. The following characteristics of eastern U.S. earthquakes represent significant differences when compared to the western U.S.

- More than an order of magnitude lower seismicity rates (longer recurrence periods for the same magnitudes).
- General lack of surface faulting, such that it is difficult to define source models
- Slower attenuation of ground motions with distance, which implies larger areas of damage for the same earthquake magnitude.
- Higher high-frequency content of seismic ground motions to larger distances.
- Relatively higher site amplification where soft soil is over rock (considered to be more significant in glaciated areas where the contact with highly competent rock is abrupt; Youd et al., 2001).
- Greater uncertainty in quantitative hazard assessments because the historic seismicity record (300 years) is too short compared to the recurrence periods of major damaging events.
- Few sets of eastern strong-motion data exist. They marginally constrain the attenuation of shaking with distance, as well as the dependence of local ground motion on magnitude, distance and depth of the earthquake.
- Higher frequency content of eastern earthquakes may lead to a greater number of cycles for the same magnitude.

In spite of the differences between eastern and western U.S. seismic events and the limitations of the eastern U.S. database, these factors can be accounted for in a seismic hazard analysis. The high-frequency motions associated with eastern earthquakes are generally limited to near-field rock sites. These motions tend to attenuate rapidly when they propagate through soil, which effectively reduces the amount of energy and the number of pertinent ground motion cycles that could contribute to the hazards of seismically-induced strength loss or ground deformation. Therefore, as noted by Youd et al. (2001), the duration differences between eastern and western soil sites are not likely to be significant when evaluating strength loss and ground deformations.

Compared with a plate boundary environment like California, an intra-plate environment like the central and eastern U.S. is difficult to characterize. Although there have been many recent advances in the understanding of earthquake occurrence based mainly on discoveries of paleoliquefaction phenomena, many gaps still exist in the knowledge of why and how often earthquakes occur in the central and eastern U.S., as summarized by the USGS Geologic Hazards Team (Crone and Wheeler, 2000) that supports the National Earthquake Hazard Reduction Program (NEHRP).

Defining a seismotectonic model for the central and eastern U.S. requires considerable judgment and is a subject of ongoing research. It is anticipated that it will be necessary to review the status of ongoing research whenever new seismic hazard assessments are required. This Manual includes some of the concepts and sources of information suitable for the derivation of seismic hazard at the time of publication, as summarized in the following subsections.

7.7.2.1 Regional Tectonic Framework

One of the major accomplishments with respect to the definition of seismic hazard in the central and eastern U.S. over the past 20 years is the definition of potential seismic sources on the basis of tectonic evidence. The zones where there has been Quaternary fault movement are summarized in [Figure 7.20](#). Fault sources are the dominant means for deriving seismic hazard in the western U.S. Fault sources are poorly defined in the central and eastern U.S., but recent work has identified a tectonic framework for earthquake occurrence, as summarized in Crone and Wheeler (2000). Recent data for the New Madrid Seismic Zone (NMSZ) is presented in Tuttle et al. (2002).

In terms of conducting a deterministic analysis, there is no agreement regarding the actual definition of the main seismic sources affecting the central and eastern U.S. Nevertheless, it is practical to use the sources that are currently defined by the USGS Geologic Hazards Team. The zones where Quaternary tectonic movements have been documented are predominantly in the New Madrid Seismic Zone, and the modeling of this zone has been considered to be as fault zones of varying probability, as shown in [Figure 7.20](#). This zone has significant influence to the southern Illinois Basin, as documented in the probabilistic hazard map shown in [Figure 7.18](#) for a 500-year return period and in [Figure 7.19](#) for a 2,475-year return period.

Another relatively recent discovery is the presence of paleoliquefaction in southern Illinois and Indiana ([Figure 7.20](#)), which was identified by Crone and Wheeler (2000) as the Wabash Seismic Zone. These widespread paleoliquefaction effects have been documented and interpreted to be associated with a large earthquake ($M \sim 7.5$) possibly centered in the Wabash Valley area between southern Illinois and Indiana that occurred about 6,100 years before the present (BP). Specific faults that produced the paleoliquefaction features have not yet been identified.

Within the Appalachian Basin coal fields, the most significant source is the Eastern Tennessee Seismic Zone, a belt of seismicity in northeastern Alabama, northwestern Georgia and much of eastern Tennessee ([Figure 7.20](#)). The largest historical shock was magnitude 4.6, and occurred in 1973. No evidence for larger prehistoric shocks has been discovered, yet the microearthquake data suggest coherent stress accumulation within a large volume (Chapman et al., 2002). The largest earthquake within the Appalachian system had a Modified Mercalli Intensity (MMI) equal to VIII ($M = 5.9$) and occurred on May 31, 1897 in Giles County, Virginia in the general area where evidence of Quaternary faulting has been uncovered. This faulting is referred to as the Pembroke Fault zone by Crone and Wheeler (2000). There is no surface expression of these faults and it is uncertain if they are due to tectonic movements or from solution collapse.

The third significant earthquake source in the eastern U.S. is the Charleston, South Carolina Seismic Zone. Paleoliquefaction data indicate that for characteristic large earthquakes in the Charleston, South Carolina region, the recurrence interval is approximately 550 years, as presented by Talwani and Schaeffer (2001). The USGS (Frankel et al., 2002) have assigned two source zones for this area with an equal probability of their validity. Although a significant seismic source in the eastern U.S., the effects of this zone do not significantly affect the Appalachian coal fields.

The definition of seismic source zones in the central and eastern U.S. based strictly on tectonics is still very much an evolving science. In conducting a deterministic analysis it will be necessary to carefully evaluate the most recent work of the USGS and other organizations, especially universities, involved with ongoing research into the identification of seismogenic tectonic structures. For example, the Mid-America Earthquake Center (MAE Center) is a good source of information for the central and eastern U.S. seismic hazard. The MAE Center, headquartered at the University of Illinois at Urbana-Champaign, is a consortium of nine core institutions funded by the NSF and each core university, as well as through joint collaborative projects with industry and other affiliations.

7.7.2.2 Historical Seismicity

The seismic hazard derived for locations in the central and eastern U.S. needs to be at least as severe as has been historically recorded. The National Earthquake Information Center of the U.S. Geological Survey and the Engineering Research and Development Center of the U.S. Army Corps of Engineers compile source and magnitude information for earthquake events. These sources also provide access to isoseismal maps of historical events and available strong motion records, although few are available for the central and eastern U.S. The seismic hazard evaluation process should consider the historical maximum Modified Mercalli Intensity experienced at the site, and the design ground motion should not be less than that corresponding to the maximum MMI. The correlation of MMI to PGA is not an exact science, but correlations developed for California such as developed by Wald et al. (1999) and adapted for use in the central U.S. by Atkinson and Kaka (2006) are worth considering.

7.7.2.3 Selection of Seismic Sources

To define the source zones for deriving seismic hazard, the distribution of earthquakes needs to be evaluated in the context of available information regarding Quaternary tectonic activity. In the western U.S., careful evaluation of surface and near-surface faults should be conducted in association with a review of historical seismicity, which is often of limited quality. It may be necessary to conduct site-specific studies of faults whose rupture could control the seismic design in order to determine their degree of activity and their physical characteristics, as summarized in detail by Slemmons and DePolo (1986). Such studies are seldom practical in the central and eastern U.S.

In many cases in the central and eastern U.S., earthquake distribution by itself is the basis for defining a seismic source. For example, the Eastern Tennessee Seismic Zone is defined primarily based on the distribution of instrumentally determined epicenters. The overall active zone in the New Madrid area has been similarly defined.

The seismic sources most critical to the central and eastern U.S. coal fields are those identified in [Figure 7.20](#). The fault sources that are significant to the definition of seismic hazard in the western U.S. coalfields are too numerous to describe in this Manual, and the reader is referred to lists and discussions provided by the USGS or state geological surveys. The interpretation presented in [Figure 7.20](#), which represents the current best interpretation of the USGS, and forms the basis for the National Seismic Hazard Maps (Frankel et al., 2002), examples of which are shown in [Figures 7.18](#) and [7.19](#), illustrates the current uncertainty with respect to the main sources affecting central and eastern U.S. coal fields. It should be emphasized that the presence of earthquakes is not an absolute criterion for delineating a seismic source zone. For example, the Wabash Valley Seismic Zone shown in [Figure 7.20](#) was developed based on the identification of paleoliquefaction phenomena. Other than for special areas of relatively high seismic hazard, the approach of the USGS to defining seismic hazard has been to construct hazard maps directly from the historic seismicity data following the procedure in Frankel (1995). The number of events greater than the minimum magnitude are counted on a grid with spacing of 0.1° in latitude and longitude. Accordingly, to develop the seismic hazard following a DSHA, it is necessary to develop source models more fully than the main sources defined by the USGS.

In addition to the USGS, there has been considerable effort by other organizations to delineate seismic sources in the central and eastern U.S. In particular, from 1981 to 1989, Lawrence Livermore National Laboratory (LLNL) developed a PSHA methodology for the eastern United States (Bernreuter et al, 1989), followed in 1993 by improvements in the handling of the uncertainties (USNRC, 1993). Differences between these results and those of a utilities-sponsored study (Electric Power Research Institute, 1989) led to the formation of the Senior Seismic Hazard Analysis Committee (SSHAC) to identify the sources of differences and give guidance on how to perform a state-of-the-art PSHA (USNRC,

1997). This work continues to be reviewed and updated (Savy et al., 2002). These documents provide different expert opinions regarding appropriate source models for the central and eastern U.S., and they are important sources for detailed information regarding the seismotectonics of the central and eastern U.S. Nevertheless, it is cautioned that the USGS modeling is not one of the source models considered, and that some of the experts involved in development of the seismic source models for the LLNL studies hold widely divergent interpretations, as documented in the review of the seismic hazard at USDOE sites (USDOE, 1996).

Another source of seismotectonic modeling information is the U.S. Army Corps of Engineers (USACE). The USACE seismic design manual, *Response Spectra and Seismic Analysis for Concrete Hydraulic Structures* (USACE, 1999), provides a detailed seismotectonic interpretation of the central U.S. in terms of a source model based on a comprehensive review of seismotectonic data, and it is a notable reference for the definition of seismic source zones in this area.

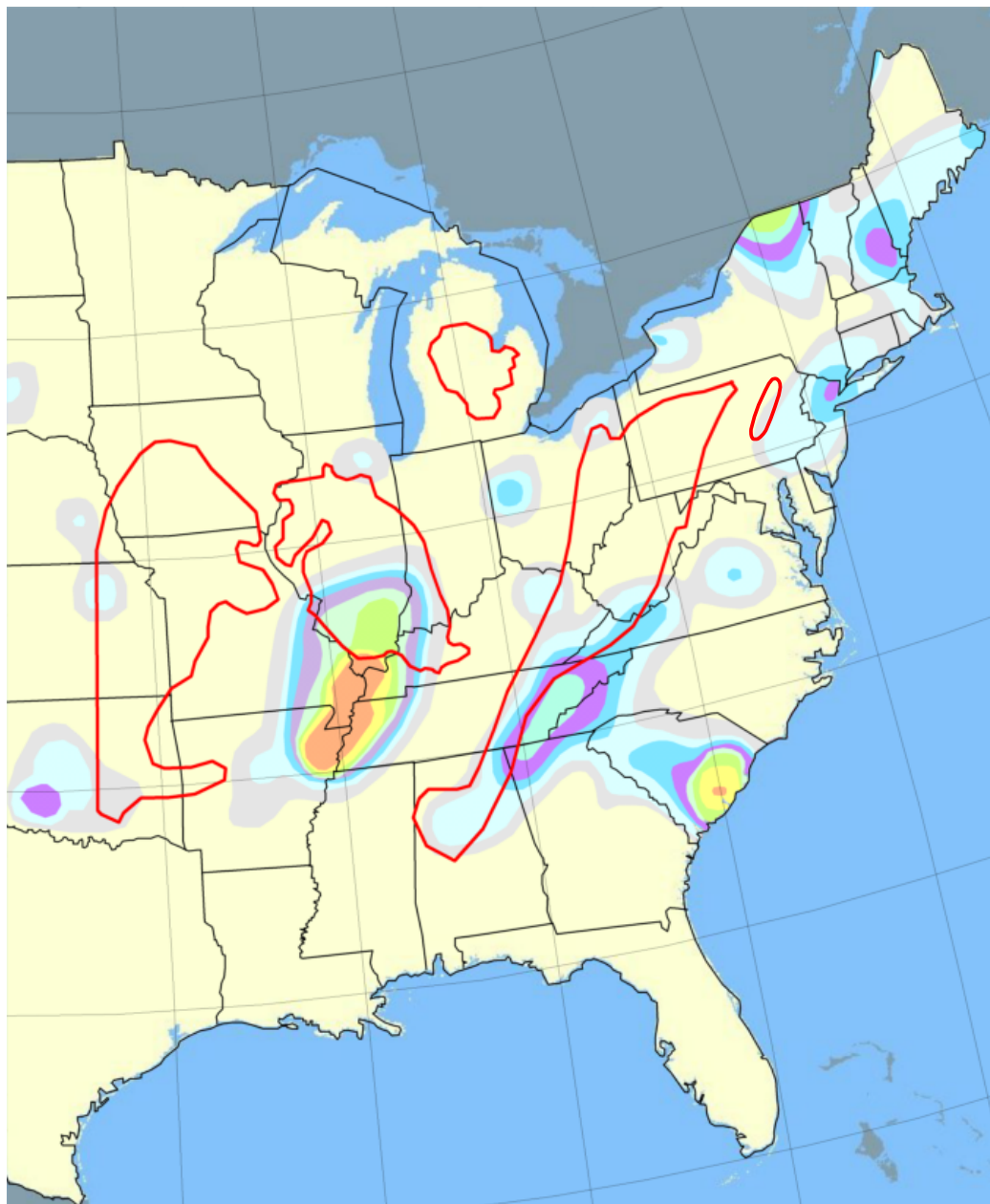
7.7.2.4 Maximum Magnitude

In either a deterministic or probabilistic analysis, it is necessary to identify the strongest earthquake that has occurred within each source and then determine if there is a reason to consider that a larger earthquake could reasonably be expected to occur. Substantial judgment is required for this assessment. For example, it may be reasonable to assume that the 1811-1812 earthquakes in the New Madrid Seismic Zone are a maximum event. However, the known historical seismicity in southern Illinois does not encompass the largest earthquake that could be produced in that area, given the widespread paleoliquefaction phenomena that have been mapped.

In an intraplate environment, the evaluation of maximum magnitude is especially problematic because the source mechanisms are poorly defined. Where source characteristics are well defined, such as along a mapped fault, common practice is to use relationships developed between earthquake magnitude and total fault length, rupture area, maximum displacement per event, fault slip rate and seismic moment (Slemmons and Depolo, 1986; Wells and Coppersmith, 1994 or several others). With some exceptions such as the Meers Fault in Oklahoma, these relationships can be applied only with considerable judgment in the central and eastern U.S.

DSHA is intended to define the worst-case ground motion and should therefore be based on the least favorable combination of earthquake source characteristics and location, and the strongest ground motion that could be generated by this scenario. In practice, DSHA generally uses the logarithmic mean or mean-plus-one-standard-deviation level of ground motion from predictive equations (Krinitzsky, 2002). If a mean plus a standard deviation is used, the ground motion will be conservative 84 percent of the time. A more detailed discussion of the difficulties in defining maximum magnitude is summarized by Bommer et al. (2004). Because of the uncertainties in the definition of maximum magnitude, the best approach is one of targeting a consensus opinion, such as is provided by the USGS Geologic Hazards Team (Frankel et al., 2002).

Another potential source of information regarding maximum earthquake magnitude is to consider probability of occurrence. In addition to the PGA hazard maps, the USGS (Frankel et al., 2002) also provides maps of the probability of occurrence of earthquakes of various magnitudes within specific distances of a given location as a function of return period. An example of a map depicting the probabilities (in terms of return periods) that an earthquake with $M > 5.5$ will occur within a distance of 50 km of different locations within the central and eastern U.S. is presented in [Figure 7.21](#). As this map was prepared by considering earthquake recurrence with a return period up to 10,000 years, the results show that large earthquakes are only reasonably conceivable in limited areas of the central and eastern U.S. and, conversely, that earthquakes of $M > 5.5$ are a remote possibility in most areas of the central and eastern U.S.



LEGEND

RETURN PERIOD IN YEARS FOR AN EARTHQUAKE OF $M > 5.5$ AT A DISTANCE OF LESS THAN 50 KM.

	9999
	7500
	4000
	3000
	2000
	1000
	500
	300

NOTE: 1. IMAGE REDRAWN FROM 2002 MAP BY THE USGS OF RETURN PERIOD FOR AN $M > 5.5$ EVENT AT A DISTANCE OF LESS THAN 50 KM.

2. ANTHRACITE AND BITUMINOUS COAL FIELDS ARE DENOTED BY RED BORDERS.

FIGURE 7.21 RETURN PERIOD FOR $M > 5.5$ EVENT AT A DISTANCE LESS THAN 50 KM

7.7.2.5 Earthquake Recurrence

The evaluation of earthquake recurrence for each source considered is a requirement of the PSHA. Recurrence is of interest to a DSHA if the distribution of earthquakes within a source as determined from the historical seismicity and geologic data as appropriate is suggestive that a maximum magnitude other than the historic maximum should be considered.

The determination of earthquake recurrence requires several steps:

1. Identification of both historical and instrumentally-located earthquakes within each postulated source.
2. Conversion of the available data into a common magnitude base. There are several magnitude scales, but for about the past 25 years it has been common practice to define magnitude in terms of seismic moment, as defined by Kanamori (1977) and Hanks and Kanamori (1979). Moment magnitude is the scale most commonly used for engineering applications and is the scale preferred for calculation of liquefaction resistance. The relationship between moment magnitude M and other commonly used magnitude scales can be reviewed as a chart published by Youd et al. (2001). In the central and eastern U.S., the most commonly derived magnitude scale is m_{blg} , which was developed by Nuttli (1973). Frankel et al. (1996) provide the following conversion to moment magnitude:

$$M = 3.45 - 0.473 m_{blg} + 0.145 (m_{blg})^2 \quad (7-8)$$

3. Evaluate the completeness of the earthquake catalog after the removal of statistically dependent events – aftershocks and foreshocks. Determination of catalog completeness is a function of location (e.g., earthquake history is better defined for a longer period in Charleston, South Carolina than in central Montana). Procedures for evaluating completeness are presented by Veneziano and Van Dyck (1985).
4. Formulate earthquake recurrence for each source. The most common means of defining recurrence is the Richter formula (Richter, 1958):

$$\log N = a - b m \quad (7-9)$$

where:

- m = earthquake magnitude
- N = number of earthquakes of magnitude m or greater per year per unit area
- a, b = constant coefficients defining a linear relationship between $\log N$ and m

This simple exponential recurrence model has been found to have good applicability for area sources, but there are many other ways to define the probability of earthquake recurrence, particularly when specific faults are considered (Schwartz and Coppersmith, 1986). It should also be noted that the simple Richter formula can be non-linear for the highest magnitudes and that caution should be used when estimating the recurrence of large magnitude events on the basis of limited historical data.

7.7.3 Design Ground Motion

The basic seismic data needed for determination of an MDE, including the MCE, is a time history(ies) representative of the source magnitude of the earthquake and a duration (number of cycles of strong ground motion) consistent with the source magnitude. The derivation of an MCE for a high-hazard-

potential dam involves a seismic-hazard assessment, and this Manual describes procedures for performing a seismic-hazard assessment using a DSHA with comparison to published probabilistic hazard assessments, such as those available from the USGS or the USNRC. The MCE should be shown to be an extremely remote event. FEMA (2005b) indicates that a PSHA can aid in deciding whether mean, or mean-plus-one-standard-deviation, or even greater estimates of ground motion are justified in a deterministic ground motion analysis for the MDE to achieve an acceptably low probability of exceedance. Until published guidance from federal dam safety agencies is available, the designer should consider that for high-hazard-potential facilities in areas of medium to high seismic hazard, the primary role of a PSHA is to serve as technical support in the selection of an MCE consistent with FEMA (2005b).

The OBE, as well as the MDE for significant-hazard-potential dams, can be defined on the basis of a probabilistic analysis, which could simply be obtained from published results of the USGS. As noted in the introduction to this chapter, a probabilistic analysis considering a 500-year return period can serve as the basis for defining an OBE, and a return period of the order of 2,500 years may be reasonable for establishing the MDE for a significant-hazard-potential dam.

Another means for evaluation of the results of a DSHA is to review the design basis for nuclear power plants, which have all been designed on the basis of a DSHA. The location of nuclear power plants with respect to U.S. coal fields is presented in [Figure 7.22](#). [Table 7.7](#) provides the Safe Shutdown Earthquake (SSE) peak horizontal ground accelerations (PGA) that formed the basis for seismic design for each nuclear plant. The SSE PGA values for these nuclear plants should be considered as minimum values for a MCE. The conservatism associated with the seismic input for a nuclear power plant has proven to be the overall spectral shape of their seismic input, rather than the PGA. Furthermore, earthquake magnitude values associated with the SSE are generally not defined, because the practice for defining seismic hazard in the 1960s and 1970s, when these nuclear power plants were licensed, was to base the design on Modified Mercalli intensity (MMI) relationships.

As noted in [Section 7.7.2](#), much of the areas mined for coal in the central and eastern U.S. have a low seismic hazard. For these areas a simplified approach is recommended for defining a minimum standard for seismic design. [Section 7.7.3.7](#) of this Manual proposes standard seismic inputs for design in areas of low seismic hazard, and these inputs are believed to be reasonably conservative for coal refuse impoundments. If the designer judges that less conservative inputs than recommended herein are appropriate, it is acceptable to perform a complete hazard analysis to justify less conservative project-specific and/or site-specific seismic design inputs. The following sections present more detailed information regarding the definition of design ground motion for an MCE for a high-hazard-potential dam.

7.7.3.1 Selection of Design Earthquakes

The MCE for each seismotectonic structure or source area within the region examined needs to be defined by a common parameter, preferably by moment magnitude M , but in a manner that is compatible with the attenuation function used to derive site ground motion. It is recommended that the maximum historical site MMI be evaluated as an additional estimate to site ground motion, but it is recommended that the historical MMI be converted to magnitude based on scientific evaluations of the ground effects. Such studies are usually available for the most significant historical events. For example, using a new method for evaluating magnitude by directly inverting observations of intensities, Bakun and Hopper (2004) determined a moment magnitude M of 7.4 (7.0 to 7.7 at a 95 percent confidence level) for the largest New Madrid earthquake in the 1811-12 sequence. Scientific publications for evaluation of the magnitude of historical earthquakes are generally available.

Where the earthquake history is incomplete or where there is no geologic evidence regarding past earthquake activity, judgment is required in assigning a maximum magnitude to each source. Where



NOTE: 1. THE SAFE SHUTDOWN EARTHQUAKE (SSE) DESIGN PEAK HORIZONTAL GROUND ACCELERATIONS FOR THESE NUCLEAR POWER PLANTS ARE PROVIDED IN TABLE 7.5.
2. ANTHRACITE AND BITUMINOUS COAL FIELDS ARE DENOTED BY RED BORDERS.

FIGURE 7.22 LOCATION OF NUCLEAR POWER PLANTS WITH RESPECT TO U.S. COAL FIELDS

fault sources are inferred to be present, fault movement within the range of 35,000 to 100,000 years BP is considered recent enough to warrant an “active” or “capable” classification, and they should be modeled as sources according to their fault dimensions and histories. The assignment of a maximum magnitude to each source should consider the concepts presented in [Section 7.7.2.4](#).

The MCEs identified for each source potentially affecting the site are candidates for one or more controlling MCEs at the site. It is also important to look at a variety of earthquakes that have a long duration and are rich in lower frequency contents, but do not necessarily cause the highest peak acceleration at the coal refuse site. For coal refuse impoundments, this longer-duration earthquake may be the controlling event if it triggers strength loss of the embankment/foundation materials. Seismic input for a coal refuse impoundment facility may be defined by both near-field and far-field events. For purposes of clarification, a near-field event is an earthquake that is postulated to have an epicenter at or very near a site of interest and a far-field event is one where the earthquake is not expected to occur near the site.

7.7.3.2 Ground Motion Attenuation

The difference in ground-motion attenuation between the western and eastern U.S. is significant and needs to be accounted for in the hazard analysis. This is a topic that has been extensively researched and there are a number of attenuation functions that have been developed for eastern U.S. ground motion. Examples include Toro et al. (1997), Frankel et al. (1996), Atkinson and Boore (1995, 2006), Somerville et al. (2001) and Campbell (2003). The attenuation relationships were developed based on

numerical modeling and sparse strong-motion records from small earthquakes, and while subject to uncertainty, they are considered to be appropriate.

7.7.3.3 Selection of Peak Ground Motion Parameters

The MCE is defined as the most severe ground motion calculated from the selected ground motion attenuation relationship(s) from the various potential MCEs identified from the possible sources. The credible severe combination(s) of magnitude (preferably moment magnitude) and distance will define the basis for the MCE. The ground motion associated with the credible severe combinations of magnitude and distance is normally defined in terms of peak ground acceleration (PGA).

In many cases the most severe PGA is associated with a relatively small nearby earthquake, especially in the areas of relatively low seismic hazard. Where there is moderate to high risk, just deriving the credible severe PGA from a small local earthquake is not sufficient, and it is necessary to supplement this MCE with a credible severe earthquake from a relatively distant large magnitude source where the PGA might be lower than a small local event, but will be associated with more cycles of ground motion.

7.7.3.4 Selection of Acceleration Time Histories

A time-history representation of the seismic input is generally presented in terms of the ground accelerations (accelerograms) where the variation of ground motion is plotted as a function of time. Actual strong motion recordings of earthquakes are time histories of the earthquake ground motion. Ultimately, the goal of selecting a time history for use in design is to be able to match the MDE ground motion with a PGA and number of cycles of ground motion defined for design. There are two ways to obtain time histories for engineering design and analysis: (1) actual ground motion records or (2) synthetic ground motions.

Actual ground motion records can be obtained from the USGS or COSMOS (Consortium of Organizations for Strong-Motion Observation Systems) web sites. If actual strong motion recordings are used as seismic input, they need to be selected to match as closely as possible the source magnitude and expected faulting mechanism, recognizing that faulting mechanisms may not be known if the site is in the central or eastern U.S. Although distance is a consideration in the selection of the ground motion, it is more significant that the earthquake simulate the PGA derived for the design MDE(s) and that the duration/number of cycles of ground motion be consistent with the number of cycles derived with the simplified approach for liquefaction analysis. In addition, care should be taken to select records that are well represented in the frequency range of interest to an embankment dam (approximately 0.5 to 1.5 Hz). In order to effectively bound the range of possible ground motions, several hypothetical design ground motions, or a synthetic time history rich in all possible frequencies of interest, should be used.

As noted in [Section 7.7.3.2](#), most of the strong motion records available as potential design time histories in the range of a central and eastern U.S. MCE will be from areas with different attenuation characteristics (e.g., the western U.S.). There are very few records from the central and eastern U.S., especially for moderate to strong earthquakes of magnitude M greater than 5.0. Nevertheless, as noted in [Section 7.7.2](#), in spite of the differences associated with western U.S. records and limitations to the eastern U.S. database, these differences can be accounted for in a seismic hazard analysis because, within soils where strength loss occurs, it is expected that western and eastern ground motions will be similar (Youd et al., 2001). If actual strong ground motion records are used as the basis for defining the MCE, it is recommended that at least three records be selected for the analysis and that justification provided for their selection. If the site is in an area of medium to high seismic hazard, more than three time histories should be used.

Although real time histories are the preferred means for defining ground motion, an alternative approach for defining a design time history that is often used in the central and eastern U.S. is to derive

synthetic ground motions. The most widely used methods to generate synthetic ground motion are the stochastic point- and finite-source models (Hanks and McGuire, 1981; Toro and McGuire, 1987) and the stochastic finite-fault model, which can simulate some of the near-source effects (Atkinson and Silva, 1997; Beresnev and Atkinson, 1997). With the improvement of computers, it has become possible to use more sophisticated numerical methods for simulating strong ground motion based on empirical or theoretical source functions and two- and three-dimensional wave propagation theory, which has been successfully used in ground-motion simulations for many earthquakes (Somerville et al., 2001; Saikia and Somerville, 1997). Zeng et al. (1994) also developed a composite source model that has been recommended for use in generating synthetic ground motions for seismic design and analysis of highway bridges in Kentucky.

TABLE 7.7 SAFE SHUTDOWN EARTHQUAKE (SSE) PEAK HORIZONTAL GROUND ACCELERATIONS FOR U.S. NUCLEAR POWER PLANTS

Plant	SSE PGA (g)	Plant	SSE PGA (g)
Arkansas Nuclear 1, 2	0.21	Millstone 2, 3	0.17
Beaver Valley 1, 2	0.13	Monticello	0.13
Braidwood 1, 2	0.19	Nine Mile Point, 1, 2	0.15
Browns Ferry 1, 2, 3	0.21	North Anna, 1, 2	0.13
Brunswick 1	0.17	Oconee 1, 2, 3	0.11
Byron 1, 2	0.19	Oyster Creek	0.27
Callaway	0.19	Palisades	0.19
Calvert Cliffs 1, 2	0.15	Palo Verde 1, 2, 3	0.19
Catawba 1, 2	0.17	Peach Bottom, 2, 3	0.15
Clinton	0.21	Perry 1	0.15
Columbia Generating Station	0.25	Pilgrim 1	0.15
Comanche Peak 1, 2	0.13	Point Beach 1, 2	0.13
Cooper	0.21	Prairie Island 1, 2	0.13
Crystal River 3	0.11	Quad Cities 1, 2	0.27
D.C. Cook 1, 2	0.21	River Bend 1	0.11
Davis-Besse	0.15	Robinson 2	0.19
Diablo Canyon 1, 2	0.80	Saint Lucie 1, 2	0.11
Dresden 2, 3	0.21	Salem 1, 2	0.21
Farley 1, 2	0.11	San Onofre 2, 3	0.63
Fermi 2	0.15	Seabrook 1	0.25
FitzPatrick	0.15	Sequoyah 1, 2	0.17
Fort Calhoun	0.19	South Texas 1, 2	0.11
Ginna	0.19	Summer	0.15
Grand Gulf 1	0.15	Surry 1, 2	0.15
Harris 1	0.15	Susquehanna 1, 2	0.11
Hatch 1, 2	0.15	Three Mile Island 1	0.15
Hope Creek 1	0.19	Turkey Point 3, 4	0.15
Indian Point 2, 3	0.15	Vermont Yankee	0.19
Kewaunee	0.13	Vogtle 1, 2	0.19
La Salle 1, 2	0.21	Waterford 3	0.11
Limerick 1, 2	0.15	Watts Bar 1	0.19
McGuire 1, 2	0.15	Wolf Creek 1	0.13

(ADAPTED FROM SOBEL, 1994)

7.7.3.5 Applicability of Design Ground Motion

The end result of a seismic hazard assessment is to derive the ground motion that will affect the base of the impounding structure. Most ground-motion-attenuation relationships derive motion for bed-rock or stiff (firm) soils. Where the site foundation consists of less stiff/dense or deeper soil deposits, or otherwise deviate from the site conditions for which the attenuation relationships are applicable, the derived ground motion should be applied at the top of rock and the ground motion (at the ground surface) estimated from local site response analyses based on computer simulation with programs such as SHAKE, QUAD4M, or DESRA (Schnabel et al., 1972; Finn et al., 1977). For these analyses it is necessary to use a time history input as discussed in Section 7.5.

7.7.3.6 Application of Seismic Parameters in Design Process

Figure 7.23 presents a flow diagram for seismic hazard assessment to determine the design earthquake inputs (M , PGA, ground motion). At a minimum, the design M and PGA are required, as these data are used in the Youd, et al. (2001) pore-pressure-based triggering analysis, to establish a minimum number of cycles of loading for cyclic shear strength testing, in very simplified dynamic response analyses, and for other general purposes. More rigorous dynamic response, seismic stability, and deformation analyses require design ground motions (acceleration versus time histories) to estimate the amplification or de-amplification of the ground motion from the appropriate input horizon (e.g., top of rock, top of stiff soil, or base of structure), up through the foundation and overlying structure; calculate peak accelerations at critical locations within the foundation and structure; conduct more refined and sophisticated triggering analyses; calculate seismically-induced stresses and strains; and identify the likely modes and estimate the range in magnitude of deformation.

7.7.3.7 Simplified Design Ground Motion for Areas of Low Seismic Hazard

As noted in the introduction to Section 7.7.3, a substantial portion of the areas mined for coal in the central and eastern U.S. have a low seismic hazard. The definition of what constitutes low seismic hazard is judgmental, but coal refuse disposal facilities in the area where the *Documentation for the 2002 Update of the National Seismic Hazard Map* (Frankel et al., 2002) indicates that the PGA with a return period in 2,500 years is less than or equal to 0.10g can be considered to be representative of low seismic hazard (Figure 7.19). This zonation is effectively similar to the area where the return period for an earthquake of $M > 5.5$ within 50 km of a given location is greater than 10,000 years (Figure 7.21).

For structures in areas of low seismic hazard that warrant evaluation for a MCE, a simplified approach can be used. The simplified minimum design earthquake should have a moment magnitude M of at least 5.5 ($M \geq 5.5$) at a distance no farther than 50 km from the source. For evaluations of triggering or deformations requiring both M and PGA, adopt 150 percent of the PGA associated with a 2,500-year return period based on the USGS PSHA hazard maps, but not less than $PGA = 0.10g$. When needed, select earthquake ground motion records based on M and the other considerations outlined in Section 7.7.3.4. In areas of low seismic hazard, it is not necessary to consider more distant earthquakes with $M > 5.5$.

Commentary: A simplified approach is recommended by the authors to define a minimum standard for seismic design in low-seismic-hazard areas, with inputs believed to be reasonably conservative for coal refuse impoundments. It is based on published seismic hazard mapping, subject to periodic updating and widely available from the USGS. Based on the project site location, a designer can directly determine the M and PGA using the above procedures for the simplified minimum design earthquake. If a designer judges that other (or potentially less conservative) inputs are appropriate, it is acceptable to perform a seismic hazard assessment. As indicated in Table 7.6, the minimum standard is appropriate for projects only in low-seismic-hazard areas, and a seismic hazard assessment is necessary in moderate to high seismic hazard areas.

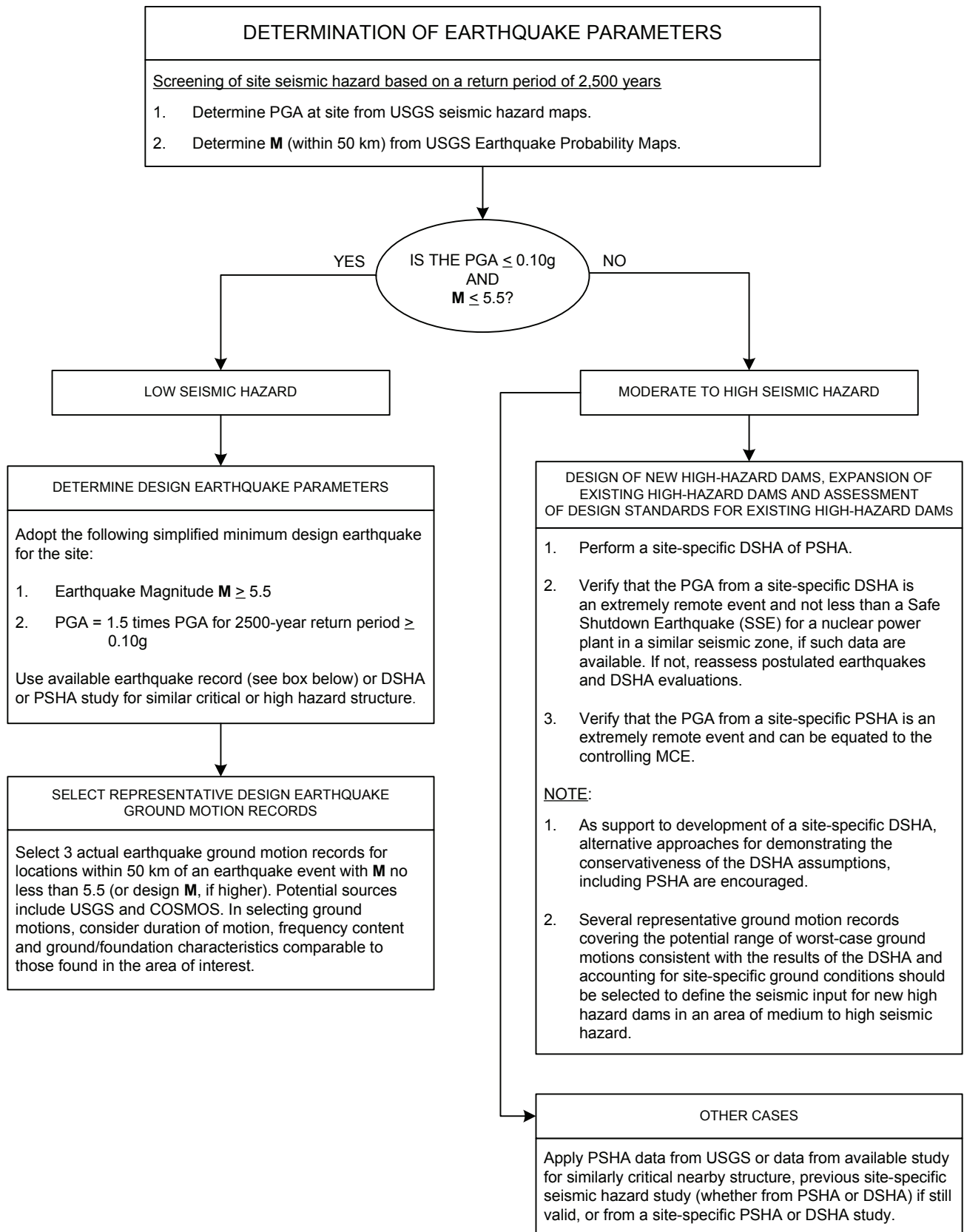


FIGURE 7.23 SEISMIC HAZARD ASSESSMENT FLOW DIAGRAM

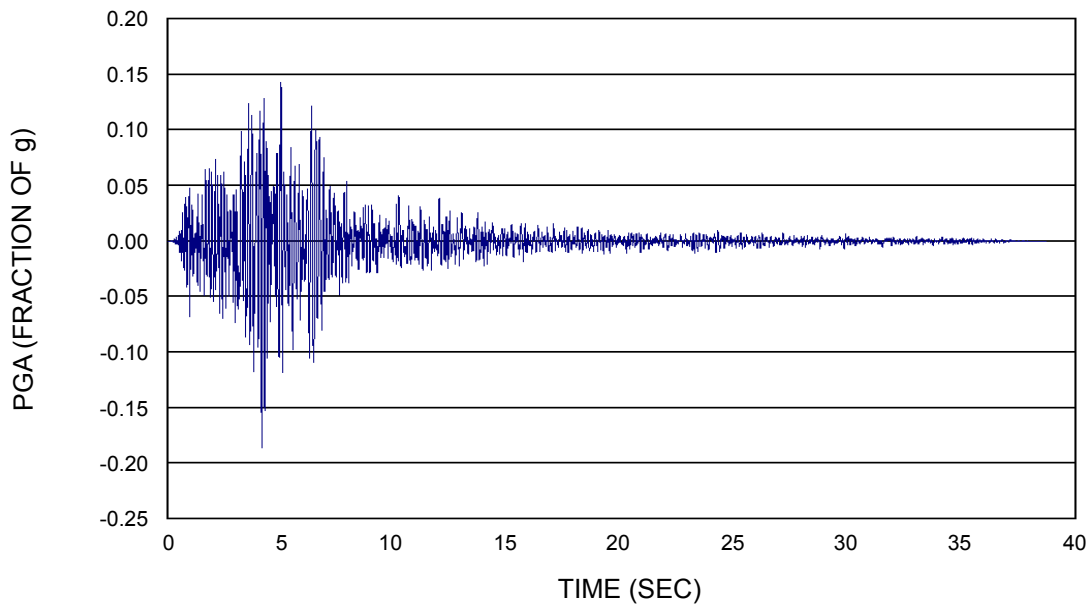
Selection of time histories of acceleration for structures in areas of low seismic hazard should consider earthquake records that are reflective of the site-specific design parameters (M and PGA) and foundation conditions. Attributes of the time histories of acceleration should include: (1) the M and PGA are at least equivalent to the site-specific design parameters, (2) near-field event with hypocentral distance of 50 kilometers or less, (3) foundation conditions similar to site-specific conditions (otherwise, some adjustment of the time history may be warranted), (4) several cycles with a representative band of acceleration in proportion to the design PGA, and (5) some cycles at or near the frequencies of interest for the structure (low frequencies for dams). [Section 7.7.3.4](#) presents reference sources for ground motion histories. The following time histories illustrate the selection of candidate records for low-seismic-hazard areas:

- [Example 1 \(Figure 7.24\)](#) – Time history for low-seismic-hazard area, and the site is distant from widely recognized seismic source zones. This example illustrates a time history that can be considered for a site in the eastern or central U.S., with a design M and PGA of at least 5.5 and 0.1g, respectively. This example has a high PGA (much greater than the site specific design PGA) and lacks cycles of substantive acceleration at lower frequencies, which is not uncommon.
- [Example 2 \(Figure 7.25\)](#) – Time history for low-seismic-hazard area, but the site is close to a boundary of moderate seismic hazard (as reflected by a site-specific PGA much greater than 0.1g). This example illustrates a time history that may be considered for a site in the eastern or central U.S. (close to a recognized seismic source zone) with a design M of at least 5.5 and a design PGA much greater than 0.1g (e.g., 0.12 to 0.15g) with significant low frequency content. This example could also be conservatively applied to sites in low-seismic-hazard areas that are distant from widely recognized source zones.
- [Example 3 \(Figure 7.26\)](#) – Time history for low-seismic-hazard area, and the site is distant from widely recognized seismic source zones. This example illustrates a time history for an actual eastern North American earthquake that could be considered for a low-seismic-hazard site in the eastern US.

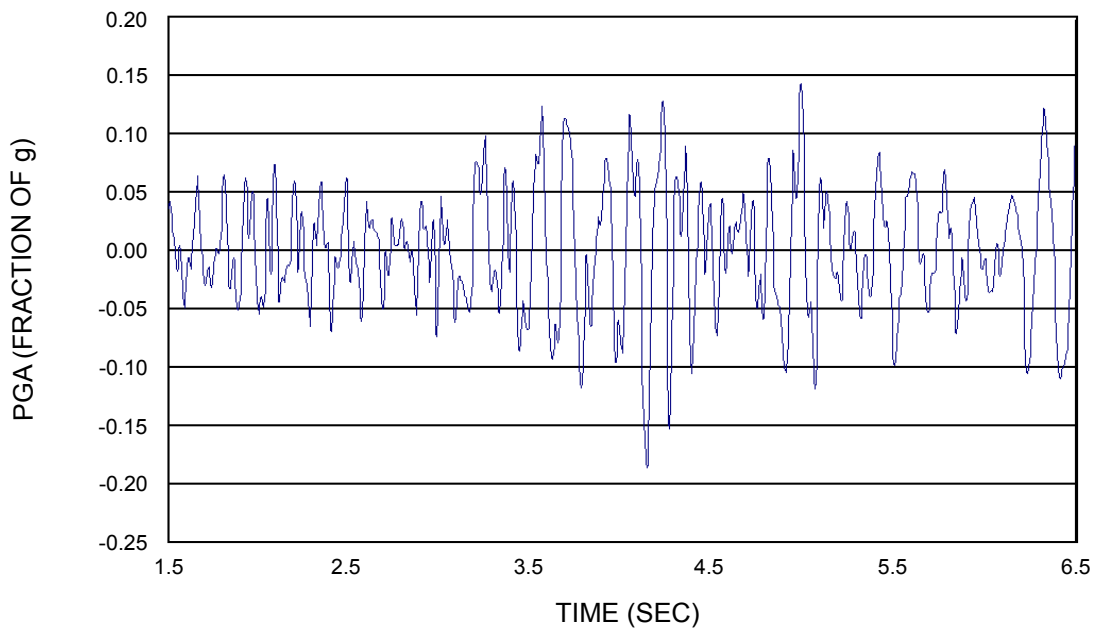
7.8 SEISMIC DESIGN OVERVIEW

Gardner and Wu (2002) presented an overview of the challenges in evaluating strength loss and seismic stability at coal refuse disposal facilities, including a summary of available pore-pressure-based empirical methods and strain-based laboratory methods that MSHA has used in their review and approval of impoundment plans. Wu et al. (2003) cite common MSHA review issues with seismic stability including: (1) defining materials subject to strength loss, (2) sampling and testing protocols, (3) defining ground motion parameters applicable to the site, (4) determining the appropriate margin of safety, (5) and dealing with questions concerning the applicability of available technical information for fine coal refuse. There are no documented case histories of a fine coal refuse impoundment being affected by significant earthquake loading, and as a result, there is little direct confirmation of methods that have been employed for estimating strength loss. Thus, MSHA has been faced with reviewing impoundment design plans with minimal factors of safety, often without mitigating design features that would enhance seismic stability such as provisions for internal drainage of fine refuse deposits.

This chapter has presented credible, documented methods and procedures for the evaluation of seismic design including stability and deformation analyses considered applicable for materials encountered at coal refuse disposal facilities. A flow chart illustrating the steps involved in evaluating seismic design, stability and deformation was presented in [Figures 7.1a, 7.1b](#) and [7.1c](#), and [Section 7.1.2](#) provides a discussion of the basis for the design guidance, including:



7.24a OVERALL RECORD



7.24b SAMPLE TIME SEGMENT

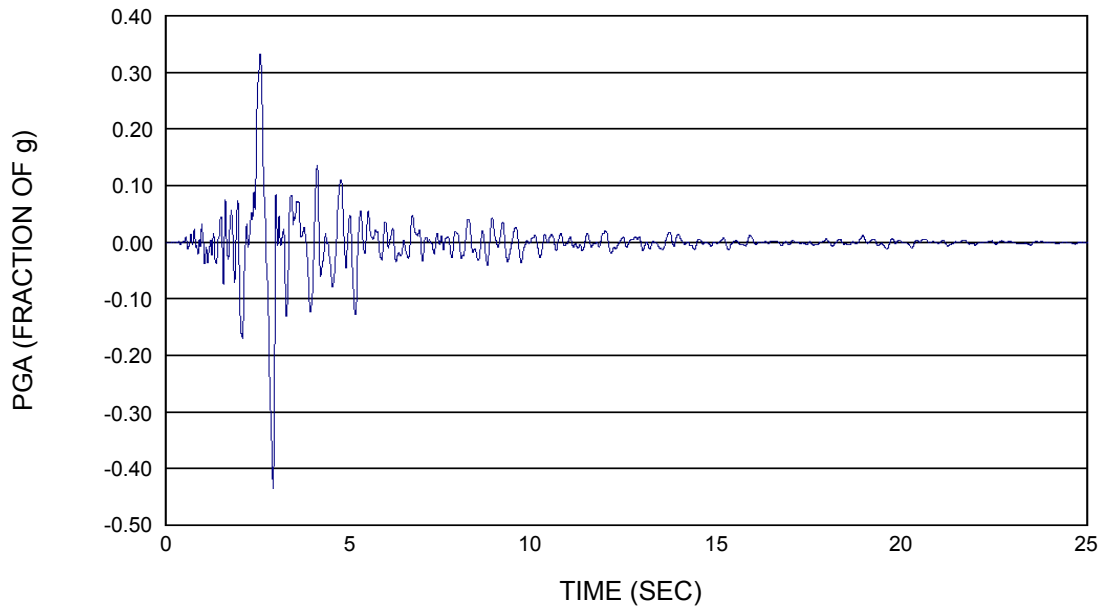
WHITTIER NARROWS - STATION: 24399 MT. WILSON - CIT SEISMIC STATION
 OCTOBER 1, 1987 $M = 5.99$, DISTANCE FROM FAULT RUPTURE = 21.2 KM, $V = 822$ M/SEC (ROCK)

- ATTRIBUTES:
1. M AND PGA > SITE-SPECIFIC DESIGN M AND PGA
 2. NEARER FIELD, FAULT-DRIVEN EVENT WITHIN 50 KM
 3. FIRM ROCK COMPARABLE TO PROJECT SITE CONDITIONS
 4. MANY CYCLES WITHIN REPRESENTATIVE BAND OF PGA.
 5. LIMITED CYCLES AT LOWER FREQUENCY.

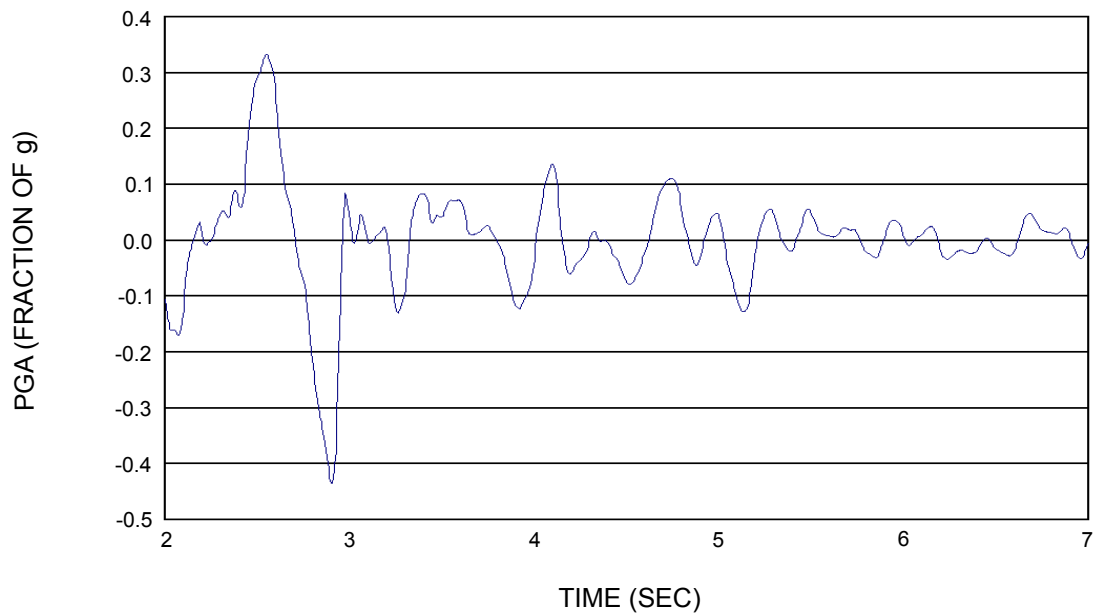
NOTE: SITE IS DISTANT FROM WIDELY RECOGNIZED SEISMIC SOURCE ZONES

(UNIV. OF CAL., 2007a)

FIGURE 7.24 EXAMPLE 1: TIME HISTORY FOR LOW-SEISMIC-HAZARD AREA



7.25a OVERALL RECORD



7.25b SAMPLE TIME SEGMENT

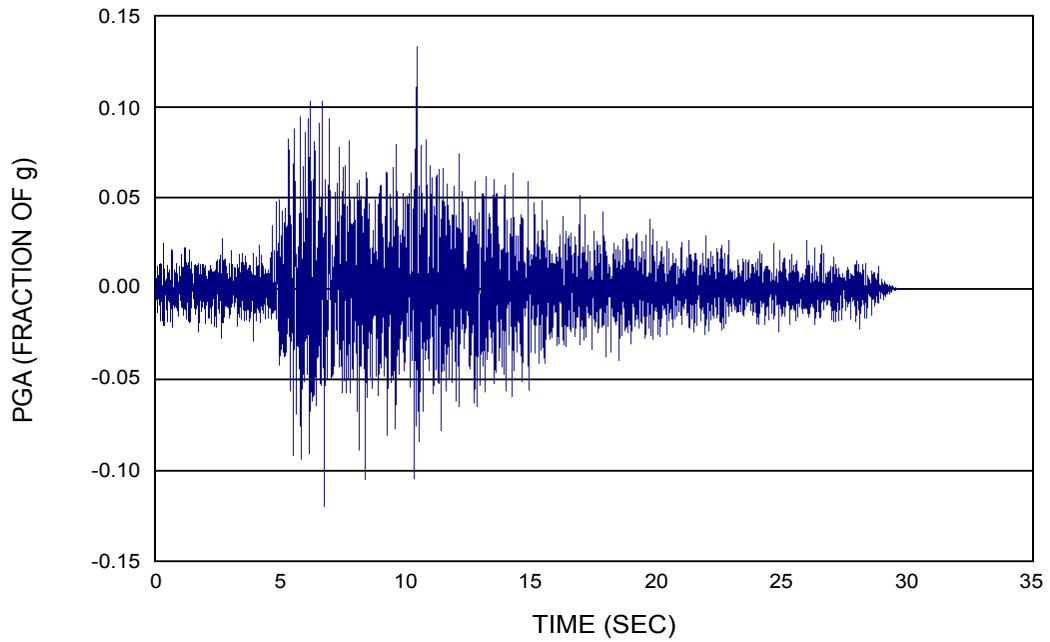
COYOTE LAKE - GILROY ARROY #6, 230 (CDMG STATION 57383)
 AUGUST 6, 1979 $M = 5.7$, HYPOCENTRAL DISTANCE = 9 km, $V = 663$ m/sec (SOFT ROCK)

- ATTRIBUTES:
1. M AND PGA > SITE-SPECIFIC DESIGN M AND PGA
 2. NEAR FIELD EVENT MUCH CLOSER THAN 50 km
 3. SOFT ROCK COMPARABLE TO PROJECT SITE CONDITIONS
 4. INCLUDES PERTINENT LOW FREQUENCY CYCLES.
 5. SIGNIFICANT ACCELERATION SPIKES AT LOWER FREQUENCY.

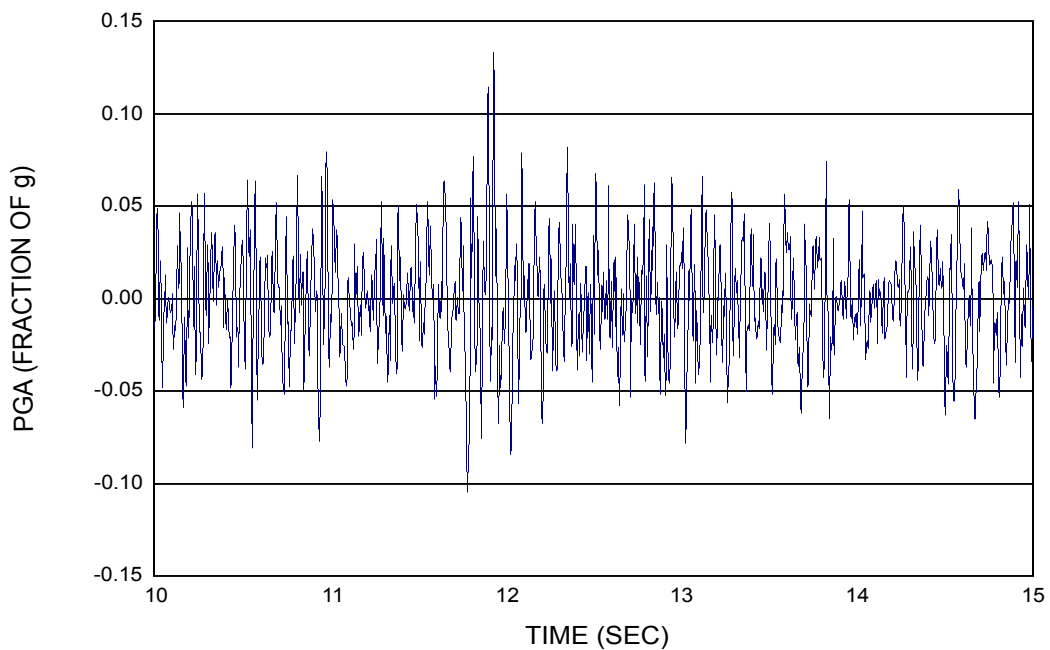
NOTE: SITE IS CLOSE TO THE BOUNDARY OF MODERATE SEISMIC HAZARD

(UNIV. OF CAL., 2007b)

FIGURE 7.25 EXAMPLE 2: TIME HISTORY FOR LOW-SEISMIC-HAZARD AREA



7.26a OVERALL RECORD



7.26b SAMPLE TIME SEGMENT

SAGUENAY - W. CHICOUTIMI NORD (SITE 16 T)
 NOVEMBER 25, 1988 **M** = 5.9, HYPOCENTRAL DISTANCE = 50 KM (HARD ROCK)

- ATTRIBUTES:
1. **M** AND PGA > SITE-SPECIFIC DESIGN **M** AND PGA
 2. EASTERN NORTH AMERICA
 3. ROCK RECORD
 4. MANY CYCLES WITHIN REPRESENTATIVE BAND OF PGA
 5. RELATIVELY LONG DURATION OF STRONG SHAKING > 0.05g (~12 SEC)

NOTE: EASTERN U.S. EARTHQUAKE, DISTANT FROM WIDELY RECOGNIZED SEISMIC SOURCE ZONES

(UNIV. OF CAL., 2007c)

FIGURE 7.26 EXAMPLE 3: TIME HISTORY FOR LOW-SEISMIC-HAZARD AREA

- Appropriate levels of analysis, depending on the type of facility.
- Methods for identifying and evaluating material susceptibility to strength loss, including available field and laboratory techniques.
- Simplified methods for estimating post-earthquake strength, as well as more sophisticated methods for evaluating if triggering of strength loss occurs.
- Alternatives for evaluating seismicity depending on the level of seismic hazard of the region.
- A recommended factor of safety for seismic stability of 1.2 based on a static stability analysis using post-earthquake strengths, which also helps achieve designs with predicted deformations within acceptable limits.

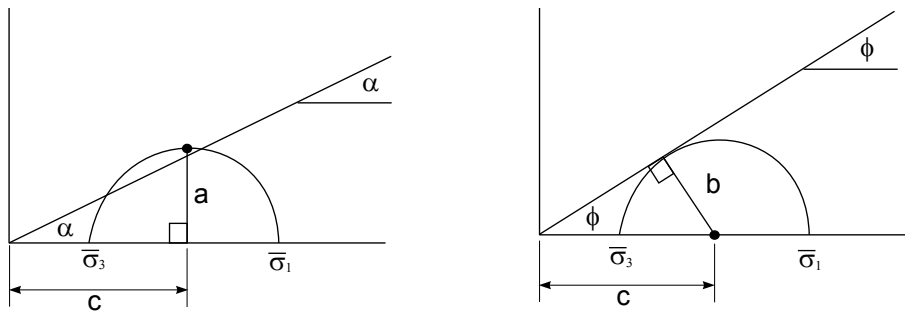
Section 7.1.5 provides recognized, simplified steps and procedures that utilize basic site data and component material properties for development of conservative embankment dam designs in regions of low seismic hazard that constitute most of the areas of coal mining, as discussed in Section 7.7. More sophisticated analyses and procedures may be needed for some facilities built by upstream construction, and these are also discussed in Section 7.1.5, with additional details presented in Section 7.4. These more sophisticated analyses and procedures can reduce conservatism and potentially provide the experienced designer with more expertise additional options for design. These types of analyses may be needed in those limited regions where seismic hazard is moderate to high. Basic screening methods for evaluating deformations are discussed in Section 7.1.5, and the applicability of both screening and analysis procedures is presented in Section 7.5.

Other credible methods and procedures may be acceptable or may become accepted in practice, provided that documentation and testing support their application, and these methods should not be precluded from use in seismic design.

Appendix 7A

DERIVATIONS OF BASIC EQUATIONS FOR STEADY-STATE LABORATORY TESTING

7A.1 COMPARISON OF α AND ϕ ENVELOPES AT STEADY STATE



MOHR'S CIRCLE AT STEADY STATE

α ENVELOPE DRAWN THROUGH MAXIMUM SHEAR STRESS ON MOHR'S CIRCLE

ϕ ENVELOPE DRAWN TANGENT TO MOHR'S CIRCLE

DEFINE $\bar{p} = \frac{\bar{\sigma}_1 + \bar{\sigma}_3}{2}$ MEASURED IN TRIAXIAL TEST AT STEADY STATE

DEFINE $q = \frac{\bar{\sigma}_1 - \bar{\sigma}_3}{2}$ MEASURED IN TRIAXIAL TEST AT STEADY STATE

$$a = b = q$$

$$c = \bar{p} = \bar{\sigma}_3 + q$$

$$\tan \alpha = \frac{a}{c}$$

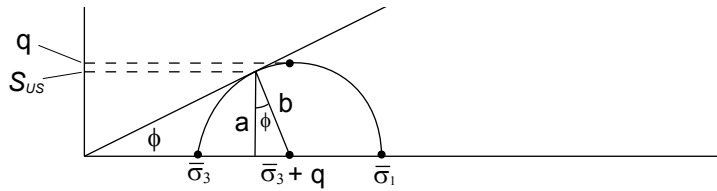
$$\sin \phi = \frac{b}{c}$$

$$a = b$$

THEREFORE $\sin \phi = \tan \alpha$

AND $\phi = \sin^{-1} \left(\frac{q}{\bar{p}} \right)$

7A.2 RELATIONSHIP BETWEEN S_{US} AND σ_3 AT STEADY STATE



MOHR'S CIRCLE AT STEADY STATE

$$b = q = \frac{\bar{\sigma}_1 - \bar{\sigma}_3}{2} = \text{RADIUS OF MOHR'S CIRCLE}$$

$$a = b \cos \phi = S_{US}$$

THEREFORE: $S_{US} = q \cos \phi$

FROM TRIANGLE GEOMETRY: $\sin \phi = \frac{b}{\bar{\sigma}_3 + q} = \frac{q}{\bar{\sigma}_3 + q}$

$$\sin \phi = \frac{\frac{S_{US}}{\cos \phi}}{\bar{\sigma}_3 + \frac{S_{US}}{\cos \phi}} = \frac{S_{US}}{\bar{\sigma}_3 \cos \phi + S_{US}}$$

$$\bar{\sigma}_3 \cos \phi \sin \phi + S_{US} \sin \phi = S_{US}$$

$$\bar{\sigma}_3 \cos \phi \sin \phi = S_{US} (1 - \sin \phi)$$

THEREFORE: $\bar{\sigma}_3 = S_{US} \left(\frac{1 - \sin \phi}{\cos \phi \sin \phi} \right)$

Appendix 7B

VOID-RATIO MEASUREMENTS DURING UNDISTURBED TUBE SAMPLING AND LABORATORY TESTING

7B.1 INTRODUCTION

The purpose of this appendix is to present methods for accurate measurement of the void ratio of triaxial specimens and the changes in void ratio of undisturbed tube samples from conditions in situ to conditions during shear in the triaxial test. Accurate void ratio measurements are needed in order to correct the undrained steady-state (residual) strengths measured in the triaxial test to obtain in-situ strengths using the procedures described in Poulos et al. (1985). Specifically, the required void-ratio values are:

- Undisturbed specimens – both the void ratio in situ and the void ratio during undrained shear in the triaxial test must be determined. To obtain these values one measures the void ratio changes that occur at various stages of the sampling and testing process, as subsequently discussed.
- Remolded specimens (tested to obtain the slope of the steady-state line) – the actual void ratio in the triaxial cell during shear is needed. For drained tests, the void ratio changes during shear, and the value when the specimen reaches steady state is needed.

In the discussion that follows, undisturbed specimens are addressed first, and then the differences in the procedures for remolded specimens are presented. The procedures discussed below include some measurements that are not directly needed in the Poulos et al. (1985) procedure. However, these extra measurements provide important checks of the measurements that are directly needed. These procedures relate to soils ranging from slightly silty sands to slightly clayey silts. Note that, in this appendix, the term “sample” is used to refer to an entire tube sample obtained from the field. The term “specimen” refers to a portion of the sample trimmed from a tube or prepared in the laboratory.

7B.2 USE OF AVERAGE VOID RATIO

In all cases it is assumed that the average void ratio of the entire specimen during shear is representative of the strengths and pore-pressure measurements being made in the triaxial test. If localized shear straining develops, as evidenced by shear planes or localized bulging, this assumption is no longer valid because the average void ratio of the specimen is no longer representative of the soil being sheared. Tests with shear planes or localized bulging cannot be used unless localized measurements of void ratio are carried out using esoteric techniques such as impregnation with resins followed by microscopic examination.

Similarly, tests on specimens with significant stratification within the specimen (e.g., layers of slightly silty sand alternating with layers of slightly clayey silt) cannot be used, because the average void ratio is not representative of either soil type. Past experience with coal refuse indicates that careful

selection of sampling zones based on CPT data has resulted in stratification not being an issue and not causing concentration of deformations in any zone within the test specimen.

7B.3 UNDISTURBED TUBE SAMPLING

Sampling in borings can be accomplished using a thin-wall tube (3-inch O.D. with wall thickness of one-sixteenth inch) with either a fixed-piston sampler with piston rods extending to the ground surface (Hvorslev sampler) or a hydraulically-actuated piston sampler (Gus or Osterberg sampler). Hand-carved samples can be obtained in test pits using a tripod tube sampler. Detailed sampling procedures for the Hvorslev sampler are presented in Appendix 7C. Similar procedures should be used for other samplers.

High quality galvanized-steel, brass, or stainless-steel tubes should be used. The cutting edge should have a clearance ratio of between 0.5 and 1.0 percent ([Appendix 7C](#)) and should be filed sharp and smooth immediately prior to use.

Measurements required during sampling are:

- Sampler penetration into the material (to the nearest millimeter).
- Length of recovered sample (to the nearest millimeter).
- Inside diameter of the sample tube cutting edge (to nearest 0.1 millimeter, using calipers).
- Inside diameter of the sample tube (to nearest 0.1 millimeter, using calipers).

The volume change during sampling is computed from:

- In-situ sample volume = distance pushed times tube area at cutting edge
- In-tube sample volume = sample length recovered times inside area of tube

When measuring the length recovered, it is expected that the bottom of the sample is flush with the bottom of the tube. If a section of the bottom of the sample is missing, it can be assumed that it fell during withdrawal of the sampler from the borehole and thus should be considered to be part of the measured length recovered.

There are potential errors in this part of the procedure. In general, the errors overstate any decrease in volume. For example, the sample may be flush with the bottom, but may have slid downwards. The shorter measured recovery would be assumed to be a volume decrease with an associated decrease in void ratio, which is conservative in the overall estimation of in-situ strengths. However, very large apparent void ratio decreases should be considered unreasonable, and the sample should not be used for testing.

Experience indicates that it is possible to keep volume changes during sampling generally below one percent, with the change being usually in compression, but some slightly clayey silts may actually expand slightly during sampling.

After the length of recovered sample is measured, a section of the sample at the bottom should be removed to allow installation of the packer. The tube should be maintained in an upright position at all times. The packer may have drain holes to allow drainage in sands, but should be solid for soils exhibiting any plasticity. The top should be cleaned and a loose packer or other disk placed on top of the sample. The distance from the top of the tube to the disk should then be accurately measured. This measurement should later be rechecked to determine if the sample settled during transport.

7B.4 HANDLING AND TRANSPORTATION

Sample tubes must be kept upright at all stages of handling and transportation. The tubes should be transported in private vehicles and cushioning should be provided around each tube and between the tube rack and the vehicle to minimize the transmission of vibrations from the vehicle to the samples. Freezing of the samples must be avoided. Any volume change that occurs during handling and transportation can be computed as the change in vertical distance from the top of the tube to the top of the disk resting on the sample. Volume changes that occur during transportation and handling are normally negligible even for sand, if reasonable care is taken.

7B.5 TUBE CUTTING AND EXTRUSION

Tube cutting must be performed using a method that does not produce vibration or deformations of the sample tube. Typically a tube cutter is used. Low pressure is applied to the tube, and stiffener rings are placed above and below the cut to minimize tube deformation. The tube must be maintained in a vertical position. The distance to the top of the sample will indicate if volume changes have occurred. If the described procedure is carefully followed, the volume changes during tube cutting should be negligible.

After the tube section containing the triaxial test specimen is cut, the ends of the specimen are typically trimmed away from each end of the tube section by about one-half inch, so that: (1) the ends of the tube section can be deburred and (2) a packer can be installed in the tube to keep the sample in place. The following measurements should be made:

- Total weight of the sample and tube (this is a back-up measurement)
- Length of tube section – length of the tube minus the distance from each end of tube to the ends of specimen (all measurements to the nearest 0.5 millimeter; each measurement should be the average of three points taken around the circumference of the tube).
- Inside diameter of the tube section (to the nearest 0.1 millimeter, using calipers).

The volume of the specimen in the sample tube after cutting and trimming can be computed from the above measurements.

From this point on, all soil in the tube section must be recovered and the dry weight measured. This requires that extreme care be taken because: (1) some soil will stick to the sample tube during extrusion, (2) some will stick to the membrane after triaxial shear, and (3) some will be used for index testing after the triaxial shear testing is performed. The total dry weight of soil, encompassing all of the above, and the measured volume of the specimen should be used to compute the void ratio.

The specimen must be extruded upward from the tube, i.e., in the same direction that it entered the tube during sampling. During extrusion, any soil that stuck to the tube and any other soil that for whatever reason did not make it to the triaxial cell must be recovered.

Depending on the ability of the soil sample to stand vertically, it may need to be extruded directly into a close-tolerance membrane stretcher using a membrane that is then used to transfer the sample to the triaxial cell pedestal. A small vacuum may need to be applied to the sample to complete placement of a second membrane and attachment of the drainage lines to the top cap. Membrane thicknesses should be measured prior to use. After the sample is safely in the triaxial cell under a small vacuum, measurements of sample length and diameter should be made, with the latter requiring correction for membrane thickness. Note that these are backup measurements.

7B.6 SATURATION

Once the triaxial cell is assembled, a cell pressure must be applied at the same time that the vacuum is released so that the effective stresses in the specimen remain about constant. As the vacuum is released, some water may enter the specimen as air bubbles are reduced in size, but this does not mean that there was a volume change.

Backpressure should then be applied keeping the effective confining stress constant. Note that the process must be done very slowly so that: (1) the backpressure is equalized at all times throughout the sample and (2) the pressure regulators are keeping up with the required pressures. The water that enters the specimen in this process does not correspond to a volume change but to compression of air bubbles in the voids of the soil and eventually their solution into the pore water. For undisturbed samples obtained below the water table, the volume change due to saturation should be negligible. For remolded specimens prepared at low water contents, there may be a collapse due to saturation and a substantial volume change, particularly for silts or very silty sands.

7B.7 CONSOLIDATION

Volume change during consolidation of the saturated specimens can be accurately determined from the water expelled from the samples. If the loading piston is attached to the top cap, height change measurements can also be made accurately, provided that an axial load is applied to the piston to compensate for the upward force in the piston caused by the cell pressure (in order to maintain the desired consolidation stress ratio – typically one). It is advisable to consolidate the sample in stages so that a compression curve (e versus $\log p$) can be obtained. Comparison of compression curves among the various tests can be used as a means of judging unusual results. The changes in void ratio during the consolidation phase are by far larger than for any of the other stages including sampling, transportation, and extrusion.

7B.8 SHEAR AND DISASSEMBLY OF TRIAXIAL CELL

Since undisturbed samples are usually sheared undrained, there is no volume change during shear of saturated samples.

The procedure for disassembling the triaxial cell and removing the sample at the end of a test should allow for two key measurements, namely the water content and the dry weight of the full specimen. The specimen should be sliced in half longitudinally, and any stratification should be noted. A vertical slice should be taken for specific gravity measurement. For coal tailings, a specific gravity measurement should be made for every test specimen. For natural soil, 2 or 3 measurements should be adequate for a given soil layer. Other vertical slices may be taken for Atterberg-limits, grain-size, or hydrometer tests, but at least half of the specimen should be used for the water content measurement. The wet weight of the water content specimen should be measured quickly, before it begins to dry.

As mentioned above, all soil from the triaxial specimen must be recovered so that the full dry weight can be determined. This includes the soil used for index testing, soil stuck to the membrane or end caps, and any other soil trimmings. The wet weight of the water content specimen should be measured to the nearest 0.01 gram. The dry weight of the water content specimen and of all other material from the triaxial specimen and from the specimen removed during tube trimming should also be measured to the nearest 0.01 gram.

To make the test specimen firmer during disassembly of the triaxial apparatus, it may be desirable to reconsolidate the specimen at the end of the test, but, if this is done, the amount of water expelled during reconsolidation must be recorded. The water expelled during reconsolidation must be included in the computation of the water content of the specimen during shear.

7B.9 COMPUTATIONS OF VOID RATIO

Void ratio computations are discussed in the following text and are summarized in [Table 7B.1](#). The following notation is used in the table:

W_s	dry weight
D	diameter
H	height or length
V	volume
w	water content
e	void ratio
γ	unit weight
γ_w	unit weight of water
G_s	specific gravity of soil grains
Δ	incremental change

Stages of sampling and testing are noted by the following:

is	in situ
t	in tube after sampling
tt	in tube after transportation
ts	in tube section after cutting the sampling tube and trimming the ends of the test specimen
txi	in triaxial cell – initial condition under small vacuum
txc	in triaxial cell – after consolidation and during undrained shear

The required values of void ratio are:

- Void ratio during shear in the triaxial cell
- Void ratio in situ

The void ratio during triaxial shear is computed simply from the measured water content of the specimen at the end of the test, using the relationship $G_s w = e$ (assuming 100 percent saturation). As mentioned previously, for coal tailings a specific gravity measurement should be made for every test specimen. For natural soil, 2 or 3 specific-gravity measurements should be adequate for a given soil layer.

Sampling, transportation and tube cutting can result in changes in void ratio from the in-situ condition that can be determined directly from the measured changes in volume, using the formula:

$$\Delta e / (1 + e) = \Delta V / V$$

Changes in void ratio should be averaged for the full tube sample. Subsequent to tube cutting, volume changes and resulting void ratio changes are associated with the tube section from which the triaxial specimen is extruded.

The table at the end of this appendix lists the measured and computed quantities considered to be the primary values, the formulas used, and the secondary values that can be used to compare with the primary measured or computed values. The primary measured and computed quantities should

TABLE 7B.1 VOID RATIO MEASUREMENT FOR UNDISTURBED TUBE SAMPLES⁽¹⁾

Stage	Volume (V)	Dry Weight (W_s)	Void Ratio (e)	Comments
1. In situ Change	ΔV (meas.)		$e(is)$ ↑ Δe (2) ↑	$e(is) = e(t) + \Delta e$ (during sampling) Measure ΔV from V (sampled) versus V (recovered). Compute Δe .
2. Full tube after sampling Change	ΔV (meas.)		↑ $e(t)$ ↑ Δe (2) ↑	$e(t) = e(tt) + \Delta e$ (during transport) Measure ΔV from the height change of the sample during transport between the field and the laboratory
3. Full tube after transport, but before cutting Change	ΔV		↑ $e(tt)$ ↑ Δe (2) ↑	$e(tt) = e(ts) + \Delta e$ (during cutting) Measure ΔV from the height change of the sample measured during tube cutting. ΔV is normally zero. Compute Δe (normally zero).
4. Tube section after cutting and trimming Change	$V(ts) \rightarrow \rightarrow \rightarrow$	$W_s(ts) \rightarrow \rightarrow$ ↑ ↑ ↑ ↑ ↑ ΔW_s	↑ $e(ts)$ (3)	Measure $V(ts)$ from the I.D. of the tube and sample length. Compute $e(ts)$ for $V(ts)$ and $W_s(ts)$. From this point on, all solids should be saved so that $W_s(ts)$ can be measured. The sample in the tube section should also be weighed. This can later be used to estimate the water content and saturation of the sample at this stage. ΔW_s is the soil left in the tube during extrusion.
5. In triaxial cell, following extrusion from tube Change	$V(txi)$ (meas.) $V(txi)$ (comp.) ↑ ↑ ↑ ΔV	↑ $\approx W_s(txi)$ $= W_s(txi)$	$e(txi)$ (3)	$V(txi)$ (meas.) is from measurements of triaxial sample when set up in the cell under small vacuum. $V(txi)$ (comp.) is from $V(txc)$ and ΔV during consolidation. Large differences between the two indicate a potential problem. ΔV is measured during consolidation.
6. In triaxial cell after consolidation and during undrained shear	↑ $V(txc)$ (3,4) ← (Not necessarily needed, but good practice.)	$W_s(txc) \rightarrow \rightarrow$ $w(txc)$ (Computation starts after above are measured.)	$e(txc)$ (4)	Use w and G_s after test (txc) to compute consolidated as-tested void ratio, considering that the sample is saturated at this point. This is the primary method for obtaining $e(txc)$. Also measure W_s for the entire sample. W_s is needed for computation of $e(ts)$ in Stage 4. W_s may also be used to obtain $V(txc)$. $V(txc)$ and ΔV measured during consolidation can then be used as a check on $V(txi)$.

Note: 1. Measurement of ΔV are made from Stage 1 onward, as sampling and testing proceed. The arrows indicate the order of void ratio computations. Computations begin following measurement of $W_s(txc)$ and $w(txc)$ in Stage 6. Computations proceed along the path of the arrows.

$$2. \Delta e = (1 + e) \Delta V / V$$

$$3. e = (G_s \gamma_w V / W_s) - 1$$

$$V = W_s (1 + e) / (G_s \gamma_w)$$

$$4. e = G_s w \text{ (} w \text{ is in percent, assumed to be 100 corresponding to complete saturation.)}$$

be used for estimating in-situ strengths. However, there may be cases where comparison of primary and secondary quantities may indicate that the secondary quantities are more believable and should be used. Some measurements mentioned in the text are not included in the table, but they can also be used to compare to the primary values.

As previously discussed, consolidation should be performed in stages. However, for clarity, consolidation is treated as a one-stage process in the table.

7B.10 REMOLDED SAMPLES

The purpose of testing remolded samples prepared at various void ratios from a uniform batch of soil is to determine the steady-state line for the soil batch, the slope of which is needed for correcting the results from testing of the undisturbed samples. Thus, primarily, we are interested in the void ratio during shear, i.e., the last line in [Table 7B.1](#). However, in planning the tests one targets specific after-consolidation void ratios and confining pressures at which to perform tests so as to achieve sufficiently wide coverage of void ratio and stresses in the steady-state plot. For this purpose, it is important to develop the compression curves for each test (by consolidating in stages) and also to estimate void ratio changes, if any, that would be expected upon saturation.

Assuming that the samples are prepared in a mold of known volume, the process of computing void ratios at various stages is similar to the one shown in the table for undisturbed samples, except that it starts at the “tube section after trimming” stage, which is equivalent to an “in the compaction mold stage” for the remolded samples.

Often when samples are compacted at relatively low water contents, there is substantial compression upon saturation. Thus the volume change from the t_{xi} to the t_{xc} stage includes not only the effect of consolidation, but also the effect of saturation. Since saturation would occur under backpressure, it would occur with the cell assembled, and thus there would not be access to the sample to measure its height and diameter after saturation but prior to consolidation. An alternative procedure would be to cause near-saturation by circulating de-aired water very slowly through the specimen with vacuum applied at the upper end while slightly opening the lower valve to allow the de-aired water to be sucked in, but not opening the valve so much that the vacuum is lost at the lower end of the sample. This process will not result in full saturation, but it will cause collapse and thus allow measurement of the sample prior to cell assembly and the application of cell and backpressures.

Appendix 7C

PROCEDURE FOR UNDISTURBED, FIXED-PISTON SAMPLING OF COHESIONLESS SOIL

The procedures presented herein have been developed for a fixed-piston sampler with piston rods (actuating rods) that extend up to the ground surface (often referred to as a Hvorslev sampler). Similar procedures should be employed for sampling using hydraulically-actuated samplers or tripod-tube samplers.

7C.1 ADVANCING THE HOLE

7C.1.1 General

1. The hole should be started as close to vertical as possible. This is necessary because the actuating rods will be placed through a bracket 10 feet directly above the borehole. If the hole is not vertical, the actuating rods will bend. Also, when the drill rods are pushed, they may slip off the drill head if they are not vertical.
2. The drill head should be almost all the way forward when starting the hole. This allows for maximum horizontal travel of the head. Usually, drillers will do this as routine procedure.

7C.1.2 Casing

1. It is best to use 4-inch-I.D. casing. If larger-diameter casing is used, the velocity of the drill fluid return is reduced, which increases the amount of coarse wash in the borehole. If the casing is smaller, the sampler will be a tight fit. Either flush-joint casing or hollow-stem augers can be used depending on soil conditions.
2. In general, the casing should be advanced to within about 1 foot of the proposed sampling depth. However, this may not be necessary if thick drilling fluid is used and the borehole remains open below the casing. This is referred to as "open-hole" drilling. If Revert drilling fluid is used in open-hole drilling, it is prudent to advance the casing to the bottom of the borehole at the end of the work shift.

7C.1.3 Drilling Fluid

1. It is generally best to use a drilling fluid that has a high unit weight, such as bentonite mixed with water, rather than plain water. This will help to carry cuttings to the surface and will increase the pressure on the bottom of the sample during withdrawal from the borehole. Usually, the governing factor in preparing the drill fluid is the ability of the pumping equipment to circulate the fluid through the drill rods. It is advantageous to use a drill fluid that has a slippery feel.
2. When drilling through a dam, the potential for hydraulic fracturing at the bottom of the borehole should be evaluated. If hydraulic fracturing is possible, special drilling procedures should be used. These procedures may involve maintaining the fluid level in the borehole well below the ground surface and using augers to advance the boring. Tube samples can be obtained through large hollow-stem augers, or small-diameter solid augers may be used to clean out the hole inside casing.

- Several types of drilling fluids are available. Some of these include Revert, Quick Gel, and Kim-Mud. Revert is an organic material that decomposes a few days after mixing with water. It is commonly used if piezometers or a groundwater observation well are to be installed in the borehole. All three of these muds have worked well for removing sand-sized particles from boreholes.

7C.1.4 Mud Tub

It is important to have a mud tub with baffles that create settling basins for the cuttings. A mud tub with three or more settling basins is preferred. Cuttings should be shoveled out of the mud tub at frequent intervals to keep the drill fluid clean.

7C.1.5 Hole Advancement

- Drill bits must have deflectors that prevent drill fluid from jetting downward and disturbing the material below the drill bit. Tricone roller bits are available with a deflector attached to one of the cones that prevents drill fluid from jetting directly downward. It may be necessary to weld a bead on fishtail or chopping bits to deflect the drill fluid. Some bits have side or upward discharge of the drill fluid. The bit should be checked by flushing water through it above the ground surface.
- Drill bits should be slightly smaller than the I.D. of the casing. If 4-inch casing is used, the drill rods should be N or NW size to reduce the annular space between the casing and drill rods. This will increase the upward velocity of cuttings and will help to reduce wash at the bottom of the borehole.
- Advancement of the bit should be done at a slow rate of about 1 foot per minute maximum. Drill fluid pressure during drilling should be kept low to minimize disturbance to the material. After the required depth is reached, the bit should slowly be lifted a distance of about 3 feet above the bottom of the borehole. Then the drill fluid pressure can be raised to wash cuttings out of the hole.
- The drill bit and rods should never be allowed to rest on the bottom of the borehole. They should always be suspended from the drill rig. This is important so that potentially loose material is not densified or disturbed by the weight of the drill rods.

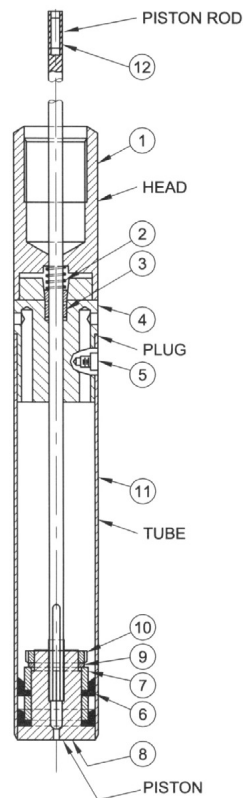
7C.2 PREPARATION OF SAMPLER

7C.2.1 Definition of Sampler Parts

TABLE 7C.1 STATIONARY PISTON SAMPLER WITH STEEL TUBE

Size	Sample Tube Length	Rod Conn.	Part No.	Weight	
				(lb)	(kg)
2" O.D. x 1 $\frac{7}{8}$ " I.D. ⁽¹⁾ (50.8 x 47.6 mm)	30" 762.0 mm	AW	22056-16	25.0	11.3
2 $\frac{1}{2}$ " O.D. x 2 $\frac{3}{8}$ " I.D. (63.5 x 60.3 mm)	30" 762.0 mm	AW	22053-16	28.0	12.6
3" O.D. x 2 $\frac{7}{8}$ " I.D. ⁽¹⁾ (76.2 x 73.0 mm)	30" 762.0 mm	NW	22041-43	30.0	13.6
3 $\frac{1}{2}$ " O.D. x 3 $\frac{3}{8}$ " I.D. (88.9 x 85.7 mm)	30" 762.0 mm	NW	22057-34	32.0	14.5
4 $\frac{1}{2}$ " O.D. x 40 $\frac{3}{8}$ " I.D. (113.7 x 110.5 mm)	30" 762.0 mm	NW	22065-34	36.0	16.3

Note: 1. Meets ASTM, AASHTO, DCDMA Standards for tubes.



7C.2.2 General Operation of Sampler

With the sampler at the bottom of the borehole and the actuating rods fixed relative to the ground surface, the drill rods are pushed down. All of the parts, except the actuating rods and piston, move down. The locking cone allows one-way (upward) movement of the actuating rods and piston relative to the sampling tube. After the push, the piston cannot move down because the locking cone jams the actuating rods in place.

7C.2.3 Sampler Tube Preparation

7C.2.3.1 Cutting Edge

1. Before the drilling program begins, the cutting edge of each sampling tube should be machined to achieve the desired clearance ratio (CR) defined as:

$$CR = \frac{D_{IT} - D_{CE}}{D_{CE}}$$

where:

D_{IT} = inside diameter of tube (should be 2 7/8 inch)

D_{CE} = inside diameter of cutting edge

Usually, there is less chance of sand sliding out the bottom of the tube if the clearance ratio is relatively high. However, more disturbance of the sand occurs when the clearance ratio is relatively high because the sand expands outward to meet the sides of the tube.

Typically, sampling tubes obtained from Acker Drilling Company have clearance ratios of about 1.3 to 1.5 percent. For sand sampling, this clearance ratio is too high. Tubes should be machined to have clearance ratios between about 0.5 and 1.0 percent.

TABLE 7C.2 OPTIONS AND SPARE PARTS – STATIONARY PISTON SAMPLER⁽¹⁾

No.	Diameter and Head Thread Connection	2" O.D.		2½" O.D.		3" O.D.		3½" O.D.		4½" O.D.	
		AW	Wt. (lb)	AW	Wt. (lb)	NW	Wt. (lb)	NW	Wt. (lb)	NW	Wt. (lb)
		Part No.	(kg)	Part No.	(kg)	Part No.	(kg)	Part No.	(kg)	Part No.	(kg)
1	Head	120140-9	2.0 0.9	1201140-7	6.0 2.7	120140-10	6.0 2.7	120140-12	8.0 3.6	120140-16	11.0 4.9
2	Clamp Spring	120136	(1)	120136	(1)	120136	(1)	120136	(1)	120136	(1)
3	Cone Clamp Assembly	220042-1	(1)	22042-1	(1)	22042-1	(1)	22042-1	(1)	22042-1	(1)
4	Plug	120221	3.0 1.3	120189	5.0 2.2	120142	7.0 3.1	120226	10.0 4.5	120243	12.0 5.4
5	Socket Head Cap Screw (4 required)	120660	(1)	120652	(1)	120652	(1)	120652	(1)	120652	(1)
6	Packing Cup (2 required)	150045	(1)	150045-14	(1)	150045-11	(1)	150045-12	(1)	150045-18	(1)
7	Piston Spacer (2 required)	120222	(1)	120190	(1)	120138	1.0 0.45	120145	1.0 0.45	120297	1.0 0.45
8	Piston	120223	(1)	120295	1.0 0.45	120143	1.0 0.45	120225	1.0 0.45	120242	2.0 0.90
9	Lock washer	90399-04	(1)	90399-065	(1)	90399-08	(1)	90399-10	(1)	90399-15	(1)
10	Locknut	90400-04	(1)	90400-064	(1)	90400-08	(1)	90400-10	(1)	90400-15	(1)
11	Steel Tube – 30"	120021-4	3.0 1.3	120086-4	4.0 1.8	120037-4	5.0 2.2	120093-11	7.0 3.1	120095-4	7.0 3.1
11	Brass Tube – 30"	120245-4	3.5 1.5	120246-4	4.00 1.8	120038-4	6.0 2.7	120092-10	6.0 2.7	120094-4	7.0 3.1
11	Stainless Steel Tube – 30"	120245-4	3.5 1.5	120246-4	4.0 1.8	120230-1	5.0 2.2	120027-7	6.5 2.9	120244-4	7.0 3.1
12	Piston Rod-Master	120139-1	1.5 0.67	120139-1	1.5 0.67	120139-1	1.5 0.67	120139-1	1.5 0.67	120139-1	1.5 0.67
(3)	Act. Rod – 2 ft	120219-2	1.5 0.67	120219-2	1.5 0.67	120219-2	1.5 0.67	120219-2	1.5 0.67	120219-2	1.5 0.67
(3)	Act. Rod – 5 ft	120219-4	5.0 2.2	120219-4	5.0 2.2	120219-4	5.0 2.2	120219-4	5.0 2.2	120219-4	5.0 2.2
(3)	Act. Rod – 10 ft.	120219-5	7.0 3.1	120219-5	7.0 3.1	210219-5	7.0 3.1	210219-5	7.0 3.1	210219-5	7.0 3.1

Note: 1. For optional tubes, see Item 11.
1. Less than one pound or 0.45 kilogram.
2. Not shown.

(REPRODUCED FROM ACKER DRILL COMPANY INC. SOIL SAMPLING TOOLS CATALOG, 1978)

- Any nicks in the cutting edge should be repaired. A small machinist's file is useful for this purpose.
- The cutting edge I.D. should be measured at three to four locations so that an average cutting edge diameter can be determined. Also, the I.D. and O.D. of the tube should be checked. They are normally exactly 2⅞ and 3 inches. Field calipers should be used. Make sure that the calipers are aligned properly.

7C.2.3.2 Deburring and Cleaning

- The four holes at the top of the tube should be deburred using a file so that the plug can be inserted into the top of the tube.
- Wash all steel filings from the inside of the tube.

7C.2.4 Sampler Assembly

7C.2.4.1 Initial Cleaning of Parts

1. Locking Cone – should be free of all sand. Ball bearings should rotate freely. Spray with WD-40 (or similar light lubricant) to lubricate bearings.
2. Spring – a new spring should have the ends turned inward so that the ends do not become jammed between the locking cone and the plug. Clean spring of all sand.
3. Piston Rod – make sure that the beveled edge occurs on the threads of the piston rod only. The bevel should not extend below the threads. The piston rod must be deburred (filed smooth) above the threads so that the locking cone slides freely along the shaft. This should be done between each sampling attempt. The female threaded end of the piston rod should be thoroughly cleaned and lubricated with grease.
4. Plug – squirt water through the ports to clean out the sand and mud. Clean the female threads in the four side holes. Make sure the beveled hole at the top is free of sand and that the male threads are free of sand.
5. Head – clean thoroughly. Make sure there is no sand in the female threads.
6. Piston – make sure that sand is removed from the area behind the leathers. Clean the female threads with water. Make sure that the piston rod screws into the piston very easily (do not grease these threads). Leathers, which are referred to as packing cups (Part 6 in [Table 7c.2](#)), should be kept in water so that they remain pliable. Leathers should not have major cracks. The leathers should be coated with a thin film of high vacuum grease.

Initially, the piston and piston rod should be checked to make sure they are able to hold a vacuum beneath the piston. Put the piston near the bottom of a sampling tube with the piston rod screwed in position and place in a bucket of water. Pull up on the piston rod to check if water can be raised into the sampling tube.

7C.2.4.2 Assembly

1. Screw the piston rod tightly to the piston.
2. Place the tube horizontally on a table.
3. Push the piston from the top to the bottom of the tube. Make sure the piston bottom is flush with the cutting edge.
4. Install the plug and four screws. The screws should be finger tight.
5. Slide the cone into position. Use a screwdriver to push it in as far as possible.
6. Push hard on the piston rod to make sure the cone is seated. Check that piston has not moved out of the tube more than one-sixteenth inch.
7. Measure the stick-up of the piston rod above the plug top. This measurement will be used to determine the actual movement of the piston during sampling.
8. Install a rubber or plastic seal around the actuating rod and push it down over the locking cone. This seal can be made from a plastic end cap typically used to seal the ends of the tubes or from an old rubber glove. This seal minimizes the entry of sand into the cone. Failure of the locking cone has been attributed to sand getting below the cone preventing movement of the cone required for locking the piston rod.
9. Install the spring over the cone.
10. Install the head. Make sure that the spring seats properly into the recess in the head. Put thick strings between the head and plug and grease the threads. Tighten as tight as possible by hand. Later, this connection will be broken while soil is in tube. The string and grease make it easier to break the connection without shaking the tube.

11. If an NW-AW sub is used, record the stick-up of the actuating rod above the sub. This will be used to determine if the actuating rods and piston moved up in the tube while the tube was being lowered down the borehole.
12. Put the plastic cap over the cutting edge of the tube to protect it.
13. Do not rest the sampler on the piston because the piston can move up into tube.

7C.3 SAMPLING PROCEDURE

7C.3.1 Preparation of Actuating Rods inside Drill Rods

All actuating rod threads should be cleaned and greased.

7C.3.1.1 Separate Drill Stem and Sampling Stem

It is often more efficient to use two sets of drill rods (with only one set down the hole at any one time). One set would have actuating rods inside and be used for sampling only. Using two sets of drill rods is especially beneficial when the depth of the hole extends beyond 30 feet.

7C.3.1.2 One Drill Stem

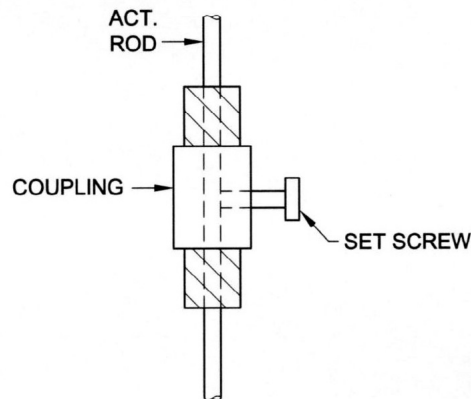
1. After drilling is completed, actuating rods can be placed down the drill rods and rest on the roller bit so that the entire string can be lifted out as a unit.
2. Protection for the male actuating rod thread at the bottom should be provided.
3. It is important to have a bleeder pipe (2-foot length of rod with holes through the side) just above the drill bit to allow the escape of drilling fluid from the rods.
4. It is desirable to have a short length of actuating rod at the bottom of the actuating rod string so that the actuating rods stick up above each corresponding drill rod by about 2 to 18 inches.

7C.3.2 Attaching Sampler to Drill Rods

1. Have drill rods ready with the actuating rods inside.
2. Make sure that the bleeder pipe is at the bottom of the drill stem.
3. Screw the sub part way onto the bottom of the drill rods.
4. Put a vise grip at the bottom of the actuating rods and a vise grip on the piston rod.
5. Raise the drill rods high enough to attach the sampler.
6. The driller should hold drill rods so they don't move. They usually extend far above the drill rig and must be held securely.
7. The helper and inspector attach the tube – do not allow the bottom of tube to rest on any surface.
 - a. Connect the actuating rod to the piston rod with vise grips, making sure the piston rod is not turned.
 - b. Unscrew the sub from the drill rods and screw the sub onto the sampler head. Make sure a string is in the joint.
 - c. Lift the sampler and the actuating rods that have been attached to the piston rod, and screw the sampler to the drill rods (this is the hardest part).
8. Remove the plastic cap and check that the piston has not moved. Note how much the piston is protruding below the cutting edge. This procedure is easier if NW drill rods are used because then an NW-AW sub is not required. The procedure for attaching the sampler to the drill stem will vary from one project to another and with the available drilling equipment.

7C.3.3 Lowering Sampler down Hole

1. Carefully place the tube into the hole without nicking the cutting edge. If the cutting edge is nicked, start over.
2. Slowly lower the sampler down the hole. When connecting actuating rods, never turn the lower actuating rod as this will release the vacuum port in the piston. Measurements of the stick-up of the actuating rods above the drill rods should be made whenever drill rods are joined as a check on the location of the piston in the sampling tube.
3. Stop lowering sampler about 1 to 2 feet above the bottom of the hole.
4. Measure the stick-up on the actuating rods. Is it correct? If the sampler hit a lot of wash, the actuating rods will be higher. String between joints of drill rods may make the drill stem slightly longer. Measure the drill rods if a problem is suspected.
5. Fix the actuating rods to the drill rods with a special coupling with a set screw. See sketch below.

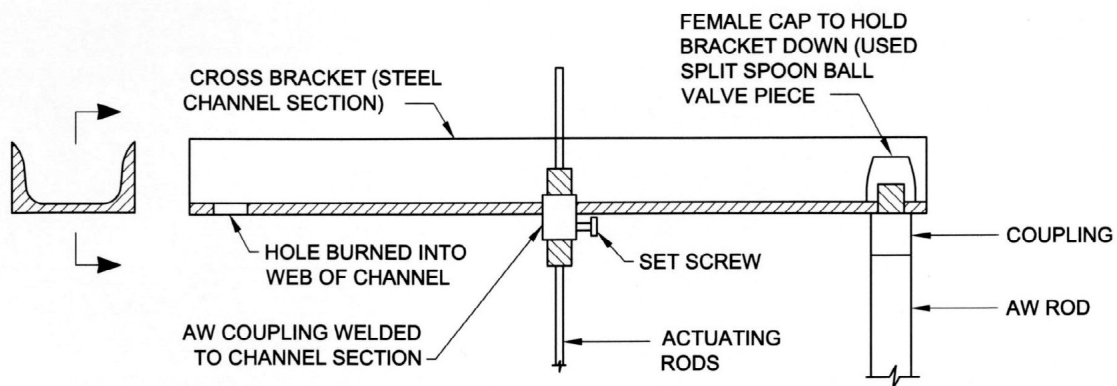
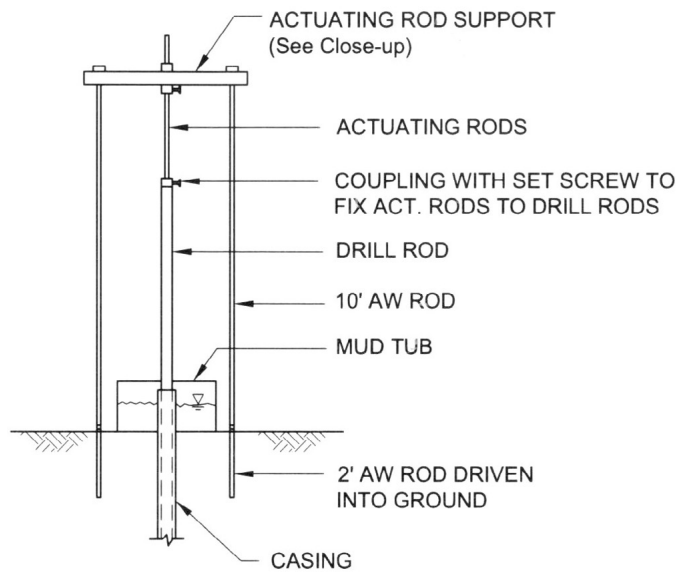


6. Put a keel line just above the coupling.
7. Very slowly, with the hydraulic cable (or cathead and rope) and pull ring, lower the sampler until it rests on the bottom. First put a keel mark on the drill rods so that the keel mark will line up with the top of the casing when sampler is supposed to reach bottom. This will warn when the sampler is getting close.
8. Check to make sure that the actuating rods did not slip in the coupling.

7C.3.4 Preparation for Push

Make sure that there is a stable surface for making measurements of the drill rod relative to the casing. Use the top of the casing itself, or the pull-plate resting on the casing.

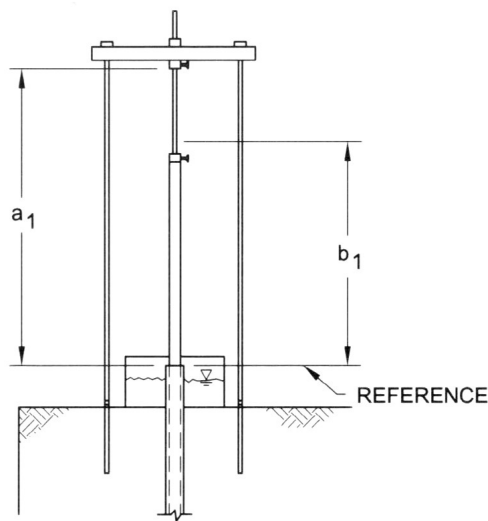
1. As soon as the sampler is resting on bottom of borehole, measure the actual depth of the bottom of the piston sampler.
2. Put a mark on the drill rod 24 inches above reference. Do this immediately, in case the sampler creeps down before push.
3. Set up frame to fix actuating rods. The frame shown on the following page is suggested:



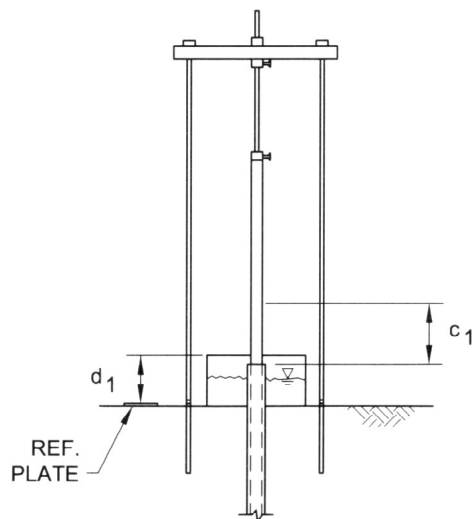
The 2-ft AW rods driven into the ground should be as close as possible to the mud tub to minimize the span length of the upper cross bracket.

Fixing the actuating rods to the rig has proven unreliable because the rig can move (lift up) during sampling. Using cables to hold the actuating rods is very bad because they allow movement due to slack in cables.

4. Tighten set screw in top cross-bracket (very tight). Place a vise grip very tightly on actuating rod just above top coupling as a safety measure to keep actuating rods from moving down.
5. Measure the distance from the bottom of the top coupling to the reference plate (a_1) to the nearest one-sixteenth inch.
6. Measure distance from reference plate to an arbitrary point on the actuating rod just above drill rods (b_1) to nearest one-sixteenth inch. This will give the actual movement of the actuating rod, including slippage if it occurs.



7. Check that mark on drill rods is still 24 inches (c_1) above reference plate. This will be used to determine actual push length.
8. Measure distance from a reference plate on the ground to a mark on the AW rods (d_1). This will be used to determine whether the support footings move during sampling.



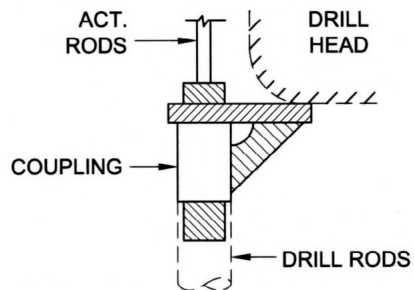
9. Determine the required rate of push and have driller set controls to achieved desired rate. The driller can experiment with rig controls.

On many drilling rigs, the hydraulic pressure gauge indicating downward pressure on the drill head will be very useful. If gravel is present in sandy soils, the tube may crumple if the cutting edge hits a large piece of gravel. By experimentation, a limit hydraulic pressure can be set which, if exceeded, would mean that the tube was hitting gravel, and, if not exceeded, would mean that the tub penetrated relatively easily for the entire push length.

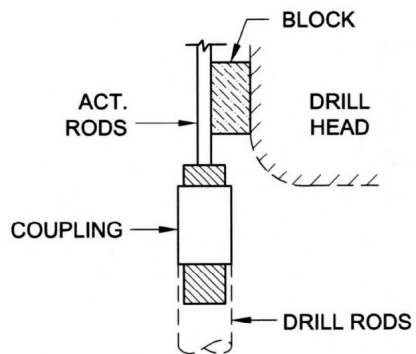
On some drilling rigs, the hydraulic pressure gauge will not be informative because it is not sensitive to resistance against the drill head. Before sampling, determine how the hydraulic pressure gauge works.

- a. Determine hydraulic pressure for the drill head moving down with no resistance (reference pressure).
 - b. Determine hydraulic pressure change for the case of the rig weight acting on the drill stem.
 - c. Decide if monitoring the gauge during sampling will be useful
10. It is important to have a stable connection between the drill head and the drill rods during the push.

On most drilling rigs, the drill heads are rounded and do not provide a good pushing surface. A special bracket can be fabricated to allow the head to push down on the drill rods, as shown in the sketch below:



Alternatively, a right-angle block that allows direct pushing on the drill rods can be attached to the drill head.



7C.3.5 Advancing Tube

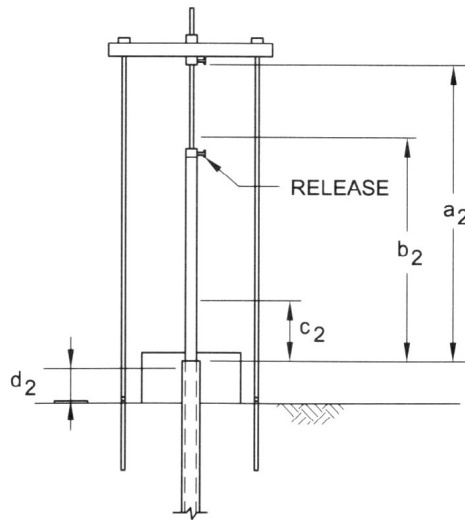
7C.3.5.1 From Weight of Rods

With the actuating rods fixed to top bracket, release the actuating rods from the drill rods. Then re-measure a , b , c , and d and record on data sheet. Compute the following:

1. Penetration due to weight of rods = $c_1 - c_2$
2. Movement of actuating rods = $b_1 - b_2$
3. Movement of cross bar = $a_1 - a_2$
4. Movement of support rods = $d_1 - d_2$

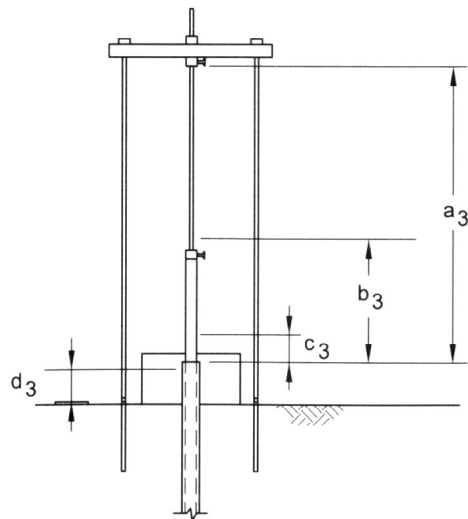
7C.3.5.2 From Drill Head Push

1. The tube should be pushed in a smooth continuous motion, if possible.
2. The driller should be given a mark on the drill stem to watch.
3. It is prudent to push only 22 to 23 inches because there is not much space (less than 1 inch) between the top of the piston and the bottom of the plug when a 24-inch push is completed. If fines have settled out on top of the piston and the fines encounter the plug, the soil in the tube will be compressed and the actuating rods will probably slip in the cross frame.
4. The inspector or helper should time the push. If necessary, the hydraulic pressure gauge should be observed by the inspector. The driller should watch the mark on the rods.
5. After pushing the tube, back off the drill head of the rig.



7C.3.6 Post-Push Measurements

1. Total Penetration – The total penetration ($c_1 - c_3$) includes penetration from the weight of the drill rods.
2. Movement of Actuating Rods – Measure and record b_3 . Record the net movement of the actuating rods
3. Movement of Actuating Rod Support – The actuating rods are now fixed to the bracket and are in tension and may have pulled the support bracket down. Measure and record a_3 . Record the net movement of actuating rod supports.
4. Movement of Support Footings – Measure d_3 and record. Also record the net movement of the support footings.
5. Release Actuating Rods from Bracket – Have the driller release the actuating rods from the top of the bracket. Measure and record a_4 (top bracket may have sprung upward when it was released from the act. rods). Measure and record d_4 . Record net movements of a, b, and d.



7C.3.7 Lifting Sampler up Borehole

1. Disassemble actuating rod support frame.
2. Put a full head of drill fluid in the borehole.
3. Rotate tube about twice – initially, the drill rod joints will come together. The actuating rods should not be tightened to drill rods. As soon as the actuating rods begin turning along with the drill rods, stop rotation. Measure b_5 and c_5 (initial distances from a reference to points on the actuator rods and the drill rods). Rotate the rods two full revolutions (or less, if specified), then re-measure b_6 and c_6 . Compute $c_5 - c_6$ (penetration during shear). Rotation should be performed more than 10 minutes after the push.
4. Lifting the tube the first 2 feet is one of the most critical parts of the operation. As the sampler is lifted, a vacuum will develop at the bottom of the tube tending to suck the soil out of the tube. The tube should be lifted as slowly as possible without jarring or vibrating the drill stem. At the same time that the tube is being lifted, the drill stem should be rotated carefully in a manner such that the rods do not whip and the wrench does not slip. Lifting the first 2 feet has been accomplished as follows:
 - a. A swivel can be attached to the drill stem and hydraulic cables used to lift the tube. The hydraulic cables should be operated slowly enough to lift the tube in 20 to 30 seconds.
 - b. On some drilling rigs, the cable hydraulics are not sensitive enough to lift the tube smoothly. In such cases, a rope can be wrapped around the drill head and tied around the drill rods. The drill head can then be raised as slowly as possible, using the rope to facilitate rotation of the drill stem. A full head of drilling fluid should be maintained in the borehole during this operation. Note if the drill fluid drops temporarily when the tube has been lifted approximately 24 inches. If the fluid drops, this may indicate that the soil is in the tube and the fluid has dropped into the hole formed.
5. If two drill rod stems are being used, slowly lift the drill rods and actuating rods out of hole at less than 1 foot per second. Maintain head. If the rod joints must be broken, make sure that rope has been placed in the joints. When breaking actuating rods, use vise grips to make sure that lowermost actuating rod does not move.
6. If one drill rod stem is being used, before lifting rods, remove as many actuating rods from hole as possible. If this procedure is used, the actuating rod joint at the top of the

piston rod should have been made the loosest and be well greased and not tightened all the way. Other actuating rod joints should have been tightened very tight with vise grips. Then, when unscrewing the actuating rods at the surface, all the actuating rods above the piston rod can be removed. This speeds up the operation considerably.

7C.4 SURFACE HANDLING OF SOIL-FILLED SAMPLER

7C.4.1 Removal of Sampler from Borehole

1. Maintain a head of drilling fluid at all times. When the sampler nears the surface, make sure that the water flowing into the casing is not too turbulent, which could cause erosion of the soil at the bottom of the tube. A stocking over the end of the hose can be used to reduce turbulence.
2. When the bleeder pipe is observed, reduce the rate of movement to as slow as possible, but do not decelerate too rapidly.
3. As soon as the bottom of the sampler surfaces, slide a plate under the sampler to prevent any soil from falling out. Do not put fingers under the cutting edge of the tube. Wait until the drill stem is stable.
4. Start sliding the plate away. Be very careful that fingers are not placed directly under the cutting edge.
 - a. If soil starts falling out, put the plate back. Have a piece of foam rubber approximately 3 inches in diameter and approximately 2 inches thick ready for placing at the bottom of the tube. Make a quick switch of plate and foam rubber and place a plastic cap at the bottom of the tube. Tape the plastic cap in place. The foam rubber will conform to the soil surface and provide resistance to slippage of the soil.
 - b. If soil stays in, which it probably will, make a quick observation of the shape of the bottom soil surface and record later. If soil is flush with the bottom, install plastic cap and tape. If soil is missing up to 2 inches from the cutting edge, put a cylindrical piece of foam in the bottom and cap. If soil is far up into tube, install a vented packer with an extension used for tightening. Filter paper should be placed on the packer.
5. Disconnecting the Sampler. Make sure that the sampler does not rest on a surface with the weight of the drill rods on it, because it could bend or kink.
 - a. If the actuating rods are left inside the drill rods during withdrawal of the sampler, the following procedure is suggested: (a) break the joint at the bottom of the 2-foot bleeder pipe, (b) lift the drill stem with rig hydraulics, and (c) unscrew the actuating rods.

Do not let the sampler drop. A piece of foam can be placed under the sampler so that when it is unscrewed it will drop approximately $\frac{1}{4}$ to $\frac{1}{2}$ inch onto foam (there may be considerable weight above from the actuating rods and soil in the tube).
 - b. If the actuating rods are removed prior to bringing the sampler to ground surface, unscrew the sampler at a convenient joint.

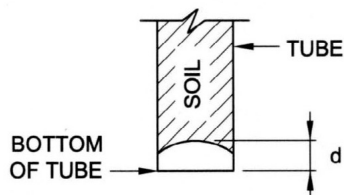
7C.4.2 Installation of Bottom Packer

The bottom packer is installed while the piston is still in place so that a vacuum holds the soil in the tube. Do not turn the tube upside down.

The sampler must be suspended above ground so that the bottom can be worked on. This can be done by mounting a chain clamp to a stationary object free from vibrations (i.e., a work bench or tree, but not the drill rig or other equipment). The head of the sampler (not the tube should be strapped in, allowing the bottom to be worked on.

Alternatively, the sampler can be suspended by a rope from the derrick of the drill rig. The 2-foot bleeder pipe should be kept on the sampler so that a swivel can be attached. The rope should be tied off at the rig. This method is less efficient than the chain clamp method because the drillers cannot advance the hole while the sample is being worked on by the inspector.

1. Remove temporary bottom cap. Note condition of cutting edge and sketch if it is distorted.
2. Measure distance from cutting edge to soil surface. Sketch profile. Record.



3. Remove soil with putty knife. Save cuttings in baggie and jar.
4. Prepare final bottom surface with trimming tool. Make flat. Final surface should be 1 $\frac{3}{8}$ inch or more from cutting edge for packer to fit.
5. Clean inside wall of tube so that packer will not slip.
6. Measure to soil at three locations.
7. Install packer, vented, with filter paper. Pull down hard on packer to confirm that it is tight.
8. Measure at three locations to bottom of packer.
9. Install bottom plastic cap with holes for drainage.

7C.4.3 Removal of Piston

Carefully place the sampler on foam and support it so it is stable and wrapped with foam or mounted in a chain clamp to minimize vibrations.

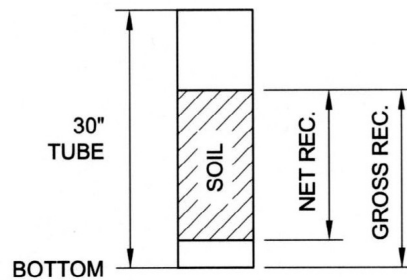
Carefully unscrew the joint between the head and the plug. Remove the head.

1. Remove spring.
2. Clean top of plug and around cone. A squeeze bottle may be used.
3. Measure from top of plug to top of actuating rod. Record distance from tube bottom to piston. Is this the same as the penetration distance?
4. Remove cone: using vise grips, rotate piston rod clockwise while putting sideways force on piston rod. The cone will climb the piston rod. After removing the cone, screw the piston rod back down to plug piston.
5. Remove plug.
6. Measure distance from top of tube to top of wash resting on piston. Did the wash push up against plug?

7. Remove fluid and wash resting on top of piston.
 - a. This can be accomplished by sucking into a long tube and/or using a squeeze bottle.
 - b. Be sure to clean the piston around the piston rod so that air (not fluid) can travel around piston rod to release the vacuum.
8. Unscrew piston rod to release vacuum. Screw piston rod back in part way to pull out piston.
9. Pull out piston slowly. Use piston rod to loosen leathers by swaying piston rod back and forth. Can use vise grips and wood block to lift if it cannot be done by hand. If vacuum is not releasing, soil may be stuck to piston. Stick a wire through port to pierce soil. It is important to prevent soil and fluid above piston from getting below piston.
10. When the piston is removed, note if soil is stuck to the piston and record thickness. This is part of gross recovery.

7C.4.4 Cleanout of Top

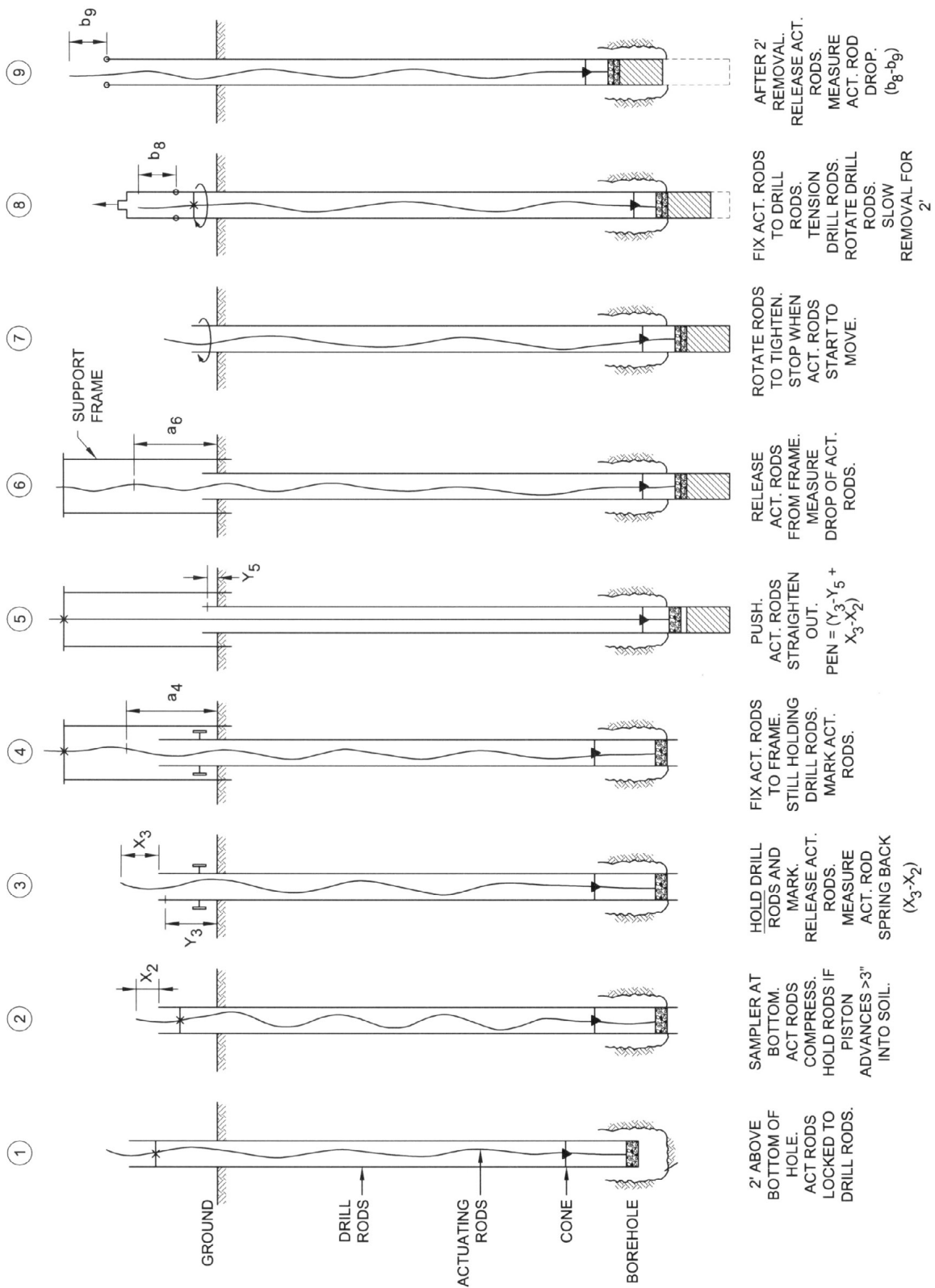
1. Measure distance from top of tube to fluid above soil and record.
2. Measure distance from top of tube to soil at three locations and record.
3. Record gross recovery and net recovery



4. Was the fluid level at the same locations as the bottom of the piston? Remove a sample of the drill fluid above the soil. Is it water or drilling fluid? Is it from the pores of the soil?
5. Remove all fluid resting on top of soil.
6. Use trimming tool to remove wash from top.
7. Note: If suction developed below the piston while the piston was being removed, some soil may have lifted. Slight pressure from a ruler will cause this to drop down.
8. Use foam rubber to remove slop from top of soil. Make sure top of soil is nearly level.
9. Measure to top of soil in three places. Record.

7C.4.5 Installation of Top Packer

1. Prepare the bottom half of a vented packer with a filter paper and a wire for future retrieval.
2. Place packer on top of soil. This provides a good level surface for measuring.



3. Measure accurately at three locations. These data will later be used for monitoring height changes during handling and shipment. Record.
4. Put a moistened paper towel in top.
5. Put a vented plastic cap on top and tape in place.

7C.4.6 Preparation for Shipment

1. Label with the following:
 - Top
 - Project Number
 - Project Name
 - Boring Number, Sample Number
 - Depths
 - Penetration, Gross Recovery, Net Recovery
2. If needed, apply vacuum below bottom packer to draw water out of sample. This will increase the stiffness of sand without significantly changing the void ratio.

Appendix 7D

COMBINING NEWMARK-TYPE DISPLACEMENTS COMPUTED USING 1D SITE-RESPONSE ANALYSES

The computer program SHAKE calculates time histories of horizontal shear stress acting at the boundaries of soil layers. To calculate a time history of acceleration for a wedge, and then a displacement, the following procedure can be used (Figure 7D.1):

1. Perform SHAKE analyses for two representative profiles through the potential wedge to obtain horizontal shear stress time histories $\tau_h(t)$ at two points A and B on the sliding surface.
2. Calculate the time history of the average acceleration $k(t)$ of the soil above the two points:

$$k_A(t) = \tau_{hA}(t) / \sigma_{vA} \quad k_B(t) = \tau_{hB}(t) / \sigma_{vB}$$

where:

$$\begin{aligned} \tau_{hA}(t) &= \text{earthquake shear stress at point A} \\ \tau_{hB}(t) &= \text{earthquake shear stress at point B} \\ \sigma_{vA} &= \text{total vertical stress at point A} \\ \sigma_{vB} &= \text{total vertical stress at point B} \end{aligned}$$

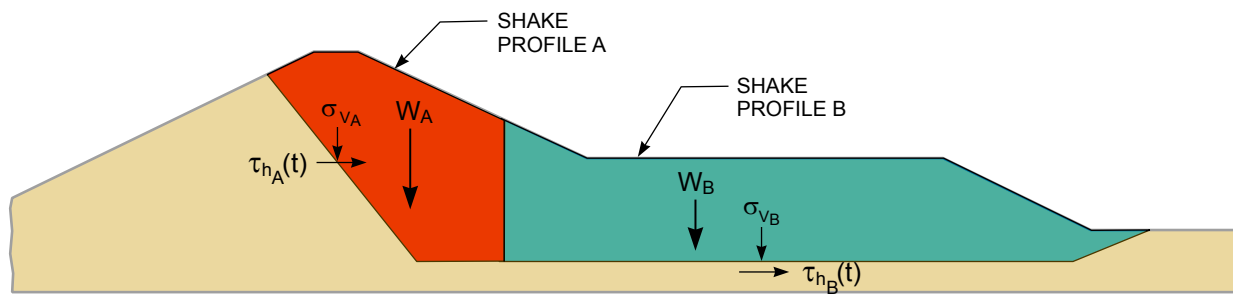
3. Integrate the $k_A(t)$ and $k_B(t)$ time histories for various values of k_y to develop curves of k_y/k_{max} versus displacement (Figure 7D.1).
4. Compute $k_{OVERALLmax}$ for the entire wedge:

$$k_{OVERALLmax} = \frac{k_{Amax} W_A + k_{Bmax} W_B}{W_A + W_B}$$

where:

$$\begin{aligned} k_{Amax} &= \text{maximum value of } k_A(t) \\ k_{Bmax} &= \text{maximum value of } k_B(t) \\ W_A, W_B &= \text{weights of portions A and B of failure wedge} \end{aligned}$$

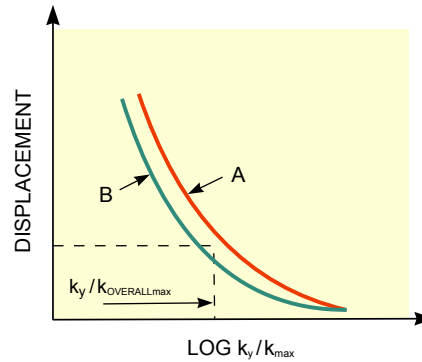
5. Using the value of k_y computed from the pseudostatic stability analyses, calculate k_y/k_{max} and enter the curves developed in Step 3 to obtain a displacement.



$$k_A(t) = \frac{\tau_{hA}(t)}{\sigma_{vA}} \quad k_{Amax} = \text{maximum of } k_A(t)$$

$$k_B(t) = \frac{\tau_{hB}(t)}{\sigma_{vB}} \quad k_{Bmax} = \text{maximum of } k_B(t)$$

$$k_{OVERALLmax} = \frac{k_{Amax} W_A + k_{Bmax} W_B}{W_A + W_B}$$



- where:
- $\tau_h(t)$ = time history of horizontal shear stress
 - σ_v = total vertical stress
 - $k(t)$ = time history of average acceleration of mass above point of interest
 - W = weight

FIGURE 7D.1 DEFORMATION ANALYSIS USING SHAKE